A Survey on Design and Performance of Higher-Order QAM Constellations

Praveen Kumar Singya[1], Parvez Shaik[2], Nagendra Kumar[3], Vimal Bhatia[2], *Senior Member, IEEE*, and Mohamed-Slim Alouini[1], *Fellow, IEEE*

arXiv:2004.14708v1 [eess.SP] 30 Apr 2020

***Abstract*—As the research on beyond 5G heats up, we survey and explore power and bandwidth efficient modulation schemes in details. In the existing publications and in various communication standards, initially square quadrature amplitude modulation (SQAM) constellations (even power of 2) were considered. However, only the square constellations are not efficient for varying channel conditions and rate requirements, and hence, odd power of 2 constellations were introduced. For odd power of 2 constellations, rectangular QAM (RQAM) is commonly used. However, RQAM is not a good choice due to its lower power efficiency, and a modified cross QAM (XQAM) constellation is preferred as it provides improved power efficiency over RQAM due to its energy efficient two dimensional (2D) structure. The increasing demand for high data-rates has further encouraged the research towards more compact 2D constellations which lead to hexagonal lattice structure based constellations, referred to as hexagonal QAM (HQAM). In this work, various QAM constellations are discussed and detailed study of star QAM, XQAM, and HQAM constellations is presented. Generation, peak and average energies, peak-to-average-power ratio, symbol-error-rate, decision boundaries, bit mapping, Gray code penalty, and bit-error-rate of star QAM, XQAM, and HQAM constellations with different constellation orders are presented. Finally, a comparative study of various QAM constellations is presented which justifies the supremacy of HQAM over other QAM constellations. With this, it can be claimed that the use of the HQAM in various wireless communication systems and standards can further improve the performance targeted for beyond 5G wireless communication systems.**

I. Introduction

With 5G deployments beginning to take place, the basic need of high data-rate multimedia applications can be met with optimum bandwidth and power efficient modulation schemes. Over a wider prospective, digital modulation schemes play a key role in attaining high data-rates with bandwidth and power efficiency. The basis of 5G and future wireless communication systems depends on the robustness of the employed modulation schemes. A digital modulation scheme for information transmission depends on various factors such as data-rates, robustness to channel impairments, bandwidth, power, and cost efficiency [1]. Data-rate describes the maximum information transmission through a channel whereas the bandwidth efficiency describes maximum utilization of the limited spectrum by accommodating more information. Power efficiency describes transmission of reliable information with optimum power. However, in practice optimization of all these factors may not be possible at the same time. For example, if power efficiency is targeted then lower order modulation is preferred which leads to lower bandwidth efficiency and lower data-rates. Hence, there is a trade-off between various expectations from modulation schemes. The optimization/trade-off of these parameters is application oriented in digital radio frequency (RF) system design. Considering a terrestrial microwave radio link design, bandwidth efficiency with low bit-error-rate (BER) is given high priority, since, the RF stations are connected to power source. Hence, power efficiency is not a prime concern and also receiver's cost/complexity is not considered because few receivers are required. On the other hand, in cellular communication, power efficiency is mainly focused since the mobile phones operate on a limited battery power. In mobile communication, both power and cost efficiency are stronger constraints than bandwidth efficiency.

Digital modulation schemes are highly impacted by noise however, this provides flexibility of multiplexing various information formats at high data-rates with good quality-of-service (QoS). Digital modulation is classified based on the variation in transmitted signal in terms of amplitude, phase or frequency with respect to the digital message signal. If the amplitude or phase of the transmitted signal is varied with respect to the message signal, the resultant signal is termed as amplitude shift keying (ASK) or phase shift keying (PSK), respectively. ASK and PSK are known as the linear modulation techniques since, they follow the principle of superposition and scaling. If the transmitted signal frequency varies with respect to the message signal, this results in frequency shift keying (FSK). Since, FSK is a non-linear modulation technique, it is not spectrally efficient as compared to the linear modulation schemes. Thus, linear modulation techniques are widely employed in wireless communications [2]. There is yet another advance modulation technique where both the amplitude and phase of the transmitted signal varies with respect to the digital message signal, known as quadrature amplitude modulation (QAM). Among the available digital modulation schemes, QAM and quadrature phase shift keying (QPSK) are widely used in communication standards because of the bandwidth and power efficiency. Further, M-ary QAM is more power efficient than M-ary PSK modulation [2] and thus, is widely preferred in the modern wireless communication standards.

In modern and future wireless communication systems,

[1]P. K. Singya and M.-S. Alouini are with the Computer, Electrical, and Mathematical Science and Engineering (CEMSE) Division, King Abdullah University of Science and Technology (KAUST), Thuwal 23955-6900, Saudi Arabia (e-mail: praveen.singya@kaust.edu.sa, slim.alouini@kaust.edu.sa)

[2]P. Shaik and V. Bhatia are with the Discipline of Electrical Engineering, Indian Institute of Technology Indore, Indore-453552, India (e-mail: phd1601202003@iiti.ac.in, vbhatia@iiti.ac.in)

[3]N. Kumar is with the Department of Electronics & Communication Engineering, National Institute of Technology Jamshedpur-831014, India (e-mail: kumar.nagendra86@gmail.com)

power efficient high data-rate transmission with efficient utilization of the limited bandwidth is a major concern. Power efficiency can be achieved by reducing the average transmit power of the constellation for a fixed BER. However, high data-rates for a limited bandwidth require high transmit power to maintain the same performance. Adaptive modulation is one such solution for spectrally efficient high data-rate communication with optimum power efficiency for the present and future wireless communication systems. In wireless communication, received signal-to-noise ratio (SNR) varies due to the multipath fading. In such scenario, adaptive modulation plays an important role by associating high data-rates to the channels with good channel conditions (high SNR) and low data-rates to the channels with bad channel conditions (low SNR) to improve overall system capacity for a limited bandwidth. Hence, an appropriate modulation scheme with variable constellation order is selected based on the channel condition. In adaptive modulation, constant SNR is maintained by varying various parameters such as transmitted power, data-rates, and modulation orders [1], [3]–[10]. Adaptive modulation is embodied in the present day wireless standards since the 3^{rd} generation (3G) [11] mobile networks. Adaptive modulation finds its applications in high-speed modems [12], [13], satellite links [14]–[16], and in the applications where high QoS is to be maintained [17].

Performance of the communication systems can be improved further by combining the spatial diversity techniques [18] with the adaptive transmission. Spatial diversity can be achieved by employing multiple antennas at the transmitter or receiver, or at both. By using multiple antennas at both the transmitter and the receiver, multiple copies of the information signal can be transmitted and hence, high data-rates can be achieved within the limited bandwidth at the cost of increased hardware and signal processing complexity. However, it is not always possible to deploy multiple antennas at each node due to the device size, cost, and implementation complexity. In such cases, spatial diversity can be achieved through cooperative relaying which is considered as virtual multiple-input and multiple-output (MIMO) system. In cooperative relaying, the end-to-end information transmission takes place through indirect links (relay nodes) by enabling the cooperation with the relays employed.

Motivated with this, in this work, a detailed study of various higher order QAM constellations is presented. This study explores star QAM, cross QAM (XQAM), and hexagonal QAM (HQAM) constellations in details. Their generation, peak and average energies, peak-to-average-power ratio (PAPR), symbol-error-rate (SER), decision boundaries, bit mapping, Gray code penalty, and BER for different constellation orders are presented. Further, applications of different QAM constellations in various communication fields are explored. In the following subsections, a detailed list of abbreviations used in this work and paper organization are presented.

A. List of Abbreviations

Various abbreviations used in this work are shown in Table I.

TABLE I: Various abbreviations used in this work.

1D	1 dimensional
2D	2 dimensional
3G	3^{rd} generation
4G	4^{th} generation
5G	5^{th} generation
ADSL	Asymmetric digital subscribers line
AF	Amplify-and-forward
APSK	Amplitude-phase shift keying
ASK	Amplitude shift keying
ASEP	Average symbol-error-probability
ASER	Average symbol-error-rate
AWGN	Additive white Gaussian noise
BER	Bit-error-rate
BEP	Bit-error-probability
CDF	Cumulative distribution function
CDMA	Code division multiple access
DF	Decode-and-forward
DVB	Digital video broadcasting
DVB-S2	Digital video broadcasting-satellite second generation
DVB-SH	Digital video broadcasting-satellite services to handheld
FEC	Forward error correction
FSK	Frequency shift keying
FSO	Free space optics
HQAM	Hexagonal QAM
i.n.i.d.	Independent and non-identically distributed
LED	Light emitting diode
LoS	Line-of-sight
MIMO	Multiple-input and multiple-output
ML	Maximum likelihood
MMSE	Minimum mean square error
MRC	Maximum ratio combining
NLA	Non-linear amplifier
NLoS	Non-line-of-sight
OFDM	Orthogonal frequency division multiplexing
OWC	Optical wireless communication
PAPR	Peak-to-average power ratio
PDF	Probability density function
PSK	Phase shift keying
QAM	Quadrature amplitude modulation
QoS	Quality-of-service
QPSK	Quadrature phase shift keying
RF	Radio frequency
RQAM	Rectangular QAM
SQAM	Square QAM
SDR	Semi-definite relaxation
SDPR	Semi-definite programming relaxation
SER	Symbol-error-rate
SEP	Symbol-error-probability
SNR	Signal-to-noise ratio
SSK	Space shift keying
STBC	Space time block codes
TDMA	Time division multiple access
TQAM	Triangular QAM
TAS	Transmit antenna selection
UVC	Ultraviolet communication
VDSL	Very high speed digital subscribers line
VLC	Visible light communication
Wi-Fi	Wireless fidelity
WiMAX	Worldwide interoperability for microwave access
XQAM	Cross QAM

B. Paper Organization

In Section II, family of QAMs is discussed is details. Section III, Section IV, and Section V discuss detailed study of some of the newer QAM constellations. In Section VI, probabilistic shaping is discussed. In Section VII, applications of various QAM constellations in wireless communication systems are discussed. Finally, conclusion and future challenges

are presented in Section VIII.

II. Quadrature Amplitude Modulation (QAM)

A. Evolution of QAM

In the late 1950s, digital phase modulation schemes gained considerable research attention along with the digital amplitude modulation for transmission. It was an extension to the amplitude modulation by considering both the amplitude and phase modulations for transmission. The QAM was first proposed by C. R. Cahn [19] in 1960. Cahn's work was extended by Hancock and Lucy in [20] where it is realized that the performance of a circular constellation can be improved by placing the constellation points on the concentric circles with lesser points in the inner circle and more points in the outer circles. They named Type I to the Cahn's constellation and Type II to their newly proposed constellation. In 1962, Campopiano and Glazer proposed properly organized square QAM constellations and denoted it as Type III constellation [21]. From the results it was concluded that the performance of Type II constellation is little better as compared to Type III constellation, but implementation and detection complexity of Type III constellation is significantly low as compared to Type I and II constellations. All three constellations are shown in Fig. 1. Later in 1971, Salz et. al. of Bell Labs proposed some actual QAM constellations [22]. They used both the coherent and non-coherent demodulations and implemented circular constellations with the help of 2 and 4 amplitude positions along with 4 and 8 phase positions. In [23], Simon and Smith proposed some tightly packed 2D spherical shaped honeycomb type structure (hexagonal QAM constellations), and simple generation and detection techniques for such constellations were discussed. In [24], Foschini et al. proposed optimum signal constellations with circular constellation envelop for large constellation size (M) which had optimum BER performance but their detection complexity was high. Foschini et al. extended their work in [25], and error optimization technique for optimum 2D signal constellations was proposed. In the same year, Thomas et al. [26] proposed empirically generated 29 amplitude-phase shift keying (APSK) signal sets, ranging from $M = 4$ to $M = 128$ to determine an optimum signal constellation through symbol-error-probability (SEP) bound for both the average and peak SNRs. In [27], Smith proposed various odd bits QAM constellations and a comparative study of rectangular and symmetric constellations was performed. In [28], Weber proposed a differential encoding technique for reducing the performance penalty by minimizing the phase ambiguity for multiple APSK systems. In [29], Forney et al. presented a detailed survey on various power efficient rectangular and hexagonal QAM constellations with coding fundamentals for band limited channels like telephone channels. Since then, applications of all these proposed constellations have widely been seen in various communication systems and standards which are discussed in the upcoming Section.

B. Various QAM Constellations

In wireless communication systems, a power efficient signal constellation which targets the best QoS with high spectral efficiency has always been an exciting research area since the genesis of early modern mobile communication systems. A breakthrough in the research on modulation schemes happened with the invention of QAM in the early 1960's. Interestingly, various QAM constellations proposed years ago are still actively being used in commercial communication systems. With the recent developments in advanced signal processing algorithms, family of QAM has gained increased attention in present mobile communication systems and is widely adopted in various wireless communication standards and commercial applications. In QAM, information is encoded in both the amplitude and phase of the transmitted signal. Hence, for a given average energy, more bits per symbol can be encoded in QAM which makes it more spectrally efficient. An overview of some of these prominent QAM constellations is presented next.

1) Square QAM (SQAM): In 1962, Campopiano and Glazer [21] extended the works done by Cahn, Hancock and Lucy, by proposing properly organized square or rectangle shaped QAM constellations. Campopiano and Glazer denoted it as Type III constellation which is later known as QAM constellation. Type III QAM provides better error performance than the predecessors Type-I and Type-II QAMs. For QAM constellations, simple maximum likelihood (ML) detection with rectangular or squared boundaries is preferred. SQAM usually takes a perfect square shape for the even power of 2 signaling points 4, 16, 64, 256, 1024, 4096, and so on. SQAM has the maximum possible minimum Euclidean distance between constellation points for a given average symbol power and requires simple ML detection technique. M-ary QAM requires less carrier-to-noise power ratio than the M-ary PSK [30]. Thus, QAM is widely considered in various wireless communication systems and IEEE standards. Lower order QAM constellations have lower spectral efficiency, provide better cell overlap control and tolerance to distortion or SER/BER performance. However, high data-rates can be achieved with higher order QAM constellations at the cost of strict SER/BER requirements, severe cell-to-cell interference, smaller coverage radii, and hardware complexity. SQAM is widely deployed in various wireless standards such as in 3G/4G/5G digital video broadcast-cable/satellite/terrestrial communications, satellite communications, wireless fidelity (Wi-Fi), worldwide interoperability for microwave access (WiMAX), asymmetric digital subscribers line (ADSL), very high speed digital subscribers line (VDSL), power line ethernets, microwave backhaul systems and others. Various QAM applications with different constellation orders are presented in Table II. As an example, 16-SQAM constellation is shown in Fig. 2.

2) Rectangular QAM (RQAM): RQAM is a Type-III QAM with non-square constellation which is commonly preferred for transmitting odd number of bits per symbol. As spectral efficiency depends on the modulation order M, higher spectral efficiency is achieved with higher value of M. Spectral efficiency also depends on the channels conditions. To improve the spectral efficiency, adaptive modulation is used in practice to maximize spectral efficiency for a given channel conditions according to M [1], [6]. Further, both the even as well as odd power of 2 constellations are required for granular

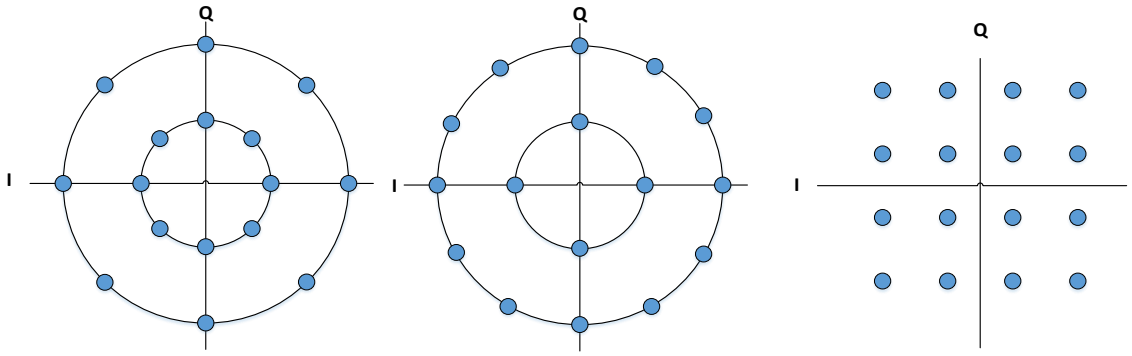

Fig. 1: Type I, Type II, and Type III QAM constellations.

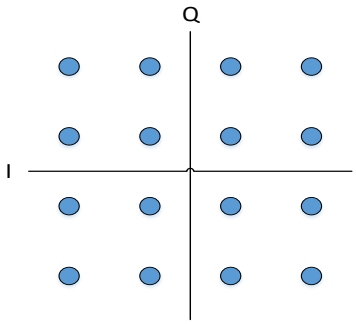

Fig. 2: 16-SQAM constellation.

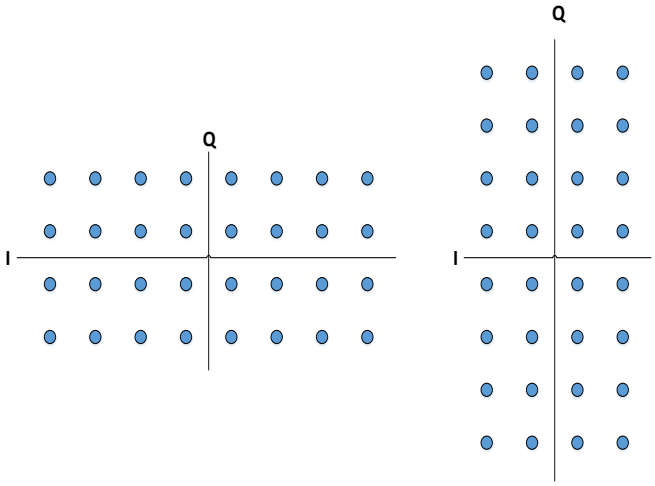

Fig. 3: 32-RQAM in-phase (left) and quadrature phase (right) constellations.

adaptation based on channel conditions. For this, rectangular QAM (RQAM) is commonly preferred due to its generalized behavior as various modulation schemes such as multilevel ASK, binary PSK (BPSK), QPSK, orthogonal binary FSK, and SQAM as its special cases [31]. RQAM is a suboptimal QAM for $M \geq 16$, since the average transmitted power required to achieve minimum distance is slightly greater than the average power required for the best M-ary QAM signal constellation. Thus, general-order RQAM is preferred in practical telecommunication systems [32], [33]. RQAM constellations can be obtained by considering the constellation points in a rectangular shape. The obtained rectangular constellation can be parallel to in-phase axis or quadrature-phase axis with identical average energy. The 32-RQAM constellations are shown in the Fig. 3.

3) Star QAM: For mobile radio applications, SQAM is widely preferred over the last few decades. However, SQAM is optimum if the communication channel is Gaussian. However, in practice, the Gaussian channel assumption does not apply and hence, severe shortcomings were observed for mobile radio channels over fading environment. Carrier recovery and automatic gain control (AGC) are required when SQAM is opted even with differential coding which are complex to achieve and sustain in a real time communication system. To avoid the use of AGC and to mitigate the false lock problem, star QAM constellation was proposed. Star QAM is a special case of circular APSK, which outperforms the SQAM in peak power limited systems. It consists of multiple concentric PSK circles with equal constellation points in each circle and identical phase angle between them. Amplitude and phase of the constellation points are mutually independent [34], [35]. Hence, differential detection can be applied successfully rather than the coherent detection, which omits the need for accurate phase tracking and channel estimation at the receiver [36], [37]. Due to the above favorable features, star QAM is adopted in various satellite communication standards such as in digital video broadcasting satellite standard-second generation (DVB-S2), digital video broadcasting-satellite services to handheld (DVB-SH), advanced broadcasting system via satellite, and Internet protocol over satellite [34], [38]. A detailed study of star QAM constellations is presented later.

4) Cross QAM (XQAM): For odd bits per symbol, RQAM is not a good choice as it has higher peak and average powers. Smith proposed [27] an improved cross shaped constellation to resolve this issue by removing the outer corner points and arranging them in a cross shape such that the average energy of the constellations is reduced. This type of constellation is named as XQAM. XQAM has lower peak and average powers than RQAM, and provides at least 1 dB gain over the RQAM constellations [76]–[78]. XQAM has been adopted in various communication system such as in ADSL and VDSL with 5-15 bits [79], [80], 32-XQAM and 128-XQAM in digital video

TABLE II: Applications of different QAM constellations in existing wireless communication systems and IEEE standards.

Standards	QAM Constellation Points	References
Digital video broadcasting- cable (DVB-C)	16, 32, 64, 128, 256	[39]–[43]
DVB-C2	16 to 4096	[43], [44]
DVB-C2-future extensions	16384 & 65536	[43]
Digital video broadcasting- terrestrial (DVB-T)	16 & 64	[45]
DVB-T2	16, 64, & 256	[46]
Digital video broadcasting satellite (DVB-S)	16	[47]
Asymmetric digital subscribers loop for copper twisted cables	upto 32768	[48]
Power line ethernets	upto 4096	[49]
Ultra-high capacity microwave backhaul systems	2048	[50]
IEEE 802.11n	16 & 64	[51]
IEEE 802.11g	16 & 64	[52]
IEEE 802.11ad	16 & 64	[53]
IEEE 802.11ac	16, 64 & 256	[54]
IEEE 802.11ad	16 & 64	[54]
IEEE 802.11ay	16, 64	[55]
IEEE 802.11af	16, 64 & 256	[56]
IEEE 802.11ah	16, 64 & 256	[57], [58]
IEEE 802.11ax	16, 64, 256 & 1024	[59]
IEEE 802.22	16 & 64	[60]
IEEE 802.22b	16, 64 & 256	[61]
CDMA 2000 1x EV-DO	16	[62]
Release 7-UMTS/HSPA- TR 25 999	16 & 64	[11], [52]
Release 8-LTE- TS 36.211	16 & 64	[63]
Release 10-LTE Advanced- TS 36.300	16 & 64	[64]
Release 14-LTE Advanced Pro- TS 36.306	16, 64, & 256	[65]
Release 15-5G support- TS 36.331	16, 64, 256 & 1024	[66]
IEEE 802.16e	16 & 64	[67]
WiMAX 1.5/IEEE Std 802.16-2009	16 & 64	[68]
WiMAX 2/IEEE 802.16m	16 & 64	[69]
IEEE 802.16-2017	16 & 64	[70]
Telephone circuit modem V.29/34	16 & 64	[71]
Optical modem	16	[72]
Digital multi-programme television distribution by cable networks	16, 32, 64, 128 & 256	[73]
H.261 Reconfigurable Wireless Video Phone System	4, 16, & 64	[74]
DCT Videophone features	16-pilot assisted	[75]

broadcasting-cable (DVB-C) [81]. XQAM has commonly been applied in applications requiring blind equalization [82]–[84]. A detailed study of XQAM constellations is presented later.

5) Hexagonal QAM (HQAM): Requirement for high data-rates at low energy further directed the research towards more power efficient 2D hexagonal shaped constellation referred to as HQAM. HQAM has the densest 2D packing which reduces the peak and average power of the constellation, and makes the constellation more power efficient than the other existing constellations. In most of the existing communication systems, SQAM is widely preferred due to its simpler ML detection than the HQAM constellation, however, with the advancement in technology, implementation complexity of HQAM detection is reduced considerably. Due to superiority of HQAM over other constellations, it can be considered in various applications such as in multicarrier systems [85], multiple-antenna systems [86]–[88], physical-layer network coding [89], small cell [90], optical communications [91], and advanced channel coding [92]–[94]. This work focuses on the HQAM constellation and a detailed study of HQAM constellations is presented later.

C. Application of Different QAM Constellations in Existing Communication Systems and Standards

QAM and QPSK are the most widely preferred constellations in various communication standards. Further, M-ary QAM has better bandwidth and power efficiency than M-ary PSK constellation [2] and thus, is widely employed in various modern communication standards. A list of various communication standards where different QAM constellations with various constellation orders are employed is shown in Table II.

III. Star QAM Constellations

In the initial studies, SQAM was widely preferred in mobile radio applications. However, severe limitations of SQAM were observed over mobile radio channels (with multipath fading) [95]. Usually, SQAM required both the carrier recovery and AGC at the receiver. In the literature, mainly two AGC methods; averaging method and forced update method were adopted for SQAM. Both performed similarly poor, however, averaging method was preferred over the other, as it has no bandwidth overhead. There were some serious issues with carrier recovery as false locks were observed not only at multiple of 90^0, but also at $26+(l\times 90)$ and $52+(l\times 90)$ degrees with $l=0,1,2,3$ as highlighted in [95]. To improve the performance and to avoid the need of AGC and false lock problem, star QAM came into existence. Star QAM consists of multiple concentric PSK circles with equal constellation points in each circle and identical phase angle between them. Star QAM consists of 8 possible lock positions for lower order constellations (16 and 32-star QAM constellations) which increases for

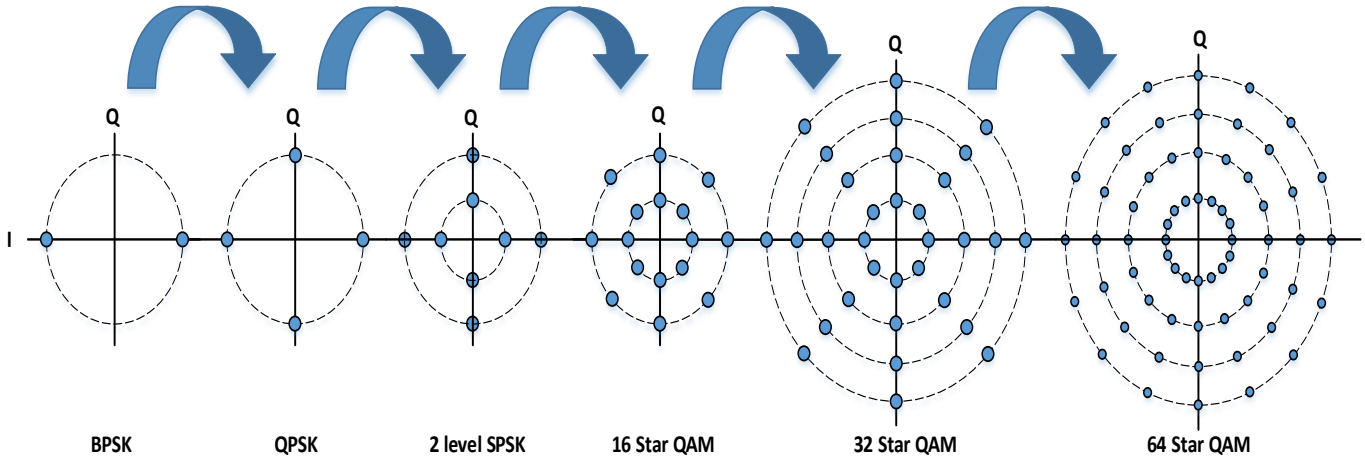

Fig. 4: Modeling of various star QAM constellations.

higher order constellations (64-star QAM constellation). All the constellation points are rotated with a fixed angle for these positions. After differential encoding, all the false lock problems can be eliminated. Modeling of various star QAM constellations is shown in Fig. 4.

A. Decision Regions

Decision regions for star-QAM are not straight-forward as compared with SQAM/RQAM regions. It does not consist of horizontal and vertical boundaries only. For decision making, inclined regions with some phase angles are also required. Let us consider 16 and 32-star QAM constellations. For decision making, initially, the entire constellation is divided into 8 sub-regions with phase angle $(2l+1)\times\pi/8$, for the constellation points situated at an phase angle of $l\times\pi/4$, where $l=0,1,...,7$. Then in each sub-region, the constellation points are separated by a boundary placed at the mid-point of the two nearby points. Hence, the decision boundaries for inner circle points are triangular regions and for mid circles points are trapezoidal regions. Decision boundaries are left open for the outer most circle points. For 16-star QAM constellation (Fig. 5 (left)), 4 bits are required to map 16 constellation points. Here, last 3 bits are used to show the change in phase angle, and remaining starting bits are used to represent the change in ring amplitudes. In this case, symbol decoding is converted into simple comparison between the current and previously decoded symbol. Let, the amplitude of inner and outer rings be r_i and r_o, respectively. Let, the received symbol amplitude are r_t and r_{t+1} at time instance t and $t+1$, respectively. Then the first bit is set to 1 only if [96]

$$\begin{aligned}\frac{r_{t+1}}{r_t} &> \frac{r_i+r_o}{2},\\ \frac{r_{t+1}}{r_t} &< \frac{2}{r_i+r_o},\end{aligned} \tag{1}$$

otherwise set to 0. If θ_t and θ_{t+1} are the phase angles of the received symbol at time instance t and $t+1$, respectively, then the demodulated angle will be [95]

$$\theta_{dem} = (\theta_{t+1}-\theta_t)\text{mod}2\pi. \tag{2}$$

Finally, the decoded angle is quantized to the closest multiple of $\pi/4$, and then a lookup table is prepared to decode the remaining bits. For 16 and 32 points star QAM constellations, decision regions are shown in Fig. 5. Similar procedure can be applied for the higher-order star QAM constellations.

B. SER Analysis

For an M-ary equiprobable digital modulation signal with arbitrary placement of constellation points in 2D plane, SEP expression over the additive white Gaussian noise (AWGN) channel can be given by the weighted sum of probabilities of each sub-regions for all the constellation points as [97]

$$\mathcal{P}_e = \sum_{u=1}^{N_S}\frac{\mu_u}{2\pi}\int_0^{\zeta_u}\exp\left[\frac{-a_u L^2\sin^2(\phi_u)}{N\sin^2(\theta+\phi_u)}\right]d\theta, \tag{3}$$

where N_S denotes the number of sub-regions, μ_u represents a priori probability that a symbol belongs to the u^{th} sub-region, and a_u, ζ_u, and ϕ_u are some important parameters related to the u^{th} sub-region for analysis which are shown in Fig. 6. Considering a 16-star QAM constellation for average SEP (ASEP) calculation as shown in Fig. 6. For analysis, perfect phase tracking is assumed at the receiver. Inner and outer ring's radius are denoted by r_i and r_o, respectively, which corresponds to a ring ratio $\mathbb{R}=r_i/r_o$. For symmetry, the ASEP is written in terms of error probabilities when symbol S_0 and S_{12} are transmitted as

$$\begin{aligned}\mathcal{P}_{S_0} &= \frac{1}{\pi}\sum_{u=1}^{2}\int_0^{\zeta_u}\exp\left[\frac{-L_u^2\sin^2(\phi_u)}{2N\sin^2(\theta+\phi_u)}\right]d\theta,\\ \mathcal{P}_{S_{12}} &= \frac{1}{\pi}\sum_{u=3}^{4}\int_0^{\zeta_u}\exp\left[\frac{-L_u^2\sin^2(\phi_u)}{2N\sin^2(\theta+\phi_u)}\right]d\theta,\end{aligned} \tag{4}$$

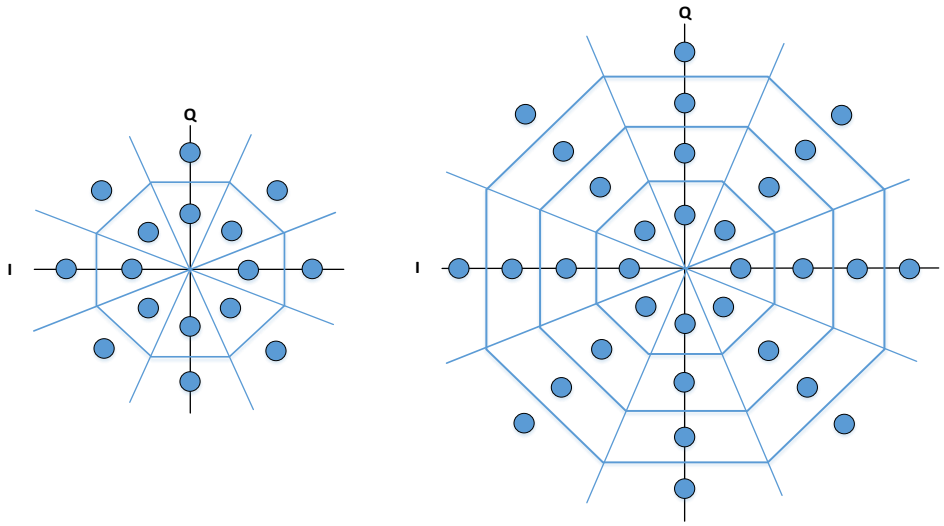

Fig. 5: Decision regions for 16-star QAM (left) and 32-star QAM (right) constellations.

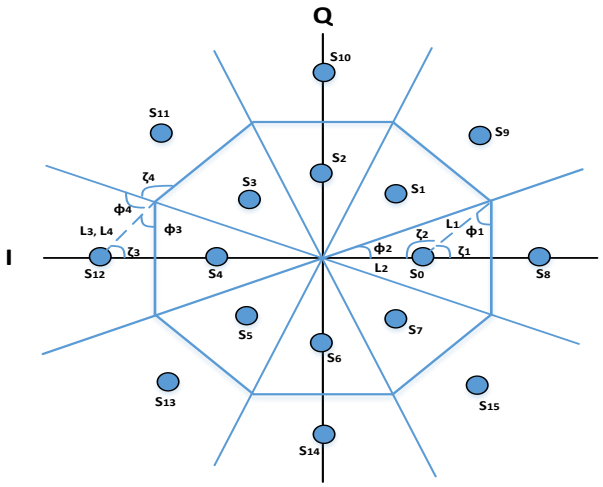

Fig. 6: 16-star QAM.

respectively, where L_u denotes the lengths (u = 1,...,4) as shown in Fig. 6. Thus, the ASEP expression of 16-star QAM can be given as [98]

$$\begin{aligned}\mathcal{P}_e =& \frac{1}{2\pi}\sum_{u=1}^{4}\int_0^{\zeta_u}\exp\left[\frac{-L_u^2\sin^2(\phi_u)}{2N\sin^2(\theta+\phi_u)}\right]d\theta,\\ =& \frac{1}{2\pi}\sum_{u=1}^{4}\int_0^{\zeta_u}\exp\left[\frac{-a_u L^2\sin^2(\phi_u)}{2N\sin^2(\theta+\phi_u)}\right]d\theta, \end{aligned} \quad (5)$$

where $\zeta_1 = \zeta_3 = \tan^{-1}\left[(\sqrt{2}-1)\frac{\mathbb{R}+1}{\mathbb{R}-1}\right]$, $\zeta_2 = (\pi-\zeta_1)$, $\zeta_4 = (7\pi/8-\zeta_1)$, $\phi_1 = \phi_3 = (\pi/2-\zeta_1)$, $\phi_2 = \pi/8$, $\phi_4 = (\pi/8+\zeta_1)$, $a_1 = a_3 = a_4 = \frac{1}{4}\left[(\mathbb{R}-1)^2+(\sqrt{2}-1)^2(\mathbb{R}+1)^2\right]$, $a_2 = 1$, and $\frac{L^2}{2N} = \frac{r_0^2}{2N} = \frac{8\gamma}{1+\mathbb{R}^2}$. Similar procedure can be followed for the higher order star QAM constellations.

C. Bit Mapping, Gray Code Penalty, and BER

Star QAM is a special case of circular APSK, where both the amplitude and phase of constellation points vary. It consists of multiple concentric PSK circles with equal constellation points in each circle. Further, there are total 8 possible phase angles for lower order constellations which increase with the constellation size. Constellation points in all the circles have identical phase angle between them. Let us consider 16 and 32-star QAM constellations whose bit mapping is shown in Fig. 7. As there are total 8 possible phase angles, last 3 bits of the bit stream are used to represent the phase angles. Remaining starting bits are used to represent the change in amplitude of the constellation points in the concentric circles. For 16-star QAM (Fig. 7, left), there are 2 concentric circles, each have 8 constellation points. There are total 8 phase angles $l \times \pi/4$ with $l = 0, 1, ..., 7$ [1]. Hence, the last 3 bits of the bit stream represent the change in phase angle by $\pi/4$ with the adjacent constellation point in the circle. If 000 is considered it means the symbol is transmitted with no phase change, if 001 is considered that means the signal is transmitted with $\pi/4$ phase shift than the previous symbol and so on. Remaining 1 bit (starting bit) represents the change in amplitude of the concentric circles. If first bit is 0, inner circles is selected, else outer circle is considered. For 32-star QAM (Fig. 7, right), there are 4 concentric circles, each have 8 constellation points. Hence, the starting 2 bits are used to represent the change in amplitude and the last 3 bits are used to show the change in phase. Similar procedure can be used for all the star QAM constellations. For 64-star QAM constellation, there are 16 possible lock positions. Hence, the last 4 bits of the 6 bits stream will be used to represent the change in phase, and the starting 2 bits denotes the change in amplitude ring.

In star QAM, each symbol shares its boundaries with maximum of 4 adjacent symbols (as can be seen from 32-

[1]The star QAM constellation can be rotated with any arbitrary angle, however, a fixed phase difference should be maintained between the adjacent constellation points in a circle.

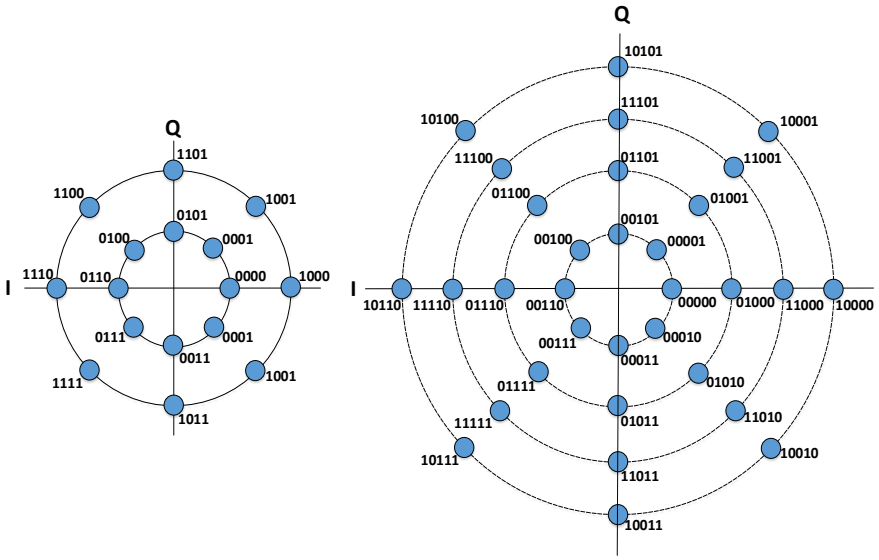

Fig. 7: Bit mapping for 16-star QAM (left) and 32-star QAM (right) constellations.

star QAM). The inner-most and outer-most ring symbols share their boundaries with 3 adjacent symbols. Hence, bit mapping is performed in such a manner that each symbol differ with maximum of 1 bit from its nearby symbol. Hence, star QAM constellations have perfect Gray coding, and their Gray code penalty (G_P) is 1. The G_p is introduced by Smith which is defined as the average bit difference between the two neighboring symbols in a constellation as

$$G_P = \frac{1}{M}\sum_{k=1}^{M} G_P^{s_k}, \tag{6}$$

where M represents the constellation order, s_k denotes the k^{th} data symbol, $G_P^{s_k}$ is the Gray code penalty of the k^{th} data symbol. For a given SEP, approximated BEP expression can be given as [27]

$$\mathcal{P}_b = G_P \frac{\mathcal{P}_s}{\log_2 M}, \tag{7}$$

where $\mathcal{P}_s$ represents the SEP which is given in (3) for the star QAM. Finally, from (7), the BEP of star QAM can be achieved.

However, if perfect coherent detection is assumed, the BER performance of SQAM is better than the star QAM as in [99], where BER performance of different 16 point constellations is compared. For the locally generated reference carrier, ambiguity arises in exact phase orientation due to the symmetric constellation which can be resolved through differential encoding. However, error propagation occurs in differentially encoded bits which degrades the BER performance. Still, the differential encoded SQAM (DE-SQAM) outperforms the star QAM which is explained mathematically in [99] for 16 point constellations.

In this work, comparative study of various QAM constellations with a fixed separation of $2d$ between the constellation points is presented. However, fixed separation of $2d$ between constellation points is not maintained in star QAM, and hence, its comparison with the other QAM constellations is not presented due to the lack of common platform.

IV. XQAM Constellations

For even bits per symbol, the transmitted signal is modulated with SQAM, whereas for odd bits per symbol, RQAM is commonly preferred. However, as discussed above, RQAM is not a good choice since RQAM constellations have high peak and average energies and hence, are power inefficient. To overcome this, Smith proposed a XQAM constellation which provides at least 1 dB gain over the RQAM constellations due to its reduced peak and average powers than RQAM [76]–[78]. If channel conditions are good, then instead of going for a constellation size of M from 2^{2n} to 2^{2n+2} as in SQAM, a more gradual increase from 2^{2n} to 2^{2n+1} is possible with XQAM which can adapt the channel conditions more efficiently than RQAM [41], [100]. Here n denotes the number of bits per symbol which can take any value greater than or equal to 2. For XQAM constellation, $M = 2^{2n+1}$, hence, $M = 32, 128, 512, 2048, ...$ are possible constellations with XQAM. Construction of 32-XQAM and 128-XQAM from 32-RQAM and 128-RQAM constellations are shown in Fig. 8. Here, corner points are shifted to top-and-bottom near the y-axis such that the peak and average energies of the constellation are reduced. In the following subsections, detailed study of the decision regions, SER, bit mapping, Gray code penalty, and BER of various XQAM constellations is presented.

A. Decision Regions

Decision regions for both SQAM and RQAM are quite straight-forward, since, in-phase and quadrature-phase bits have vertical and horizontal decision regions, respectively. However, only the horizontal and vertical decision regions are not sufficient for XQAM constellations. In XQAM, three types of symbols exist; edge symbols, corner symbols, and

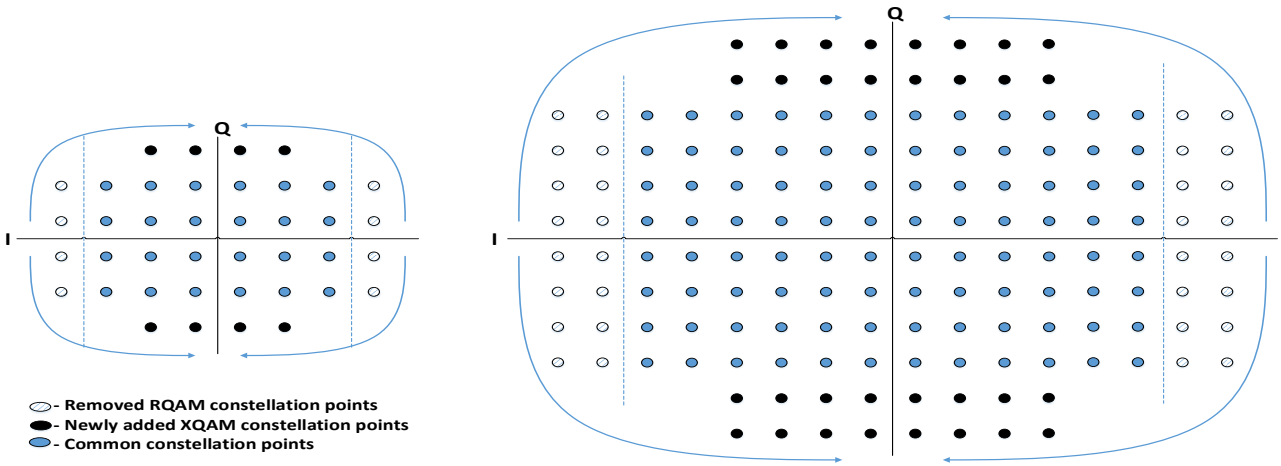

Fig. 8: 32-XQAM and 128-XQAM constellations.

interior symbols. As the XQAM constellations are symmetric around the origin, we consider only one quadrant for analysis which is shown in Fig. 9. Number of interior, edge, and corner

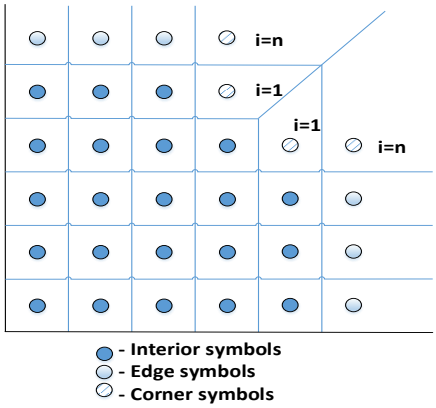

Fig. 9: Single quadrant of 128-XQAM constellation.

symbols/points in each quadrant are given as

$$\begin{aligned} N_{IS} &= (2n)^2 + 2(n-1)(2n-1), \\ N_{ES} &= 2(2n-1), \\ N_{CS} &= 2n, \end{aligned} \tag{8}$$

respectively. For XQAM constellations, the end columns symbols are moved to new cross type positions in the constellation. For interior symbols, decision regions are closed squares, however, for edge symbols, decision regions are semi-infinite rectangles. Decision regions for corner symbols are not straight-forward and consist of 45^0 lines along with the horizontal and vertical regions. As an example, we consider a 5 bits ($i_1 i_2 i_3 q_1 q_2$) 32-XQAM constellation. Decision regions for i_1 and q_1 bits are vertical and horizontal regions. However, for i_2, i_3, and q_2 bits, decisions regions are formed with horizontal, vertical, and 45^0 inclined regions, which is shown in Fig. 10. Similar procedure can be applied to obtain the decision regions for the other XQAM constellations.

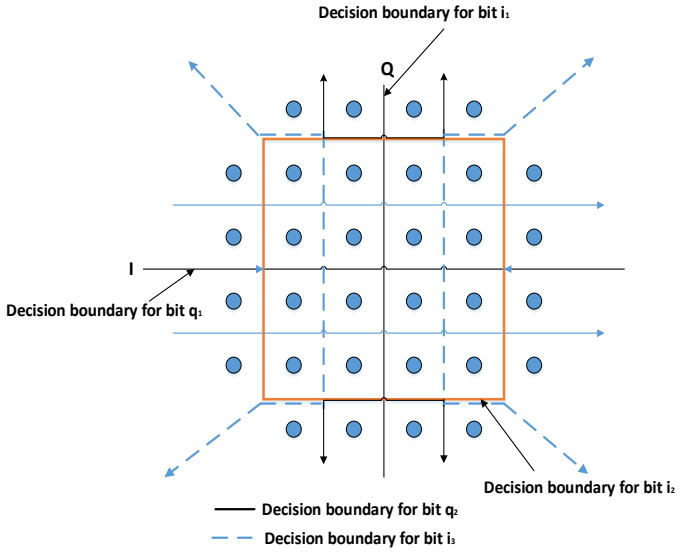

Fig. 10: Decision regions for 32-XQAM constellation.

B. SER Analysis

The 32-XQAM and 128-XQAM constellations are shown in Fig. 8. Here, corner points are shifted to top-and-bottom near the y-axis such that the peak and average energies of the constellation are reduced. For equiprobable constellation points, average symbol energy of XQAM is given as

$$\begin{aligned} E_{avg} &= \frac{4}{M}\left[2 \times 3n \sum_{i=1}^{3n} (2i-1)^2 d^2 - 2n \sum_{i=2n+1}^{3n} (2i-1)^2 d^2\right], \\ &= \frac{d^2}{\lambda}, \end{aligned} \tag{9}$$

where $\lambda = \frac{48}{31M-32}$. Thus, the SNR can be given as

$$\gamma = \frac{E_{avg}}{N_0} = \frac{d^2}{\lambda N_0} = \frac{\eta^2}{2\lambda}, \tag{10}$$

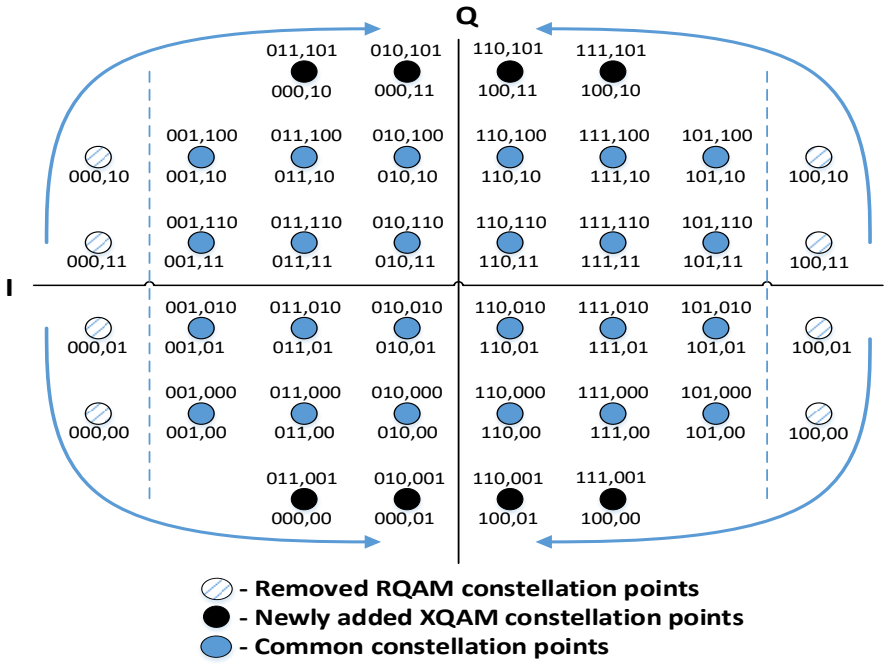

Fig. 11: Bit mapping of 32-XQAM constellation.

where $\eta = \frac{d}{\sqrt{N_0/2}}$ represents the minimum distance between a constellation point and decision boundary, $N_0/2$ denotes the two sided power spectral density of noise, and $\eta = \sqrt{2\lambda\gamma}$ from (10). For the interior and edge symbols, respective SEP expressions in terms of η can be given as [33]

$$\begin{aligned}\mathcal{P}_{IS} &= 1-(1-2Q(\eta))^2 = 4Q(\eta)-4Q^2(\eta),\\ \mathcal{P}_{ES} &= 1-(1-Q(\eta))(1-2Q(\eta)) = 3Q(\eta)-2Q^2(\eta),\end{aligned} \tag{11}$$

where $Q(\cdot)$ represents the Gaussian-Q function. SEP expressions for the i^{th} corner point from the bottom-to-top, or from left-to-right can be given as [41]

$$\begin{aligned}\mathcal{P}^i_{CP} &= 3Q(\eta)-2Q^2(\eta)+\mathbb{F}(i,\eta;\eta), \qquad i=1,2,...,n-1\\ \mathcal{P}^n_{CP} &= 2Q(\eta)-Q^2(\eta)+\mathbb{F}(n,\eta;\infty),\end{aligned} \tag{12}$$

where $\mathbb{F}(i,\eta,c_1) = \int_{\eta}^{c_1} Q(2i\eta+x)f(x)dx$, wherein $f(x) = 1/\sqrt{2\pi}e^{-x^2/2}$ represents the probability density function (PDF) of the standard normal distribution. Finally, considering all the points, exact average SEP for the generalized XQAM is given as

$$\begin{aligned}\mathcal{P}^{XQAM}(\eta) &= \frac{4}{M}\Big(N_{IP}\mathcal{P}_{IP}+N_{EP}\mathcal{P}_{EP}+2\sum_{i=1}^{n}\mathcal{P}^i_{CP}\Big)\\ &= \frac{4}{M}\Big((M-6n)Q(\eta)-(M-12n+2)Q^2(\eta)\\ &\quad +2\,\mathbb{F}(n,\eta;\infty)+2\sum_{i=1}^{n-1}\mathbb{F}(i,\eta;\eta)\Big).\end{aligned} \tag{13}$$

Finally, solving (13), the conditional SEP of general order XQAM constellation in AWGN channel can be given as [41]

$$\begin{aligned}\mathcal{P}^X_e(e|\gamma) = \Big[&g_1Q(\sqrt{2\lambda\gamma})+\frac{4}{M}Q(2\sqrt{\lambda\gamma})-g_2Q^2(\sqrt{2\lambda\gamma})\\ &-\frac{16}{M}\sum_{i=1}^{n-1}Q(\sqrt{2\lambda\gamma},\alpha_i^+)-\frac{8}{M}\sum_{i=1}^{n-1}Q(2i\sqrt{\lambda\gamma},\beta_i^+)\\ &+\frac{8}{M}\sum_{i=2}^{n}Q(2i\sqrt{\lambda\gamma},\beta_i^-)\Big],\end{aligned} \tag{14}$$

where $g_1 = 4-\frac{6}{\sqrt{2M}}$, $g_2 = 4-\frac{12}{\sqrt{2M}}+\frac{12}{M}$, $\alpha_i^+ = \arctan(\frac{1}{2i+1})$, for $i=1,...,n-1$
and $\beta_i^{\pm} = \arctan(\frac{i}{i\pm1})$, for $i=1,...,n$.
Further, $Q(x,\phi)$ is related to the 1D and 2D Gaussian Q-functions as

$$Q(x,\phi) = \frac{1}{\pi}\int_0^{\phi}\exp\Big(-\frac{x^2}{2\sin^2\theta}\Big)d\theta \qquad \text{for} \quad x\geq 0. \tag{15}$$

C. Bit Mapping, Gray Code Penalty, and BER

A detailed study about XQAM labeling is discussed in [27] and given for completeness. Binary and Gray codes for both the dimensions of an RQAM constellation are defined as

$$\begin{aligned}g^1_k &= b^1_k\\ g^l_k &= b^l_k \oplus b^{l-1}_k, \quad 1\leq k\leq (2^{n+1} \text{ or } 2^n),\\ &\qquad\qquad 1<l\leq (n \text{ or } n+1),\end{aligned} \tag{16}$$

where g^l_k and b^l_k represent the l^{th} bit of the k^{th} symbol of Gray and binary codes, respectively. However, these relationships are not valid in XQAM where the far left and far right columns symbols are shifted to a new position to form a cross structure. Hence, perfect Gray coding is not possible in XQAM. The

problem of modulation and labeling was solved by Smith [27] by adding one extra bit to create a $2n+2$ bits impure Gray coding. Here, this extra bit is not transmitted, however, it is only used for modulation and demodulation, and all the BER analysis is performed with $2n+1$ bits pseudo Gray codes. From Fig. 11, it is observed that with the use of the $2n+1$ bits pseudo Gray codes (5 bits Gray coding for 32-XQAM), topmost or bottom most blue colored symbols differ by 2 bits from its neighboring newly generated black symbols, however the other inner blue symbols only have one bit difference with its neighboring symbol. From Fig. 11, it is also observed that the $2n+1$ bits pseudo Gray codes are imperfect, and hence, G_p arise which is defined in (6). For example, G_p of 32-XQAM is calculated as

$$\begin{aligned} G_p = \frac{1}{32}\Big[&\frac{3}{2}+\frac{4}{3}+\frac{4}{3}+\frac{3}{2}+1+\frac{5}{4}+\frac{5}{4}+\frac{5}{4}+\frac{5}{4}+1+1 \\ &+1+1+1+1+1+1+1+1+1+1+1+1 \\ &+\frac{5}{4}+\frac{5}{4}+\frac{5}{4}+\frac{5}{4}+1+\frac{3}{2}+\frac{4}{3}+\frac{4}{3}+\frac{3}{2}\Big] \\ &= 1.166. \end{aligned} \tag{17}$$

As we increase the constellation order M, G_p increases accordingly. Hence, a generalized G_p for M-ary XQAM constellation can be given as $(1+\frac{1}{\sqrt{2M}}+\frac{1}{3M})$ [100]. Please note that, for a constellation with perfect Gray coding, G_p is always 1. In any constellation, bit mapping should be performed very precisely and carefully to minimize the BEP for a given SEP for the constellation. Finally, substituting the SEP given in (14) for XQAM, approximated BEP expression can be obtained. From (7), it is clear that the BEP is directly dependent on G_P since $\log_2 M$ is constant. Hence, optimum bit mapping is required to minimize the G_P for minimum BEP. Therefore, any other bit mapping results in higher G_p which increases the BEP accordingly.

V. HQAM Constellations

Energy efficient 2D signal constellation which can save considerable transmission energy is the most basic requirement of the present and future wireless communication systems. For a 2D signal constellation, SER is mainly affected by the minimum separation between the two neighboring constellation points, and average symbol energy which depends upon the mean squared distance of constellation points from the origin. Considering these points in mind, an optimum 2D hexagonal lattice based HQAM constellation is proposed where constellation points are situated at the center of the concentric spheres. For a minimum distance separation of $2d$ between the two adjacent constellation points in hexagonal constellation, area of the hexagonal region is $2\sqrt{3}d^2$ which is 0.866 times the area of the rectangle regions with the same dimensions. This allows hexagonal regions to provide around 0.6 dB gain over the rectangle regions [29]. HQAM is also termed as triangular QAM (TQAM) in the literature. Placement and separation of the constellation points on the 2D plane is same for both the HQAM and TQAM constellations. If the constellation is termed as HQAM, the constellation points are considered at the center of an equilateral hexagon and separated with the neighboring point hexagon with $2d$ distance. If the constellation is termed as TQAM, then the constellation points are considered at the vertices of well connected equilateral triangles of side-length $2d$. However, the decision boundaries are hexagonal shaped as shown in Fig. 12. Based on the placement of the constellation points, HQAM

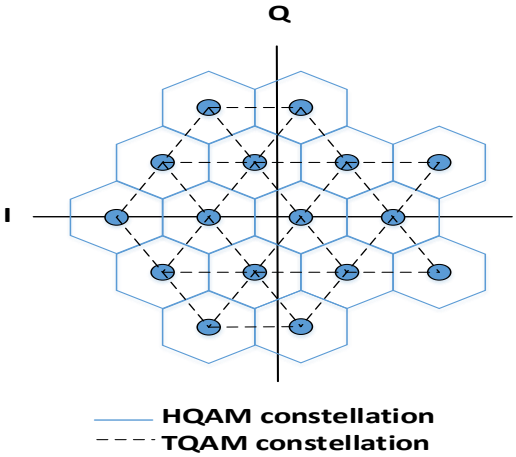

Fig. 12: 16-HQAM constellation.

constellations are further categorized into regular and irregular HQAM structures. Regular HQAM has comparatively simpler detection, its power efficiency or BER performance can further be improved for larger values of M. The irregular HQAM provides improved power efficiency and optimum performance, however, at the cost of increased detection complexity [101]. Since, the distance between the constellation points is equal, in the inner regions, the ML detection boundaries are in equilateral hexagonal shapes. However, at the boundaries, detection regions vary as per the constellation geometry. Constellation for regular HQAM, are symmetric around the origin [102], [103]. For, even power of 2, regular HQAM constellations are in square shapes [102] such as for $M = 16, 64, 256, 1024, ...$, however, for odd power of 2, regular HQAM constellations are in cross shapes [103] such as for $M = 32, 128, 512, ...$ For, irregular HQAM, constellations are in circular shapes as M increases which makes the irregular HQAM constellations more compact than others [104]. Various regular HQAM and irregular HQAM (optimum) constellations are shown in Fig. 13 and Fig. 14, respectively. Average energy of HQAM constellations is less than the SQAM constellations for any value of M except for $M = 4$. This is due to the fact, that 4-HQAM has same average energy of the constellation as 4-SQAM, however is having higher value of NNs. Further, irregular HQAM constellations have comparatively less average energy than the regular HQAM constellations, however, are more complex to generate and detect.

In the following subsection, generation of irregular HQAM from the regular HQAM constellation is explained.

1) Formation of Irregular HQAM (Optimum) Constellation from Regular HQAM: Process to generate an irregular HQAM (optimum) constellation (Fig. 15) is shown in Algorithm 1, where, d_{vs} represents the vertical spacing, E_c represents the energy of a constellation point, and $\mathbf{E}_c$ represents the array of

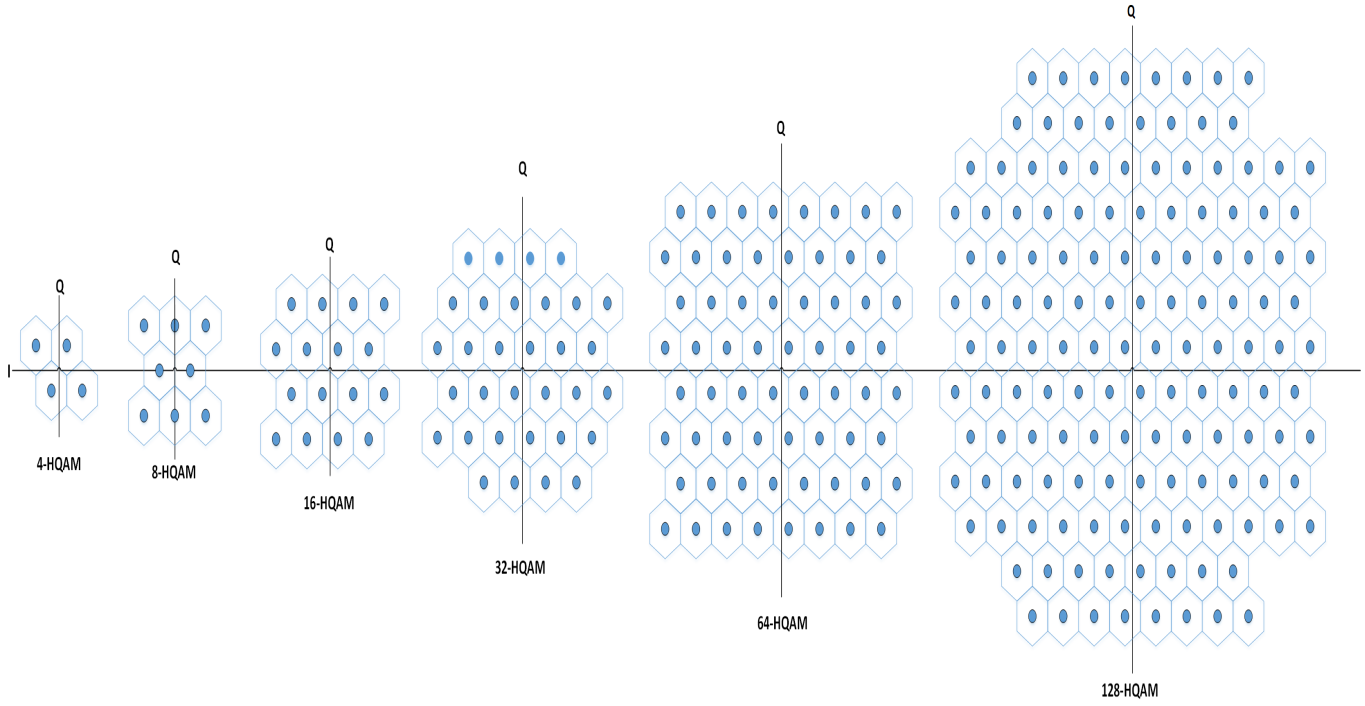

(a)

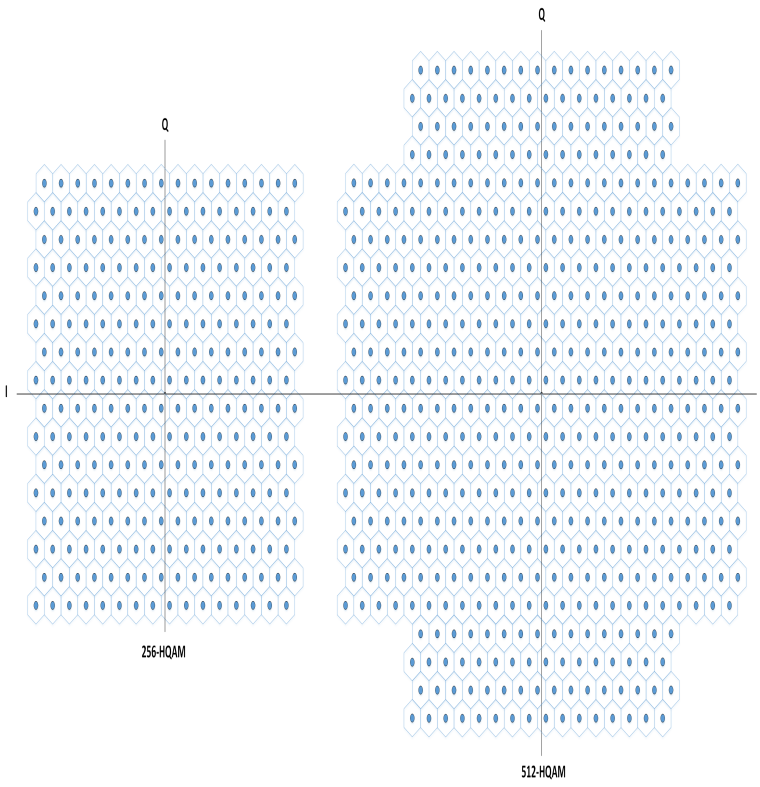

(b)

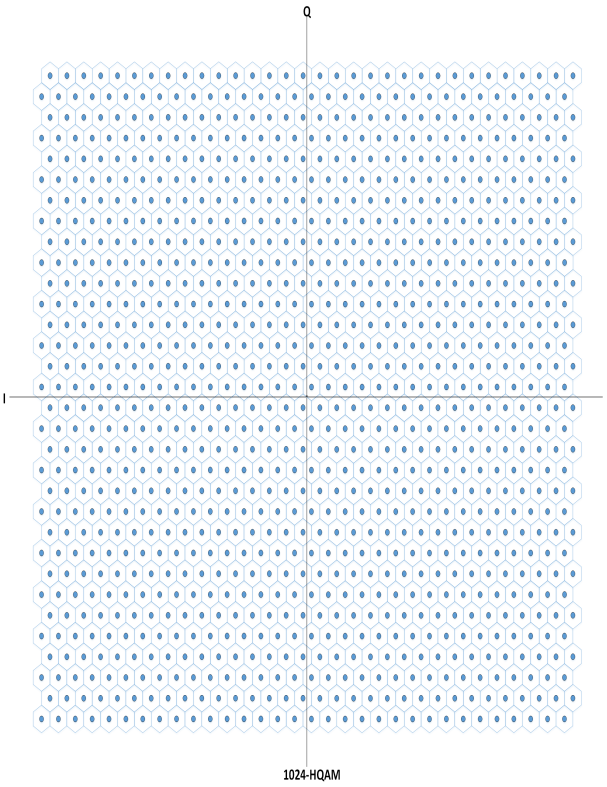

(c)

Fig. 13: Various regular HQAM constellations.

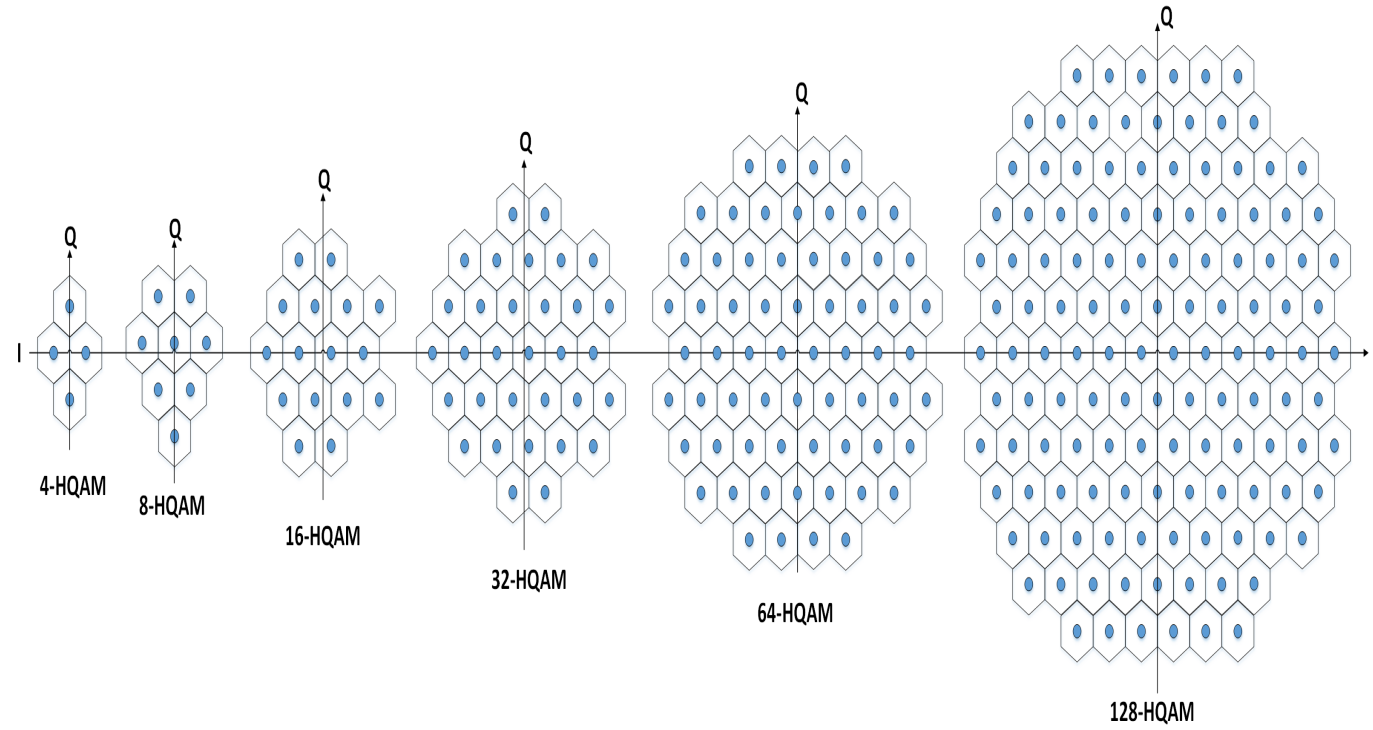

(a)

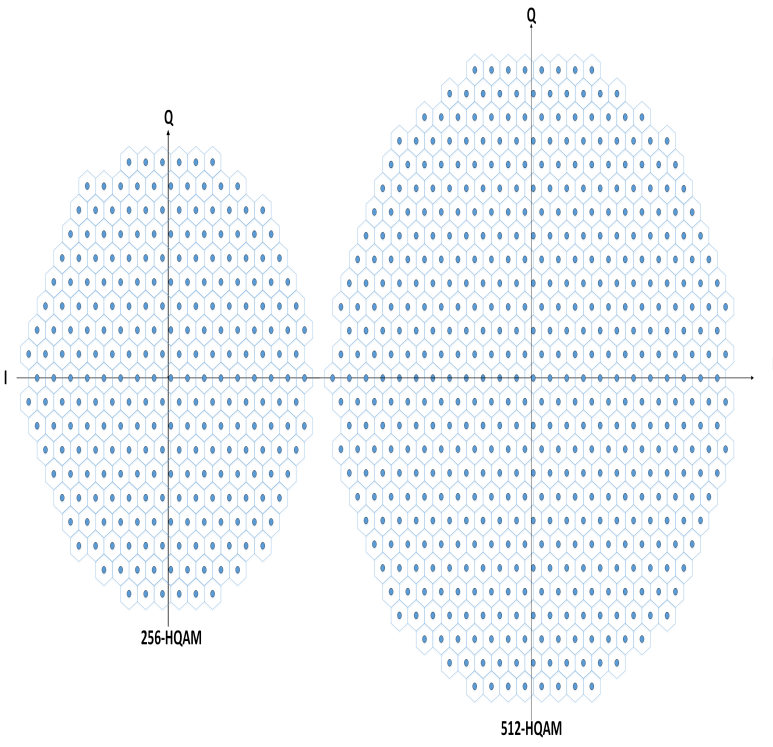

(b)

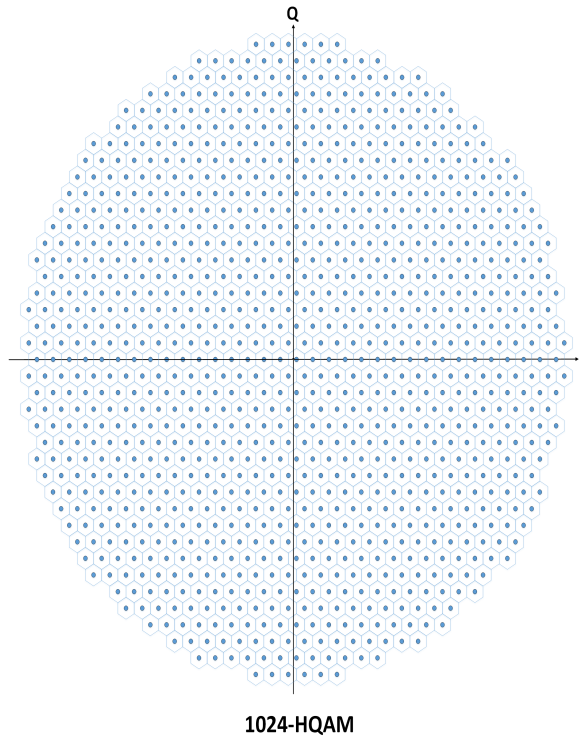

(c)

Fig. 14: Various irregular HQAM (optimum) constellations.

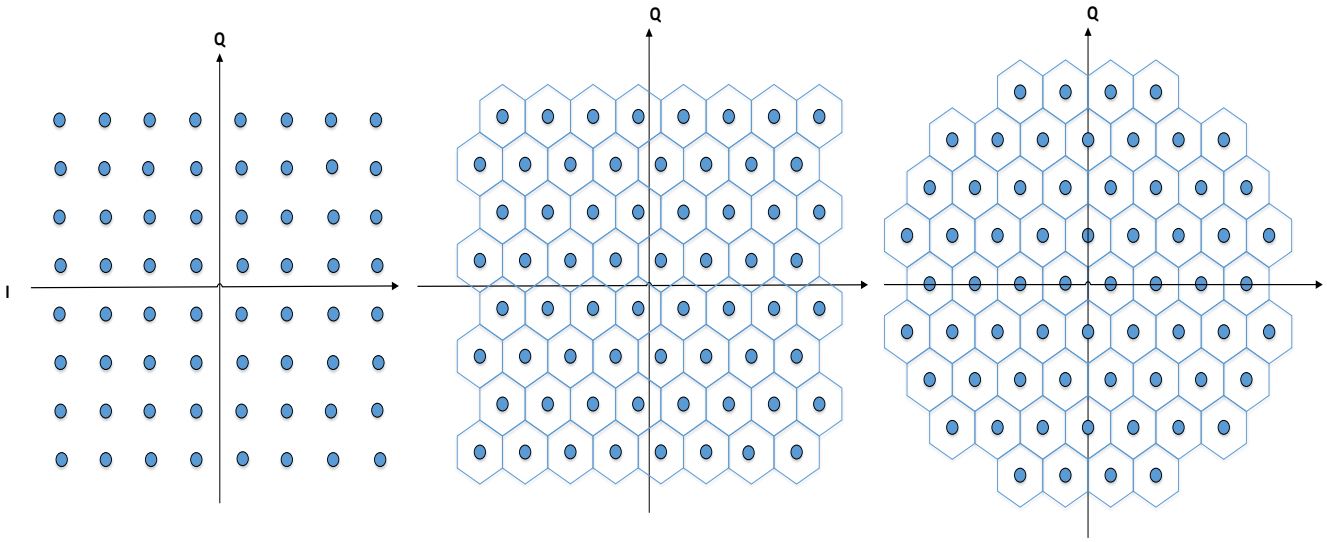

Fig. 15: Generation of optimum irregular HQAM constellation (M=64).

Algorithm 1 Irregular HQAM generation

1: **Inputs:**
M=number of constellation points.
2: **Initialize:**
Generate regular HQAM, set counter $l = 1$.
3: **if** $M \neq 8$ **then**
Shift one row of the generated regular HQAM to X-axis.
4: **else**
Shift one row of the generated regular HQAM to $\sqrt{3}/4$ distance above X-axis.
5: **end if**
6: Generate rows on both sides of the x-axis with $d_{vs} = \sqrt{3}$.
7: Identify center point of the constellation.
8: Calculate energy (E_c) of all probable constellation points and store it in an array $\mathbf{E}_c$.
9: **while** $\{l <= M\}$ **do**
10: Find $\underbrace{\min}_{1 \leq j \leq M}$ $\mathbf{E}_c(j)$, and place the constellation point at the coordinates of j^{th} index.
11: $l = l + 1$.
12: **end while**

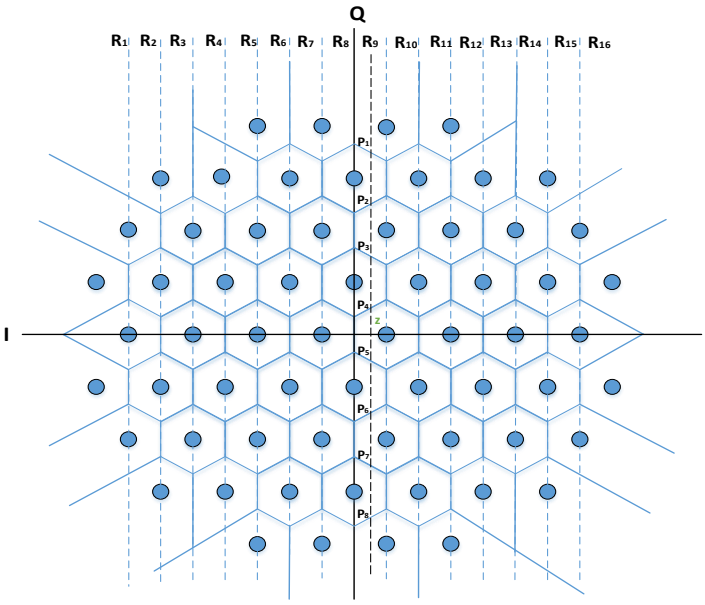

Fig. 16: Simplified detection method for irregular 64-HQAM constellation.

constellation points energies.

A. Decision Regions

ML detection is the most popularly used detection scheme where distance between each signal point and the received symbol is calculated, and decision (as an estimate of the transmitted symbol) is made to the nearest symbol. ML detection has less detection complexity however, is not applicable for HQAM detection in a straight-forward manner. Thus, an optimum and simple detection scheme for HQAM constellations is proposed where entire constellation is initially divided into vertical regions. A signal point is first located in a region and then the nearest constellation point in that region is found. This process ultimately reduces the number of distance calculations as compared to the traditional ML detection scheme [102]. In Fig. 16, a simplified detection technique for 64-ary irregular HQAM constellation is shown which is explained as follows. Initially, the entire constellation is divided into $R_1 - R_{16}$ regions. When a symbol, lets say $z = x + iy$ is received (where x and y are the constant values and $j = \sqrt{-1}$), based on the the arbitrary value x, one of the sixteen regions is selected. Further, imaginary values for the decision points are calculated and decision for a symbol is made with a comparison between the imaginary value y of the demodulated symbol and calculated imaginary boundaries. For different regions, calculated imaginary boundaries are shown in Table IV. For illustration, depending on the arbitrary value of x, initially a region (R_9) is selected for the demodulated symbol z as shown in Fig. 16. Next, to detect 9 signaling points which

TABLE III: Imaginary values of boundary points for region R_9.

$\text{Im}(P_1)$	$\text{Im}(P_2)$	$\text{Im}(P_3)$	$\text{Im}(P_4)$	$\text{Im}(P_5)$	$\text{Im}(P_6)$	$\text{Im}(P_7)$	$\text{Im}(P_8)$
$\frac{11d-x}{\sqrt{3}}$	$\frac{7d+x}{\sqrt{3}}$	$\frac{5d-x}{\sqrt{3}}$	$\frac{d+x}{\sqrt{3}}$	$-\left(\frac{d+x}{\sqrt{3}}\right)$	$-\left(\frac{5d-x}{\sqrt{3}}\right)$	$-\left(\frac{7d+x}{\sqrt{3}}\right)$	$-\left(\frac{11d-x}{\sqrt{3}}\right)$

TABLE IV: Imaginary values of boundary points for various vertical regions.

	R_9, R_8	R_{10}, R_7	R_{11}, R_6	R_{12}, R_5	R_{13}, R_4	R_{14}, R_3	R_{15}, R_2	R_{16}, R_1
$\text{Im}(P_1)$	$\left(\frac{11d-x}{\sqrt{3}}\right)$	$\left(\frac{10d+x}{\sqrt{3}}\right)$	$\left(\frac{13d-x}{\sqrt{3}}\right)$	$\left(\frac{10d+x}{\sqrt{3}}\right)$	$\left(\frac{11d+x}{\sqrt{3}}\right)$	-	-	-
$\text{Im}(P_2)$	$\left(\frac{7d+x}{\sqrt{3}}\right)$	$\left(\frac{9d-x}{\sqrt{3}}\right)$	$\left(\frac{7d+x}{\sqrt{3}}\right)$	$\left(\frac{11d-x}{\sqrt{3}}\right)$	$\left(\frac{7d+x}{\sqrt{3}}\right)$	$\left(\frac{13d-x}{\sqrt{3}}\right)$	$\left(\frac{7d+x}{\sqrt{3}}\right)$	$\left(\frac{x+d}{\sqrt{3}}\right)$
$\text{Im}(P_3)$	$\left(\frac{5d-x}{\sqrt{3}}\right)$	$\left(\frac{4d+x}{\sqrt{3}}\right)$	$\left(\frac{7d-x}{\sqrt{3}}\right)$	$\left(\frac{4d+x}{\sqrt{3}}\right)$	$\left(\frac{9d-x}{\sqrt{3}}\right)$	$\left(\frac{4d+x}{\sqrt{3}}\right)$	$\left(\frac{11d-x}{\sqrt{3}}\right)$	$\left(\frac{x-3d}{\sqrt{3}}\right)$
$\text{Im}(P_4)$	$\left(\frac{d+x}{\sqrt{3}}\right)$	$\left(\frac{3d-x}{\sqrt{3}}\right)$	$\left(\frac{x-d}{\sqrt{3}}\right)$	$\left(\frac{5d-x}{\sqrt{3}}\right)$	$\left(\frac{x-3d}{\sqrt{3}}\right)$	$\left(\frac{7d-x}{\sqrt{3}}\right)$	$\left(\frac{x-5d}{\sqrt{3}}\right)$	$\left(\frac{9d-x}{\sqrt{3}}\right)$
$\text{Im}(P_5)$	$-\left(\frac{d+x}{\sqrt{3}}\right)$	$-\left(\frac{3d-x}{\sqrt{3}}\right)$	$-\left(\frac{x-d}{\sqrt{3}}\right)$	$-\left(\frac{5d-x}{\sqrt{3}}\right)$	$-\left(\frac{x-3d}{\sqrt{3}}\right)$	$-\left(\frac{7d-x}{\sqrt{3}}\right)$	$-\left(\frac{x-5d}{\sqrt{3}}\right)$	$-\left(\frac{9d-x}{\sqrt{3}}\right)$
$\text{Im}(P_6)$	$-\left(\frac{5d-x}{\sqrt{3}}\right)$	$-\left(\frac{4d+x}{\sqrt{3}}\right)$	$-\left(\frac{7d-x}{\sqrt{3}}\right)$	$-\left(\frac{4d+x}{\sqrt{3}}\right)$	$-\left(\frac{9d-x}{\sqrt{3}}\right)$	$-\left(\frac{4d+x}{\sqrt{3}}\right)$	$-\left(\frac{11d-x}{\sqrt{3}}\right)$	$-\left(\frac{x-3d}{\sqrt{3}}\right)$
$\text{Im}(P_7)$	$-\left(\frac{7d+x}{\sqrt{3}}\right)$	$-\left(\frac{9d-x}{\sqrt{3}}\right)$	$-\left(\frac{7d+x}{\sqrt{3}}\right)$	$-\left(\frac{11d-x}{\sqrt{3}}\right)$	$-\left(\frac{7d+x}{\sqrt{3}}\right)$	$-\left(\frac{13d-x}{\sqrt{3}}\right)$	$-\left(\frac{7d+x}{\sqrt{3}}\right)$	$-\left(\frac{x+d}{\sqrt{3}}\right)$
$\text{Im}(P_8)$	$\left(\frac{11d-x}{\sqrt{3}}\right)$	$-\left(\frac{10d+x}{\sqrt{3}}\right)$	$-\left(\frac{13d-x}{\sqrt{3}}\right)$	$-\left(\frac{10d+x}{\sqrt{3}}\right)$	$-\left(\frac{11d+x}{\sqrt{3}}\right)$	-	-	-

lie in R_9 region, 8 boundary points ($P_1 - P_8$) are marked on the dotted line and their imaginary values are calculated to estimate a signaling point out of the 9 signaling points. The imaginary values of 8 boundary points for R_9 region are shown in Table III. Following similar procedure for the other regions, imaginary values for the boundaries points are calculated and summarized in Table IV. Similar procedure can be followed for the other HQAM constellations for symbol detection. For various irregular HQAM constellations (M varies from 4 to 1024), decision regions are shown in Fig. 17.

B. SER Analysis

Let us consider a set $S_M \in \{s_0, s_1, ..., s_{M-1}\}$ for M-ary HQAM constellation. SEP for HQAM constellation is based on the shape of the decision regions. For this, a suitable correction to NN approximation is applied [105] which is expressed as

$$\mathcal{P}_{NN} = \tau Q\Big(\frac{d}{2\sigma}\Big). \tag{18}$$

Here τ represents the average number of NNs and is defined as $\tau = \frac{1}{M}\sum_{k=0}^{M-1}\tau(k)$ wherein $\tau(k)$ is the number of NNs for k^{th} symbol s_k, $Q(\cdot)$ represents the Gaussian Q-function, d is the half the distance between constellation points, and σ is the AWGN standard deviation. For illustration, simplest HQAM structure is the 3-PSK structure as shown in Fig. 18. The 3-PSK consists of three symbols s_0, s_1, and s_2. Starting with s_0 which has two NNs s_1 and s_2. s_1 is also an NN of s_2. Thus, s_1 and s_2 are the couple of NNs of s_0. Two half planes with partial overlapping cover the error region in NN approximation which produces an overestimation of SEP. This can be clarified from Fig. 18. Thus, exact SEP expression for 3-PSK is given as

$$\mathcal{P}^{\text{3-PSK}} = 2Q\Big(\frac{d}{2\sigma}\Big) - C_1, \tag{19}$$

where C_1 is a correction term, used to compensate for the double counting of overlapping. For 3-PSK, C_1 is given in [33]. However, for simplification, integral can be avoided and C_1 is approximated with C_2 as [106]

$$C_1 \approx C_2 = 2Q\Big(\frac{d}{2\sigma}\Big)Q\Big(\frac{d}{2\sqrt{3}\sigma}\Big) - \frac{2}{3}Q^2\Big(\frac{d}{\sqrt{6}\sigma}\Big). \tag{20}$$

Hence, approximate SEP expression for 3-PSK can be given as

$$\mathcal{P}^{\text{3-PSK}} = 2Q\big(d/2\sigma\big) - C_2. \tag{21}$$

This correction approach is easily applicable for generalized HQAM constellation. In HQAM, multiple overlaps with a $2\pi/3$ angle occur which generate couple of NNs. Therefore, for AWGN channel, approximate SEP expression for HQAM can be given as

$$\mathcal{P}^{HQAM} = \tau Q\Big(\frac{d}{2\sigma}\Big) - \tau_c C_2, \tag{22}$$

where $\tau_c = \frac{1}{M}\sum_{k=0}^{M-1}\tau_c(k)$ is the average of couple of NNs, wherein $\tau_c(k)$ represents couple of NNs for s_k symbol. Further, considering $K = \frac{1}{\gamma}\big(\frac{d}{2\sigma}\big)^2$ with average transmit SNR $\gamma = P_s/N_0$, and substituting C_2 from (20) in (22), generalized conditional SEP of HQAM is given as

$$\mathcal{P}^{HQAM}(e|\gamma) = \tau Q(\sqrt{K\gamma}) - 2\tau_c Q(\sqrt{K\gamma})Q\Big(\sqrt{\frac{K\gamma}{3}}\Big) + \frac{2}{3}\tau_c Q^2\Big(\sqrt{\frac{2K\gamma}{3}}\Big). \tag{23}$$

Here, K is related to the average energy of the constellation which varies with M. Further, τ and τ_c are the average number of NNs and couple of NNs, respectively, which also vary according to M. Various regular HQAM constellations and irregular HQAM constellations (optimum) are shown in Fig. 13 and Fig. 14, respectively. Based on the constellations (regular or irregular HQAM) and modulation order M; different values of K, τ, and τ_c are given in Table V which are used to select various HQAM constellations with different constellation orders.

For a well connected HQAM, $\tau_c = 3T/M$, where T represents the number of equilateral triangles with sides of

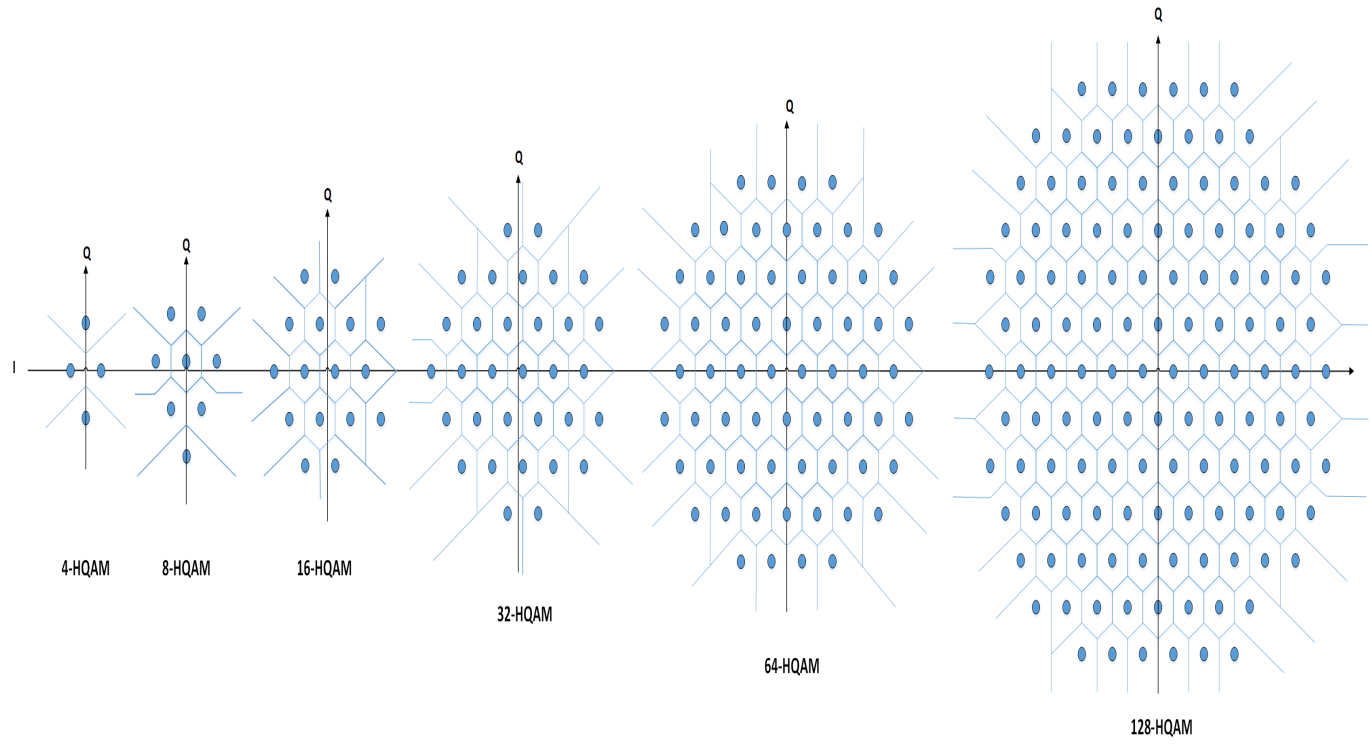

(a)

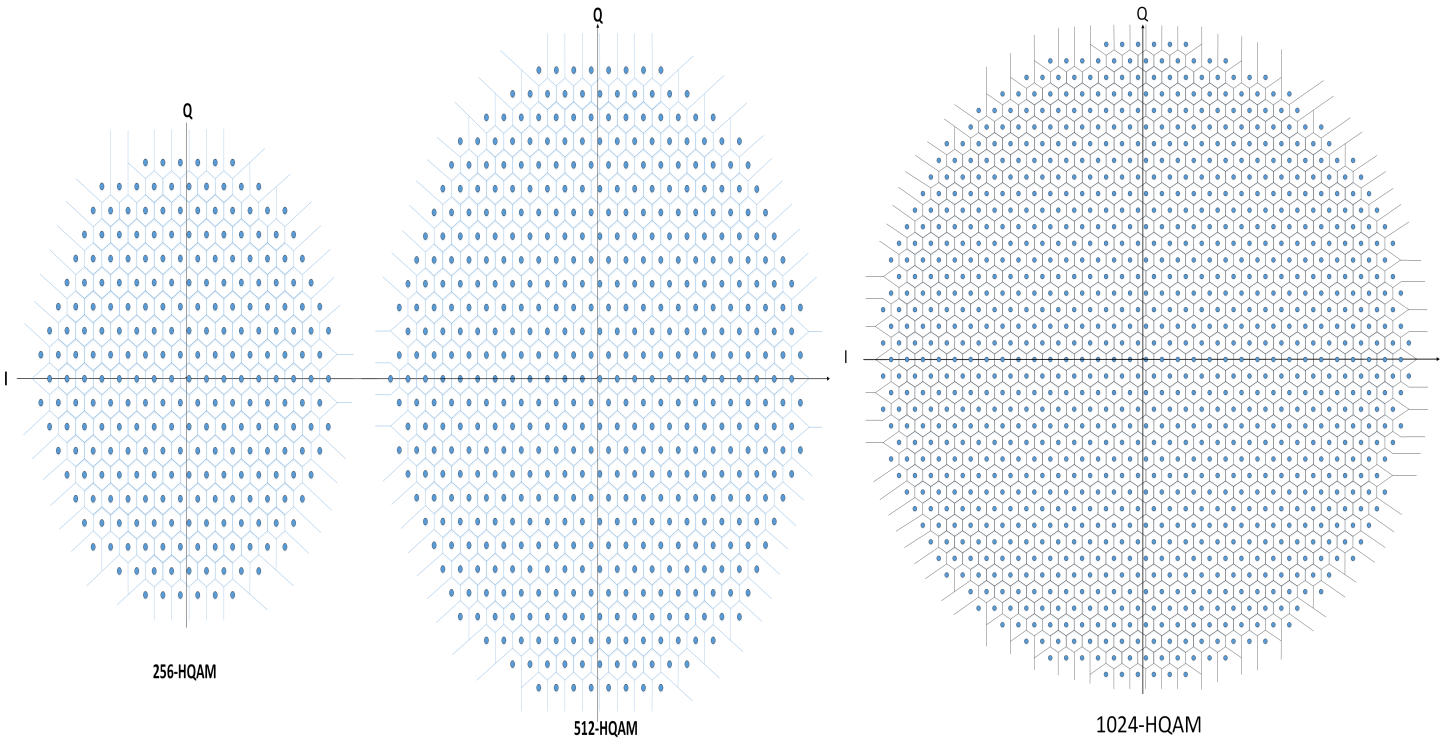

(b) (c)

Fig. 17: Various irregular HQAM (optimum) constellations with their decisions boundaries.

TABLE V: Different parameters for the various regular and irregular HQAM constellations over the AWGN channel.

	Regular HQAM						Irregular HQAM (optimum)					
M	K	τ	τ_c	E_s/d^2	PAPR	G_p	K	τ	τ_c	E_s/d^2	PAPR	G_p
4	1	$\frac{5}{2}$	$\frac{3}{2}$	2	1.5	1.166	1	$\frac{5}{2}$	$\frac{3}{2}$	2	1.5	1.166
8	$\frac{2}{6}$	$\frac{7}{2}$	$\frac{21}{8}$	6	2.16	1.275	$\frac{32}{69}$	$\frac{7}{2}$	$\frac{21}{8}$	4.3125	2.130	–
16	$\frac{2}{9}$	$\frac{33}{8}$	$\frac{27}{8}$	9	2.11	1.237	$\frac{8}{35}$	$\frac{33}{8}$	$\frac{27}{8}$	8.75	1.742	1.27
32	$\frac{8}{71}$	$\frac{75}{16}$	$\frac{33}{8}$	17.75	2.084	1.388	$\frac{512}{4503}$	$\frac{75}{16}$	$\frac{33}{8}$	17.59	1.8792	–
64	$\frac{2}{37}$	$\frac{161}{32}$	$\frac{147}{32}$	37	2.51	1.2822	$\frac{8}{141}$	$\frac{163}{32}$	$\frac{75}{16}$	35.25	1.90	1.351
128	$\frac{2}{72}$	$\frac{339}{64}$	$\frac{159}{32}$	72	2.347	1.363	$\frac{2}{70.56}$	$\frac{343}{64}$	$\frac{81}{16}$	70.562	1.96	1.48
256	$\frac{2}{149}$	$\frac{705}{128}$	$\frac{675}{128}$	149	2.74	–	$\frac{2}{141}$	$\frac{711}{128}$	$\frac{171}{32}$	141	2.03	–
512	$\frac{2}{289.06}$	$\frac{2895}{512}$	$\frac{5619}{1024}$	289.06	2.535	–	$\frac{200}{28217}$	$\frac{2911}{512}$	$\frac{5667}{1024}$	282.17	2.01	–
1024	$\frac{2}{597}$	$\frac{2945}{512}$	$\frac{2883}{512}$	597	2.86	–	$\frac{100}{28227}$	$\frac{2955}{512}$	$\frac{1449}{256}$	564.54	1.99	–

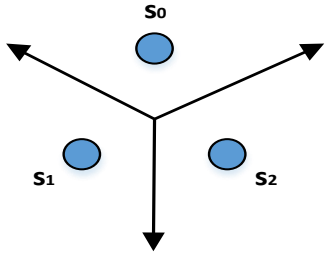

Fig. 18: 3-PSK constellation.

length $2d$, and $\tau = 2\left[\frac{\tau_c}{3} + 1 - \frac{1}{M}\right]$ [107]. For regular HQAM with even power of 2 constellations, $K = \frac{24}{7M-4}$, $\tau = 2\left(3 - \frac{4}{\sqrt{M}} + \frac{1}{M}\right)$, and $\tau_c = 6\left(1 - \frac{1}{\sqrt{M}}\right)^2$. However, for an arbitrary power of 2 constellation, no such pattern can be found in the literature for different values of K, τ, and τ_c for both regular and irregular HQAM constellations. A detailed study on various HQAM or TQAM constellations can be seen in [29], [101], [103]–[105], [107]. Solving the equations given for K, τ, and τ_c, generalized approximate values of K, τ, and τ_c, for a well connected M-ary irregular HQAM can be given as

$$\begin{aligned} K &= \frac{7}{2M-1}, \\ \tau &= 6.07 - 6.733M^{-0.456}, \\ \tau_c &= 3\left[\frac{\tau}{2} - 1 + \frac{1}{M}\right]. \end{aligned} \tag{24}$$

C. Bit Mapping, Gray Code Penalty, and BER

BER performance is significantly affected by the bit mapping of the constellation points. For an M- ary constellation, bit mapping should be done such that the bit difference between the neighboring points is minimum. The optimum bit mapping is achieved with the least average number of bit difference between neighboring symbols. In SQAM, each constellation point shares its boundaries with maximum 4 constellation points and differ with its neighbors by only a single bit. Thus, SQAM has the perfect Gray coding and its G_P is always 1 [108]. However, for HQAM, perfect Gray mapping is not possible [109], since each symbol shares its boundaries with maximum of six neighboring symbols. This generates G_P which is expressed as

$$\begin{aligned} G_P &= \frac{1}{M}\sum_{k=1}^{M} G_P^{s_k}, \\ &= \frac{1}{M}\sum_{k=1}^{M} \frac{\sum_{j=1}^{N(s_k)} b_d(s_k, s_j)}{N(s_k)}, \end{aligned} \tag{25}$$

where s_k denotes the k^{th} data symbol, $G_P^{s_k}$ is the Gray code penalty of k^{th} data symbol, $b_d(s_k, s_j)$ represents the bit difference of k^{th} data symbol with its neighboring symbol s_j, and $N(s_k)$ is the NN count of k^{th} data symbol s_k.

In any constellation, bit mapping should be performed very precisely and carefully to minimize the BEP for a given SEP for the constellation. For a given SEP, approximated BEP expression is given in (7) which is directly proportional to G_P. Hence, optimum bit mapping is required to minimize G_P to get minimum BER. Optimum bit mapping can only be obtained with exhaustive search over all the possible bit mappings for the constellation. Further, it should be noticed that there is not an unique optimum bit mapping, others may exist which have the same G_P. Practically, for an M-ary signal constellation, there are $M!$ bit mappings and finding an optimum bit mapping for optimum G_P for a large signal constellation is extremely tedious and time consuming. Thus, a sub-optimum bit mapping is preferred for a signal constellation with $M > 16$. For an M-ary signal constellation, each symbol is represented with n bits, and 2^n bit streams appear to represent all the symbols in the constellation. In practice, a sub-optimum bit mapping is preferred which is performed in three steps. Initially, regular HQAM constellations are generated with the same bit mapping as preferred for SQAM (or RQAM) constellations. Further, irregular HQAM constellations are generated by shifting the regular HQAM constellations such that the maximum signal points get matched on I/Q coordinates. Next, for the matched signaling points of irregular HQAM, the same bit mapping is preferred as used for regular HQAM constellation. Finally, for the remaining symbols, a partially optimized bit mapping is considered where each symbol picks its favorable NNs symbols from the available ones such that it has minimum

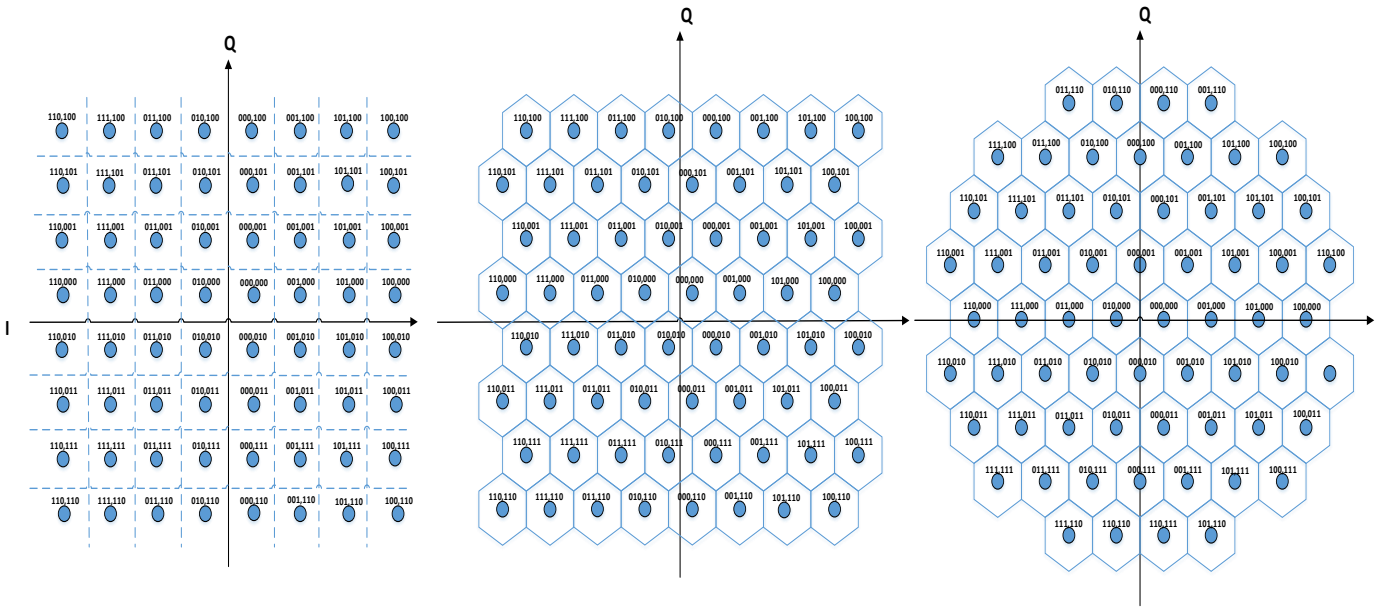

Fig. 19: Bit mapping for 64-HQAM.

TABLE VI: Comparison of various QAM constellations.

	SQAM		RQAM		XQAM		Regular HQAM		Irregular HQAM (optimum)	
M	E_s/d^2	PAPR	E_s/d^2	PAPR	E_s/d^2	PAPR	E_s/d^2	PAPR	E_s/d^2	PAPR
4	2	1	-	-	-	-	2	1.5	2	1.5
8	-	-	6	1.666	-	-	4.5	1.55	4.312	2.13
16	10	1.80	-	-	-	-	9	2.11	8.75	1.742
32	-	-	26	2.23	20	1.70	17.75	2.084	17.59	1.879
64	42	2.333	-	-	-	-	37	2.51	35.25	1.90
128	-	-	106	2.584	82	2.073	72	2.347	70.56	1.96
256	170	2.647	-	-	-	-	149	2.74	141.023	2.03
512	-	-	426	2.784	330	2.28	290	2.494	282.17	2.01
1024	682	2.81	-	-	-	-	597	2.86	564.54	1.99

bit difference with its NNs. As an example, for $M = 64$, bit mapping for irregular HQAM is shown in Fig. 19. For $M = 64 = 2^6$, 6 bits are required for mapping. Initially, 8 rows and 8 columns are selected, and 3 bits are assigned to represent the rows and rest of the 3 bits represent columns. Lower three bits represent the rows and upper three bits represent the columns. Bit mapping for irregular HQAM is completed in three steps. In the first step, regular HQAM is formed similar to SQAM formation. The same bit mapping is adopted for regular HQAM constellation as preferred by SQAM constellation. Further, irregular HQAM constellation is formed with a little shift in constellation points of regular HQAM on I/Q plane. For the matched points in irregular HQAM constellation, the same bit mapping is preferred as in regular HQAM constellation. Finally, for the remaining points, a sub-optimum bit mapping is performed by considering that s_k consists of the NNs with minimum G_P from the available signaling points. Thus, the G_P for irregular 64-HQAM is 1.35. Finally, substituting G_P and SER in (7), approximate BER expression for HQAM can be obtained. As the G_P of regular and irregular HQAM constellations are always greater than 1, the bit error performance of HQAM constellations is always poor as compared to the symbol error performance because G_P of SQAM constellations is always 1.

D. Comparison of Irregular HQAM Constellation with Other QAM Constellations

A comparative analysis between the irregular HQAM and other QAM constellations for different constellation orders is illustrated through Table VI. Here, a fixed Euclidean distance of $2d$ is maintained between the neighborhood constellation points for all the constellations and their average constellation energy or power and PAPR are calculated. From the Table VI, it can be concluded that for all the constellation orders (even as well as odd bits constellations), irregular HQAM has the reduced peak and average energies or powers. Hence, irregular HQAM can be concluded as the optimum constellation which provides better ASER performance than the other constellations. For various cooperative relay networks, this can be verified in [77], [78], [110], [111].

VI. Probabilistic Shaping

The development of optical transport networks is pushed forward due to the growing demands of Internet traffic in past decades. Advanced modulation schemes (specially the family of QAMs) are adopted for better spectral efficiency; and various multiplexing techniques are implemented for improved capacity. It is observed, for transmission and detection in the

modern day optical networks, usually uniform QAM constellations are used which results in a loss of around 1.53 dB gain towards the Shannon limit [112]. However, the Shannon limit can be achieved by implementing shaping and coding techniques. Shaping gain can be achieved through probabilistic and geometric amplitude shaping. In uniform QAM constellation, all the constellation points are equiprobable and equidistant on the 2D plain. However, in geometrically shaped QAM, constellation points are non-equidistant on 2D plain, whereas in probabilistically shaped QAM, constellation points are non-equiprobable on 2D plain. In this work, all the constellations discussed in the previous sections are geometrically shaped. However, we can further improve their performance by probabilistic shaping. Considerable works on the probabilistically shaped QAM constellations are observed in the literature. Works on the comparative study of both the probabilistically and geometrically shaped QAM constellations are presented below.

In [113], [114], probabilistically shaped QAM constellations are compared with the uniform QAM constellations for the optical communication system. In [115], for equidistant constellation points, probabilistic amplitude shaping is applied to bipolar ASK which is applied to SQAM. In [116], for non-linear fiber channel, probabilistic shaping of QAM is performed. In [117], for AWGN channel, both the geometric and probabilistic shaping are studied. In [118], generalized pairwise optimization scheme is reviewed for geometrically and probabilistically shaped constellations. In [112], [119], [120], comparison to geometrically shaped QAM; the probabilistically shaped QAM is presented for optical communication system. Most of the works focus on the probabilistic and geometric shaping in optical communication system, however, this can also be implemented in wireless systems for improved power efficiency along with the spectral efficiency.

VII. Application of QAM Constellations in Wireless Communication Systems

The QAM was first proposed by C. R. Cahn [19] in 1960 and later extended by Hancock and Lucy in [20], who termed Type I to the Cahn's constellation and Type II to their proposed constellation. Later in 1962, Campopiano and Glazer proposed properly organized square QAM constellation and denoted it as Type III constellation [21]. There were some initial works [22]–[27], where various QAM constellations were proposed. Since then, such constellations have received tremendous attention for high data-rates in various fields of communication with different applications. These areas of communication with applications are described below in details.

Further, except for some initial works on HQAM or TQAM constellations [23], [25], [26], [29], [97], significant research attention in BER/SER analysis of HQAM or TQAM constellations is reported recently in [76]–[78], [92], [101]–[105], [107], [109]–[111], [121]–[128]. In [102]–[105], [109], Park has presented an extensive research for various regular and irregular TQAM (or HQAM) constellations with different constellation orders. In these works, various TQAM constellations with their peak and average powers, bit mapping, detection regions, etc. are presented separately. In [92], for non-power of 2 HQAM constellations, multilevel coded modulation scheme is presented. In [129], performance of θ-QAM family (including SQAM and TQAM) is analyzed in both the AWGN and Nakagami-m fading channels. In [107], a non-relay system is considered and SEP of HQAM over Rayleigh fading channel is derived. For a multi-relay network over independent and non-identically distributed (i.n.i.d.) Nakagami-m fading links, ASER performance of various signal constellations such as HQAM, RQAM, XQAM, De-QPSK, and $\pi/4$-QPSK are analyzed in [76]. In [77], impact of imperfect CSI is observed on the performance of amplify-and-forward (AF) relay system over i.n.i.d. Nakagami-m fading links and closed-form expressions of outage probability and ASER of HQAM and RQAM constellations are derived. In [101], Abdelaziz and Gulliver have examined both power of 2 and non-power of 2 constellations. Further, BER performance with detection complexities of regular, irregular, and sub-optimum TQAM constellations are analyzed. Work done in [76], [77] is extended in [78], where a multi-relay AF system over i.n.i.d. Nakagami-m fading channels with both integer and non-integer fading parameters is considered in presence of imperfect CSI and NLPA at the relay, and analytical expressions of outage probability, asymptotic outage probability, and ASER of HQAM, RQAM, and XQAM constellations are derived.

The major areas of applications for various QAM constellations are:

- Mobile communications
- Broadcasting-cable, satellite, microwave
- Spatial diversity-multicarrier-(OFDM MIMO), cooperative relaying
- Optical wireless communications
- Miscellaneous

A. Mobile Communications

Due to increase in the number of wireless devices, the requirements of voice, data, and video applications are increasing day-by-day. However, to access the limited spectrum, efficient spectrum utilization techniques are required. At the same time, Internet and other data related wireless applications requires very high data-rates. Spectrally efficient high data-rate can be achieved through adaptive digital modulation schemes at an affordable cost. Hence, research is directed towards various spectrally and power efficient compact 2D constellations. In this subsection, we have explored a detailed survey on various signal constellations, adopted in mobile communications from the early days till now.

In [22], authors presented performance of a digital data modem transmission, employing combined amplitude and phase modulation. In [130], authors experimentally implemented the BER of 4-PSK, 8-PSK, and 16-QAM, for a bit-rate of 140 Mbps by considering high capacity digital radio-relay system. In [131], authors investigated the impact of multipath fading on a 200 Mbps 16-QAM digital radio system experimentally. In [132], Oetting compared various constellations up-to 16 constellation orders over AWGN channel which were applicable

to digital radio systems. In [133], Prabhu determined the co-channel interference immunity of high capacity QAM constellations for digital radio applications. In [134], the authors analyzed the impact of multipath fading over a high-speed digital radio systems operating in $4-11$ GHz band by considering offset 4-PSK, conventional 8-PSK and 16-QAM constellations. In [135], authors concluded that the decision feedback equalizer with few taps is efficient in the presence of multipath fading and constructed a 140 Mb/s 16-QAM modem. In [136], Hill et al. presented the performance of nonlinearly amplified (NLA) 64-QAM and the sensitivity over group delays and amplitude distortions was discussed for digital radio systems. In [137]–[140], authors presented their works on QAM constellations in digital radio systems. In [141], authors proposed a blind equalization technique and verified its performance of one and two carrier systems with QAM and V29 constellations. In [29], Forney et al. presented a detailed survey on various power efficient RQAM and HQAM constellations for band limited channels like telephone channels. In [142], authors proposed a futuristic mobile communication system based on the integration of a high-capacity digital cellular mobile radio system with a packet-switched routing network and discussed various modulation formats including QAM. In [143], authors presents a comparative study of 16, 32, 64, and 128-QAM in a digital radio system environment by considering the effects of filtering, interference, amplifier non-linearities, and selective fading. In [144], authors analyzed the performance of 256-QAM over distorted channels by considering amplitude distortions such as linear, parabolic, and sinusoidal characteristics along with group delay. In [145], authors analyzed the performance of 512-QAM by considering the effects of linear channel distortions. In [146], performance of transversal and decision feedback equalizers for 16-QAM and 64-QAM digital radio systems with tap spacing was analyzed. In 1987, Sundberg et al. [147], [148] considered SQAM constellation for voice communication over a Rayleigh fading channel. This was the first major consideration of QAM in mobile radio applications. In [149], authors described the performance of a 400 Mbps transmission capacity 256-QAM modem and introduced some novel approaches such as forward-error-correction (FEC) to reduce residual errors, good phase jitter performance and no false lock phenomenon to attain good system performance. In [150], authors investigated the performance of M-ary QAM by using times-four method of carrier recovery in a digital radio link. In [151], authors evaluated the effects of transmit amplifier non-linearities on digital radio link performance by considering 256-level constellations. In [152], authors presented the performance of multilevel QAM radio system over selective fading by considering adaptive baseband equalization to reduce the signatures. In [153], authors proposed a progressive filter concept for co-channel transmission with negligible interference employing 16-QAM with a 0.19 roll-off at 140 Mbps rate. In [154], technical and design requirements for 256-QAM data in voice modems such as signal processing for implementation, error correction codec etc. were described. In [155], authors reviewed the importance of coded modulation for a 1.544 Mbps data-rate in voice modems employing 256-QAM. In [156], authors presented the performance of a dual polarized M-ary QAM up-to 64 levels by considering coherence between cross talk and the desired signal. In [157], authors proposed an equalization technique for multilevel QAM systems which eliminates linear distortions with easy implementation at high data-rates. In [152], authors presented the performance of multilevel QAM radio system in selective fading by considering adaptive baseband equalization to reduce the signatures. In [158], performance of dual 16-QAM system over dispersive radio channels was analyzed by considering the cross-polarization interference cancelers. In [159], analysis of 140 Mbps 64-QAM is performed by considering the digital adaptive equalization technique. In [160], comparative study of 16, 32, 64, 128-QAM constellations at 140 Mbps by considering both linear and non-linear equalizers was presented. In [161], highly precise cross-polarization interference canceler was developed by using digital transversal filter and performance of 256-QAM at 12.5 Mbps was examined. In [162], authors performed a simulation case study of M-ary QAM constellations for a high capacity digital radio link, subjected to frequency selective fading with different types of channel encoding. In [163], authors presented the performance of 16-QAM, 64-QAM, 49-QPR, and 81-QPR over a 45 Mbps line-of-sight digital radio systems. In [164], authors investigated the impact of delay spread over non-linearly filtered QAM.

In the initial studies, the decision regions for most of the signal constellations were straight boundaries (including some special cases of QAM constellations), and exact and simple BER expressions were obtained. However, more compact 2D signal constellations such as family of QAM do not have boundaries with perpendicular angles. For such constellations exact BER expressions are not simple and consists of special functions during the integral calculation. Considering this point in mind, Craig [165] presented simple and exact BER expressions with polygonal decision boundaries for such more practical signal constellations. This approach was also considered in [166]. In [167], authors examined the performance of 16-QAM by using sub-band coded speech and BCH error correcting codes. In [96], authors presented the differential encoding technique and circular star QAM constellation mapping to improve the BER performance. In [95], author discussed about the application of variable rate square and star QAM constellations for microcellular network based mobile radio applications and the hardware development of a QAM modem. In [99], authors examined the BER performance of various 16-ary QAM constellations and observed that 16-SQAM outperforms 16-star QAM. In [168], author presented the details of best suitable QAM constellations for micro-cellular and macro-cellular personal communication systems. In [169], authors proposed a post-detection maximum ratio combining (MRC) for space diversity in digital land mobile communications by considering M-ary QAM constellations over Rayleigh fading channels. In [170], authors examined the performance of M-ary QAM constellations by considering pilot symbol aided scheme to compensate Rayleigh fading for land mobile communications. In [171], authors proposed a trellis code based 32-QAM constellation to improve the BER performance of the system for fading channels. In [172],

authors analyzed the performance of DS/CDMA system over multipath fading channel with RAKE receiver by employing non-coherent M-ary orthogonal modulation. In [173], [174], considering the amplitude and phase errors, performance of various coherently modulated non-constant envelope like M-ary RQAM constellations were studied over the AWGN and various fading channels. In [5], authors proposed an SQAM constellation for land mobile communications to achieve high data-rate with high QoS for flat and selective fading channels. In [6], authors investigated the performance of adaptive QAM constellation in the presence of co-channel interference. In [9], authors proposed a system to control both modulation level and SER according to channel conditions and monitor the channel condition based on the delay profile measurement. In [175], authors optimized the switching levels for BPSK, QPSK, 16-QAM, and 64-QAM based on received signal strength. In [176], a method of superimposing the closet codes with adaptive M-ary QAM over fading channels was proposed. In [177], authors investigated the performance of L-branch diversity reception system and the SER expressions of M-ary QAM over Rayleigh fading and AWGN channels were derived. In [178], analytical exact ASER expressions for different constellations over various fading channels were derived. In [97], Dong et al. extended the work done by Craig, and performance of various coherent 8 and 16-ary signal constellations was analyzed for both the AWGN and fading channels. In [179], authors employed non-coherent orthogonal M-ary modulation with RAKE receiver for CDMA over fast fading and combined fast fading, shadowing and power control channels. Further, authors determine the BER of the adaptive signaling constellations from 2^2 to 2^9 symbols. In [180], authors mitigated the effects of wideband multipath Rayleigh fading channel with a decision feedback equalizer for adaptive modulation and obtained the BER and bits per symbol performance of BPSK, QPSK, 16-QAM, and 64-QAM constellations. In [181], authors proposed adaptive modulation schemes for simultaneous transmission of voice and data transmission over Nakagami-m fading channels. In [182], authors illustrated the impact of power control over adaptive modulation schemes in presence of interference in a multi-user environment. In [183], authors investigated the performance of adaptive modulation over slow fading channels by considering co-channel interference. In [184], authors analyzed the performance of adaptive M-ary QAM techniques by considering channel estimation errors over Rayleigh fading channel. In [185], authors proposed the recursive algorithm for M-ary QAM constellations to obtain the accurate BER over AWGN channels. In [186], authors introduced the adaptive modulation over Nakagami-m multipath fading channels and determined the average spectral efficiency for 2L-dimensional trellis codes. In [187], authors introduced adaptive bit-interleaved coded modulation to combat the estimation errors. In [188], authors analyzed cellular network scenario by considering adaptive antennas based on fixed and channel allocation schemes. In [189], authors determined the adaptive modulation schemes under constraints of data-rate, transmit power, and instantaneous BER to maximize the spectral efficiency. In [190], authors presented the generalized expression for 1D and 2D amplitude modulations schemes encoded with gray mapping. In [191], authors derived the generalized log likelihood ratio for soft decision channel decoding for QAM constellations. In [192], authors analyzed the performance of multi-rate CDMA system and determined the optimal adaptive rate and power allocation strategies to maximize the throughput of the system. In [193], authors proposed the optimal modulation-mode switching levels for the various PSK and QAM constellations and their BER performance were analyzed. In [194], authors analyzed the performance of a turbo coded system and optimize the adaptive turbo codes and transmitter power. Further, BER performance under average power constraint was obtained. In [195], authors analyzed the performance of a cellular system with different link adaptation strategies by considering practical constraints and proposed a hybrid link to overcome losses due to the practical constraints. In [196], authors optimized the adaptive modulation schemes assisted with channel prediction of Rayleigh fading channels for uncoded M-ary QAM. In [197], authors proposed a soft decision equalization techniques with low complexity and better error performance for MIMO frequency selective channels and BER of QAM constellations was evaluated. In [198], authors analyzed the impact of CSI prediction employing the linear fading predictor over trellis coded Rayleigh fading channel with adaptive modulation and closed-form expressions of BER and spectral efficiency were obtained. In [199], authors derived the BER expressions of M-ary QAM with pilot symbol assisted channel estimation of static and Rayleigh fading channels by considering the impact of noise and the estimator de-correlation. In [200], authors analyzed the effect of linear MMSE channel estimation and channel prediction errors on BER and developed the adaptive pilot symbol assisted modulation schemes to maximize the spectral efficiency. In [201], authors developed a framework for single user throughput maximization by optimizing the symbol rate, packet length, and M-QAM constellation size over AWGN and Rayleigh fading channels. In [202], authors proposed an optimum power allocation policy for the discrete signaling constellations limited in PAPR to maximize the mutual information with arbitrary input distributions. In [203], authors analyzed the bit-interleaved coded OFDM packet transmission with adaptive modulation and determined the pairwise error probability over slow fading channels. In [204], authors investigated the performance of a slow adaptive modulation scheme employing M-ary QAM constellations with antenna diversity. In [205], authors analyzed the impact of constellation size of an M-ary QAM constellations, and the impact of trellis coded modulation on energy efficiency of wireless network through game theoretic approach was analyzed. Further, a number of research works on the BER/SER performance of various QAM constellations in wireless communication systems, operating under different fading environments have been addressed in [31], [206]–[210].

B. Cable, Satellite, and Microwave Communications

In a limited frequency band, the high data transmission through satellite leads towards the use of highly spectral efficient modulation schemes in satellite communication. Further, digital microwave radio system is an efficient way of

transmission when digitizing a communication system. In designing a microwave radio system, RF spectrum must be used in an efficient way, which can be done through adaptive modulation scheme. Hence, in this subsection, a survey on various modulation schemes used in satellite and microwave radio communications is presented.

For the very first time, Thomas et al. [26] mentioned QAM application in satellite communication and considered the non-linear distortion effect due to the use of traveling wave tube amplifier in transponder. In [211], authors implemented multi-level QAM constellations using PSK modems for realizing high baud-rate multi-level transmission for high speed digital-microwave, millimeter-wave, and satellite communication system. In [212], authors proposed a long-haul 16-QAM digital radio system with 200 Mbps in 40 MHz bandwidth as an application for satellite and microwave links. In [213], Prabhu evaluated the performance of 16-QAM in presence of co-channel interference over 8-PSK and 16-PSK by developing a theory in evaluating the error probabilities as an application for terrestrial and satellite communications. In [214], from spectral efficiency point of view, 16-SQAM constellation was adopted for digital microwave radio system operating in 4-5 GHz band. For satellite communication, a turning point came in 1982, when K. Feher proposed a new method of SQAM generation with the use of nonlinear amplifiers which was termed as NLA-QAM [215], where 16 and 64-ary NLA-QAM constellations were proposed. In [216], authors presented the work on digital communications in satellite communications. In [217], author proposed the equalization techniques for digital terrestrial radio systems employing QAM techniques by tap adaptation. In [218] author addressed FEC coded 1024-QAM modems, staggered 1024-QAM, and 256-QAM modems for microwave and cable system application for the first time, where practical constraints of phase noise, amplitude distortions, and group delays were considered. In [219], authors considered 64-256 QAM constellations to calculate the system parameters for high speed data transmission to deploy 1.54 Mbps modems in microwave radio. In [220], authors analyzed the satellite channels by considering the weather induced impairments such as scintillation and rain attenuation, and developed predictors using autoregressive models to improve the efficiency along with the adaptive modulation. In [221], authors investigated the performance of non-linear precoding to mitigate the interference in the broadband MIMO satellite communications and performed BER of uncoded BPSK and QAM constellations. Further, in [38]–[43], [81], QAM constellations were standardized for digital signal broadcasting over cable and satellite links.

C. Spatial Diversity:

Multipath fading is one of the prominent constraint which severely degrades the reliability, robustness, and coverage of a wireless communication system. To combat this, spatial diversity is one of the solutions which improves the performance of a wireless communication system. Spatial diversity can be achieved through multi-carrier system by deploying multiple antennas at the communication nodes. A communication system with multiple antennas at the transmitter and receiver is referred to as MIMO system. In MIMO systems, multiple paths between the source and destination are established with the help of multiple antennas to improve diversity of the communication system. However, multiple antennas at each node are not always possible due to hardware limitations and device size (such as in mobile handsets and sensor networks). In such cases, cooperative communication is preferred as an alternative to improve the spatial diversity of the communication system. Next, we will study the performance of such constellations.

1) Multi-carrier System-(OFDM, MIMO): Multicarrier systems are explored by using OFDM and MIMO systems. A detailed study of OFDM systems is given in [222]–[224]. Various applications employing OFDM techniques are listed as below:

a) OFDM: In [225], author proposed DFT based orthogonally multiplexed QAM system for multichannel system. In [139], authors investigate the multi-carrier system and the application of higher-order QAM constellations. In [226], authors realized the 16-QAM from scaled 4-PSK signals to reduce the peak-to-average envelope power ratio employing Golay sequences for OFDM systems. In [203], authors analyzed the bit-interleaved coded OFDM packet transmission with adaptive modulation and determined the pairwise error probability of the system over slow fading channels. In [227], authors developed loading algorithms to minimize the transmit power of OFDM system with rate and error probability constraints under three different CSI scenarios for QAM constellations. In [228], authors presented the Golay code based 16-star QAM constellation constructed from sum of two scaled QPSK to reduce the peak-to-mean envelope power for OFDM systems. In [229], authors investigated OFDM system with adaptive transmission for maximizing energy efficiency with transmit power and its allocation constraint.

b) MIMO: In [230], authors investigated the performance of M-ary QAM techniques by considering the L-fold antenna diversity over Nakagami-m fading channels with MRC receiver for independent and correlated channels and equal gain combining receiver for independent channels. In [231], authors examined the performance of MIMO system with adaptive modulation and adaptive array processing at the receiver in interference limited cellular systems. In [232], authors developed a framework for mean spectral efficiency by considering mean SNR at the cell boundary, propagation exponent, coding technique and the number of antennas. Further, authors highlighted the potential benefits of adaptive modulation with multiple transmissions in terms of spectral efficiency. In [233], authors illustrated the impact of partial CSI over adaptive MIMO OFDM QAM mapped symbols with 2D space-time coder beamformer. In [234], authors investigated the impact of imperfect CSI and outdated CSI over a multi-antenna system with adaptive modulation. In [196], authors optimized the adaptive modulation schemes assisted with channel prediction of Rayleigh fading channels for uncoded M-ary QAM. In [235], authors presented a pilot symbol assisted modulation channel predictor for MIMO Rayleigh fading channels, the impact of prediction errors on BER performance was analyzed. In [234], authors investigated the impact of imperfect and outdated CSI on a multi-antenna system based on adaptive

modulation. In [236], authors examined the multi-user multi-antenna scenario and emphasized the advantages of non-linear pre-equalization, and SER analysis was performed for QAM constellations. In [237], authors investigated the impact of both the perfect and imperfect CSI at both the transmitter and receiver under average transmit power and instantaneous constraint for MIMO systems. In [238], authors proposed adaptive resource allocation based on subcarrier allocation, power, and bit distribution for multi-user MIMO/OFDM systems based on channel conditions. In [239], authors optimized the performance of a multi-antenna system with bandwidth limited feedback link based on adaptive modulation and transmit beamforming. In [240], authors analyzed a point-to-point MIMO system with perfect CSI at transmitter and receiver, and optimized the constellation selection and linear transceiver based on BER. In [241], authors investigated the multicode CDMA systems with interference cancellers to support high data-rate communications and BER of M-ary QAM was obtained. In [242], authors analyzed the performance of rate-adaptive M-ary QAM constellations with orthogonal space time block codes (STBC) and derive the closed-form BER expressions. In [243], authors investigated cross-layer approach for transmit antenna selection to maximize the throughput of the system and also adaptive modulation to improve systems performance. In [244], authors investigated half-duplex non-orthogonal AF MIMO multi-relay network with STBC and performed diversity multiplexing trade-off and frame-error-rate analysis employing QAM constellations. In [245], authors developed a framework for opportunistic encryption to maximize the throughput with desired security constraints based on channel characteristics. Further, authors optimized the encryption, modulation, and employed FEC codes to combat bit errors. In [246], authors investigated the performance of a half-duplex cooperative MIMO system and asymptotic closed-form pairwise error probability expression was derived. In [247], authors investigated the performance of space time codes based MIMO system over Rayleigh fading channels with adaptive modulation by considering imperfections in channel estimation. In [248], authors investigated QAM mapping based multi-user MIMO OFDM system and optimized transmit power with user rate constraint. In [249], authors investigated multi-user MIMO relay cellular system with adaptive modulation and derived the upper and lower bounds for achievable sum rate. In [250], authors introduced space shift keying (SSK) employing QAM mapping for MIMO systems, and analyzed the system performance under spatial correlation and estimation errors. In [251], authors investigated the MIMO half-duplex AF one and two-way relay systems and proposed algorithms to optimize linear transceivers at both source and relay nodes with sum-rate and mean-square error constraints, and determined the BER of QAM constellations. In [252], authors presented a VLSI architecture for MIMO decoder which supports 4×4 antenna configuration with 64-QAM based on depth-first and breadth-first approach and proposed an algorithm which reduces complexity for both the soft and hard decoding. In [253], authors proposed a hybrid algorithm combining technique using reactive tabu search algorithm and belief propagation algorithm to improve the performance of large MIMO detection with higher order QAM constellations. In [254], authors proposed a near optimum detection algorithm for coherently detected space time shift keying techniques with L-point PSK and QAM constellations. In [234], [255]–[280], authors presented the works considering multiple antennas in various system models including multi-node communication and performed SER analysis of QAM constellations. In [281], authors presented a unified asymptotic framework for transmit antenna selection (TAS)-MIMO multi-relay network with various fading channels and derived the closed-form expressions of the outage probability and SER of M-ary PSK and M-ary QAM constellations. In [282], authors proposed the TAS algorithms and obtained the BER performance of the QAM constellation. In [283], authors presented an analysis of OFDM with offset QAM. In [233], authors presented the impact of partial CSI over adaptive MIMO OFDM QAM mapped symbols with 2D space-time coder-beamformer. In [238], authors proposed the adaptive resource allocation based on subcarrier allocation, power and bit distribution for multi-user MIMO/OFDM systems based on channel conditions. In [248], authors investigated QAM mapping based multi-user MIMO OFDM system and optimized transmit power with user rate constraint. In [284], authors developed a framework for OFDM based spatial modulation over Rayleigh fading channels and derived the SER expressions for QAM constellations. In [285], authors analyzed an OFDMA based cellular downlink by considering non-Gaussian intercell interference to improve the transmission rates of cell edge users, and proposed new modulation scheme frequency and QAM by combining FSK and QAM constellations. In [286], authors analyzed the performance of a MIMO OFDM system with adaptive modulation based on machine learning as an application to 5G new radio systems. In [287], authors introduced STBC using multiple transmit and receiver antennas. Further, the authors determined the maximum diversity order attained and also maximum achievable code rate for complex constellations such as QAM and PAM. In [288], authors investigated the STBC diversity systems over Rayleigh fading channels and SEP of RQAM constellations was obtained. In [289], authors analyzed the performance of half-duplex two-way AF relaying system by considering the Alamouti coding and derived the lower and upper bounds for average sum-rate and pairwise error probability by considering QAM constellations. In [290], authors investigated a MIMO system and proposed a virtual antipodal detection scheme for gray coded higher order RQAM based on semi-definite programming relaxation. In [291]–[294], authors analyzed STBC systems by considering QAM constellations. In [295]–[297], authors proposed semi-definite relaxation (SDR) approach for MIMO detection with higher order QAM constellations. In [298], for M-ary QAM constellations based systems, a semi-definite programming relaxation (SDPR) approach is proposed to combat the multiuser detection problems. In [299], authors proposed SDR based quasi-maximum likelihood algorithm for MIMO systems and introduced several relaxation models with increasing complexity and performed the SER analysis for QAM and PSK constellations. In [300], authors investigated the performance of three different SDR such as polynomial-

inspired SDR, bound-constrained SDR, and virtually antipodal SDR over MIMO channels for BPSK, QPSK, and higher order QAM constellations.

2) Cooperative Relaying: Cooperative relaying is one of the prominent techniques to achieve spatial diversity in wireless communication. Cooperative relaying is extensively explored because of its capability to provide improved capacity, coverage, and power and spectral efficiency due to the diversity gain without using multiple antennas at different communication nodes. Hence, it is also considered as a virtual MIMO system. A detailed study of cooperative relaying can be seen in [301], [302]. In this subsection, we have explored various works on the SER or BER performance of different cooperative relaying networks in various fading environments.

In [303], authors investigated single and multi-channel communication, and presented the BER analysis for M-ary constellations over Nakagami-m and Rayleigh fading channels. In [304], authors investigated the SER of M-ary PSK and QAM constellations over Nakagami-m fading channels for hybrid selection/MRC diversity. In [199], authors investigated the effect of estimator de-correlation on the BER performance of M-ary QAM constellations over Rayleigh fading channels. In [305], authors investigated the performance of cooperative relay system for three different time division multiple access transmission protocols and determined the SER of 4-QAM over fading channels. In [306], authors derived the average error rates of various M-ary constellations and outage probability using characteristic function based approach over various fading channels. In [307], authors analyzed cooperative diversity by considering arbitrary cooperative branches with arbitrary hops per branch over various fading channels and derived the SEP for various constellations including QAM. In [308], authors derived the closed-form expressions of QPSK and QAM for a cooperative systems and optimized the power allocation. In [309], author analyzed the AF cooperative multi-relay system employing selection combining and obtained the SER analysis of QAM constellations. In [255], authors investigated multi-node cooperative relay system and derived the SER expressions for M-PSK and M-QAM constellations and optimized the power allocation. In [310], authors investigated the performance of multi-hop cellular network and proposed the routing and power allocation algorithms to maximize the throughput and BER is evaluated for QAM constellations. In [311], authors analyzed the impact of channel estimation error on the BER performance of RQAM and SQAM constellations. In [312], authors analyzed the performance of cooperative multi-relay system over i.n.i.d. Nakagami-m fading channels and derived the outage probability and error rate employing QAM constellations. In [313], authors investigated the performance of cooperative relay system with DF and AF relaying protocols and analyzed the SER for M-ary QAM and PSK constellations with optimum power allocation. In [314], authors investigated the selection detection and forward and AF half-duplex OFDM relay systems and proposed margin adaptive bit and power loading techniques to minimize the transmit-power consumption, and determined the SER of QAM constellations. In [315], authors investigated the performance of clustered relay network based on STBC and evaluated the packet error rate employing BPSK and 16-QAM constellations. In [316], authors investigated the single and multi-channel diversity reception over i.n.i.d. Nakagami-m fading channels and average SEP expression of RQAM was derived. In [259], authors investigated the SER performance of multi-relay DF system over Nakagami-m fading channels for QAM constellations and optimized the power allocation. In [317], author analyzed DF based single and multi-relay systems and proposed maximum likelihood and piece-wise linear decoders for complex-valued unitary and non-unitary transmissions, and performed the SER analysis of M-ary QAM and PSK constellations. In [318], authors analyzed the performance of OFDM based cooperative relay system and optimized the BER of QAM techniques with respect data rate based on optimal power, bit, and joint power and bit loading. In [319], authors investigated the decode and forward cooperative system and derived the maximum likelihood decoder for M-ary PSK, PAM, and QAM constellations. Apart from the works presented above and reference therein, a lot of work is presented in the literature on the BER/SER performance of various constellations for various relay networks over different fading channels till now.

D. Optical Wireless Communications

Optical wireless communications (OWC) operates in $350-1550$ nm band, through visible light (VL), infra-red, and ultraviolet communication (UVC) bands; has gained significant research attention for the future wireless broadband access. OWC is affordable with high data-rates (30 Gbps) and virtually infinite bandwidth [320], [321]. Various OWC technologies are VL communications (VLC), free space optical (FSO) communication, optical camera communication, light fidelity, and light detection and ranging [322]. OWC operating in VL band ($390-750$ nm) is known as VLC. FSO is also known as terrestrial point-to-point OWC and operates near infra-red frequencies (7501600 nm) [323]. UVC is an non-line-of-sight (NLoS) communications operates in ultraviolet band (200280 nm). OWC is employed for both indoor and outdoor communications. OWC also finds its potential application in underwater communications [323], [324].

In VLC, achievable high data-rates are limited by the low modulation bandwidth of the GaN-based white light emitting diodes (LEDs) due to the slow response time. Bandwidth can be increased by using blue LEDs at the cost of intensity loss of 10 dB [325]. Spectral efficiency can be increased by employing MIMO, massive MIMO, and higher order modulation schemes like optical-OFDM (O-OFDM) [326]. However, MIMO channel are limited by the receiver position, making channel matrix either ill conditioned or rank-deficit which makes data recovery almost impossible. O-OFDM limited by Hermitian symmetry constraints, cyclic prefix, PAPR, and dynamic range of LEDs. As an alternative to O-OFDM, carrierless amplitude and phase modulation has gained significant interest in optical communications for high data-rate transmissions [327]. Bandpass CAP modulation is a QAM modulation where two orthogonal finite impulse response digital filters are employed to achieve it. Various seminal works using CAP

modulation schemes to improve the spectral efficiency of the band-limited LEDs are presented in [328]–[345].

In underwater communications, OWC provides very high data-rates and bandwidth when compared with acoustic, RF, and optical wave communications. In underwater OWC, spectral efficiency is increased by employing coherent modulation, where information is transmitted through amplitude, phase, or polarization of the optical field [346]. Coherent modulation includes M-ary PSK, M-ary QAM, and multilevel polarization shift keying. In underwater OWC, coherent modulation schemes are very attractive due to high receiver sensitivity, spectral efficiency, and robust to background noise and interfering signals with increased cost and implementation complexity [324], [346]. Some of the notable works which presented the advantages of QAM schemes over intensity-modulation direct-detection systems are [324], [347]–[357].

In UV NLoS communications, several notable works were performed employing QAM constellations to improve the spectral efficiency [126], [128], [358]–[368]. In [346], [361], [369]–[377], authors have presented the application of QAM and adaptive modulation in FSO communications.

E. Miscellaneous-Emerging Areas for High Data-rate Communications

1) Machine Learning-5G, Security: In [378], authors addressed the application of adaptive modulation schemes for 3G wireless communication systems and developed method to select the modulation and coding based on the channel conditions with minimum frame error rate constraint. In [245], authors developed a framework for the opportunistic encryption to maximize the throughput with the desired security constraints based on channel characteristics. Further, authors optimized the encryption, modulation and employ FEC codes to combat bit errors. In [210], [379]–[383], authors investigated the SER performance of different QAM constellations over $\eta-\mu$, κ-μ, and two wave with diffuse power fading channels. In [384], author presented a survey on approximation of Q function and its significance in error probability evaluation. Further, author presented the closed-form SEP of various constellations such as QPSK, QAM, HQAM, and XQAM with approximated Q-functions. In [385]–[387], authors presented a survey on 5G new radio and also discussed the application of QAM constellations. In [388]–[394], authors presented the work based on filter bank multi-carrier systems using QAM constellations as an application for future wireless communications. In [284], authors developed a framework for MIMO systems with spatial modulation schemes over generalized fading channels and computed the average BEP for PSK and QAM constellations. In [395], authors analyzed the performance of MIMO system with SSK and generalized SSK modulation by considering multiple-access interference for PSK and QAM constellations. In [396], authors presented a state-of-the-art survey on spatial modulation based MIMO system with QAM for the emerging and future wireless communications and discussed the advantages, research challenges, and experimental activities. In [38], authors investigated the performance of star constellation based spatial modulation. In [397], authors investigated the energy harvesting based distributed spatial modulation and evaluated the error probability of energy recycling DSM with QAM constellations. In [398], authors presented a survey on spatial modulation schemes and the application of spatially modulated QAM is presented. In [399]–[401], authors investigated spatial modulation techniques employing QAM.

2) Edge Caching, Energy Harvesting, Full-Duplex Communications, Game Theory: In [402], authors developed a framework to optimize the modulation scheme to be employed by reducing the energy consumption over energy constraint nodes for both coded and uncoded systems. In [403], authors investigated sensor network and proposed variable length TDMA schemes to minimize energy consumption for transmission of QAM constellations by optimizing routing, scheduling, and link adaptation strategies. In [205], authors analyzed the impact of constellation size of M-ary QAM constellations and also the impact of trellis coded modulation on energy efficiency of wireless network through game theoretic approach. In [315], authors analyzed the STBC based clustered wireless networks using cooperative communications and performed packet error rate analysis for QAM constellations to minimize the energy consumption with transmit power allocation, number of sensors, and distance between clusters as constraints. In [404]–[407], authors investigated the wireless sensor networks and presented various techniques for minimizing the energy consumption by considering QAM transmissions. In [408], authors investigated the performance of full-duplex AF relay system under residual self interference and derived the pairwise error probability for uncoded systems and BER for coded systems. In [409], authors presented a survey on solutions provided for improving energy efficiency of multimedia based battery operated hand-held devices by considering various modulation schemes for transmission including QAM constellations. In [410], authors investigated the performance of spatial modulation based full-duplex two-way relay systems and derived the tight upper bound for average BEP and asymptotic BEP for QAM constellations. In [410]–[414], authors analyzed full-duplex cooperative relay system by considering spatial modulation based QAM. In [415], authors investigated the performance of full-duplex relay system and compared the performance of media based modulation schemes with QAM.

VIII. Conclusion

As bandwidth and power efficiency are prominent constraints for 5G and beyond wireless communication systems, a detailed study of various QAM constellations has been presented in this work. This study started with an introduction to QAM constellations used since early 1960s to more complex higher order power and bandwidth efficient QAM constellations with their applications in various wireless communication systems and IEEE standards. A detailed study of star QAM is performend. Further, constellation modeling, bit mapping, Gray code penalty, decision regions, peak and average powers, and PAPR of the advance XQAM and HQAM constellations have also been discussed in details. Study of HQAM includes regular and irregular HQAM constellations

with various constellation orders. Finally, a comparison of various QAM constellations has been presented which concludes the irregular HQAM as the optimum constellation which is highly power efficient than the other constellations employed in the existing wireless communication systems and standards. From this, it can be claimed that the HQAM can be adopted in various wireless applications targeted for 5G and beyond wireless communication systems where high data-rates with good QoS is required within the limited power and bandwidth. Performance can be improved further by probabilistically shaping the HQAM constellations in the future.

REFERENCES

[1] A. Goldsmith, *Wireless Communications*. Cambridge University Press, 2005.

[2] T. S. Rappaport *et al.*, *Wireless Communications: Principles and Practice*. Prentice Hall PTR New Jersey, 1996, vol. 2.

[3] J. Hayes, "Adaptive feedback communications," *IEEE Trans. Commun. Technol.*, vol. 16, no. 1, pp. 29–34, Feb. 1968.

[4] J. Cavers, "Variable-rate transmission for Rayleigh fading channels," *IEEE Trans. Commun.*, vol. 20, no. 1, pp. 15–22, Feb. 1972.

[5] S. Otsuki, S. Sampei, and N. Morinaga, "Square-QAM adaptive modulation/TDMA/TDD systems using modulation level estimation with Walsh function," *IET Electron. Lett.*, vol. 31, no. 3, pp. 169–171, Feb. 1995.

[6] W. Webb and R. Steele, "Variable rate QAM for mobile radio," *IEEE Trans. Commun.*, vol. 43, no. 7, pp. 2223–2230, Jul. 1995.

[7] Y. Kamio, S. Sampei, H. Sasaoka, and N. Morinaga, "Performance of modulation-level-controlled adaptive-modulation under limited transmission delay time for land mobile communications," in *Proc. IEEE VTC*, vol. 1. IEEE, Jul. 1995, pp. 221–225.

[8] S. Kallel and S. M. Alamouti, "Adaptive trellis-coded multiple-phase-shift keying for Rayleigh fading channels," *IEEE Trans. Commun.*, vol. 42, pp. 2305–2314, Jun. 1994.

[9] T. Ue, S. Sampei, and N. Morinaga, "Symbol rate and modulation level controlled adaptive modulation/TDMA/TDD for personal communication systems," in *Proc. IEEE VTC*, vol. 1. IEEE, Jul. 1995, pp. 306–310.

[10] A. J. Goldsmith and S.-G. Chua, "Variable-rate variable-power MQAM for fading channels," *IEEE Trans. Commun.*, vol. 45, no. 10, pp. 1218–1230, Oct. 1997.

[11] 3GPP TR 25.999 V 7.1.0 Release 7, "Universal Mobile Telecommunications System (UMTS); High Speed Packet Access (HSPA) evolution; Frequency Division Duplex (FDD)," Apr. 2008. [Online]. Available: https://www.etsi.org/deliver/etsi_tr/125900_125999/125999/07.01.00_60/tr_125999v070100p.pdf

[12] J. A. Bingham *et al.*, "Multicarrier modulation for data transmission: An idea whose time has come," *IEEE Commun. Mag.*, vol. 28, no. 5, pp. 5–14, May 1990.

[13] P. S. Chow, J. M. Cioffi, and J. A. Bingham, "A practical discrete multitone transceiver loading algorithm for data transmission over spectrally shaped channels," *IEEE Trans. Commun.*, vol. 43, no. 2/3/4, pp. 773–775, Feb. 1995.

[14] M. Filip and E. Vilar, "Optimum utilization of the channel capacity of a satellite link in the presence of amplitude scintillations and rain attenuation," *IEEE Trans. Commun.*, vol. 38, no. 11, pp. 1958–1965, Nov. 1990.

[15] A. M. Monk and L. B. Milstein, "Open-loop power control error in a land mobile satellite system," *IEEE J. Sel. Areas Commun.*, vol. 13, no. 2, pp. 205–212, Feb. 1995.

[16] J. Rose, "Satellite communications in the 30/20 GHz band," *Satellite Commun.*, pp. 155–162, Jun. 1985.

[17] R. V. Cox, J. Hagenauer, N. Seshadri, and C.-E. Sundberg, "Subband speech coding and matched convolutional channel coding for mobile radio channels," *IEEE Trans. Signal Proc.*, vol. 39, no. 8, pp. 1717–1731, Aug. 1991.

[18] M.-S. Alouini and A. J. Goldsmith, "Capacity of Rayleigh fading channels under different adaptive transmission and diversity-combining techniques," *IEEE Trans. Veh. Technol.*, vol. 48, no. 4, pp. 1165–1181, Jul. 1999.

[19] C. Cahn, "Combined digital phase and amplitude modulation communication systems," *IRE Trans. Commun. Syst.*, vol. 8, no. 3, pp. 150–155, Sep. 1960.

[20] J. Hancock and R. Lucky, "Performance of combined amplitude and phase-modulated communication systems," *IRE Trans. Commun. Syst.*, vol. 8, no. 4, pp. 232–237, Dec. 1960.

[21] C. Campopiano and B. Glazer, "A coherent digital amplitude and phase modulation scheme," *IRE Trans. Commun. Syst.*, vol. 10, no. 1, pp. 90–95, Mar. 1962.

[22] J. Salz, J. Sheehan, and D. Paris, "Data transmission by combined AM and PM," *Bell Syst. Tech. J.*, vol. 50, no. 7, pp. 2399–2419, Sep. 1971.

[23] M. Simon and J. Smith, "Hexagonal multiple phase-and-amplitude-shift-keyed signal sets," *IEEE Trans. Commun.*, vol. 21, no. 10, pp. 1108–1115, Oct. 1973.

[24] G. Foschini, R. Gitlin, and S. Weinstein, "On the Selection of a Two-Dimensional Signal Constellation in the Presence of Phase Jitter and Gaussian Noise," *Bell Syst. Tech. J.*, vol. 52, no. 6, pp. 927–965, Jul. 1973.

[25] ——, "Optimization of two-dimensional signal constellations in the presence of Gaussian noise," *IEEE Trans. Commun.*, vol. 22, no. 1, pp. 28–38, Jan. 1974.

[26] C. Thomas, M. Weidner, and S. Durrani, "Digital amplitude-phase keying with M-ary alphabets," *IEEE Trans. Commun.*, vol. 22, no. 2, pp. 168–180, Feb. 1974.

[27] J. Smith, "Odd-bit quadrature amplitude-shift keying," *IEEE Trans. Commun.*, vol. 23, no. 3, pp. 385–389, Mar. 1975.

[28] W. Weber, "Differential encoding for multiple amplitude and phase shift keying systems," *IEEE Trans. Commun.*, vol. 26, no. 3, pp. 385–391, Mar. Mar. 1978.

[29] G. Forney, R. Gallager, G. Lang, F. Longstaff, and S. Qureshi, "Efficient modulation for band-limited channels," *IEEE J. Sel. Areas Commun.*, vol. 2, no. 5, pp. 632–647, Sep. 1984.

[30] K.-L. Du and M. N. Swamy, *Wireless communication systems: From RF Subsystems to 4G Enabling Technologies*. Cambridge University Press, 2010.

[31] D. Dixit and P. R. Sahu, "Performance analysis of rectangular QAM with SC receiver over Nakagami-m fading channels," *IEEE Commun. Lett.*, vol. 18, no. 7, pp. 1262–1265, Jul. 2014.

[32] G. K. Karagiannidis, "On the symbol error probability of general order rectangular QAM in Nakagami-m fading," *IEEE Commun. Lett.*, vol. 10, no. 11, pp. 745–747, Dec. 2006.

[33] J. G. Proakis and M. Salehi, *Digital Communications*. New York, NY, USA: McGraw-Hill, 2008.

[34] K. Ishibashi, W.-Y. Shin, H. Ochiai, and V. Tarokh, "A peak power efficient cooperative diversity using star-QAM with coherent/noncoherent detection," *IEEE Trans. Wireless Commun.*, vol. 12, no. 5, pp. 2137–2147, Mar. 2013.

[35] W. Webb, L. Hanzo, and R. Steele, "Bandwidth efficient QAM schemes for Rayleigh fading channels," *IEE Proceed. I (Commun. Speech Vision)*, vol. 138, no. 3, pp. 169–175, Jun. 1991.

[36] T. May, H. Rohling, and V. Engels, "Performance analysis of Viterbi decoding for 64-DAPSK and 64-QAM modulated OFDM signals," *IEEE Trans. Commun.*, vol. 46, no. 2, pp. 182–190, Feb. 1998.

[37] K. Ishibashi, H. Ochiai, and R. Kohno, "Low-complexity bit-interleaved coded DAPSK for Rayleigh-fading channels," *IEEE J. Sel. Areas Commun.*, vol. 23, no. 9, pp. 1728–1738, Sep. 2005.

[38] P. Yang, Y. Xiao, B. Zhang, S. Li, M. El-Hajjar, and L. Hanzo, "Star-QAM signaling constellations for spatial modulation," *IEEE Trans. Veh. Technol.*, vol. 63, no. 8, pp. 3741–3749, Feb. 2014.

[39] ANSI/SCTE, "Digital Transmission Standard For Cable Television," Jul. 2013, accessed: 2014-08-17. [Online]. Available: https://web.archive.org/web/20140817034950/http://www.scte.org/FileDownload.aspx?A=3445

[40] ETSI EN 300 468 V1.15.1, "Specification for service information in DVB systems," Mar. 2016. [Online]. Available: https://www.etsi.org/deliver/etsi_en/300400_300499/300468/01.15.01_60/en_300468v011501p.pdf

[41] X.-C. Zhang, H. Yu, and G. Wei, "Exact symbol error probability of cross-QAM in AWGN and fading channels," *EURASIP J. Wireless Commun. Netw.*, pp. 917–954, Nov. 2010.

[42] U. Reimers, *DVB: The family of international standards for digital video broadcasting*. Springer, 2013.

[43] D. Jaeger, "DVB-C2 - system aspects and performance analysis," *DVB-C2 Implementers Seminar*, Sep. 2009. [Online]. Available: https://web.archive.org/web/20120319065737/http://www.ict-redesign.eu/fileadmin/documents/DVB_TM_C2_254_Dirk_Jaeger__DVB-C2_System_Aspects.pdf

[44] ETSI EN 302 769 V1.1.1, "Frame structure channel coding and modulation for a second generation digital transmission system for cable

systems," Apr. 2010. [Online]. Available: https://www.etsi.org/deliver/etsi_en/302700_302799/302769/01.01.01_60/en_302769v010101p.pdf

[45] ETSI EN 300 744 V1.6.1, "Framing structure, channel coding and modulation for digital terrestrial television," Jan. 2009. [Online]. Available: https://www.etsi.org/deliver/etsi_en/300700_300799/300744/01.06.01_60/en_300744v010601p.pdf

[46] ETSI EN 302 755 V1.2.1, "Frame structure channel coding and modulation for a second generation digital terrestrial television broadcasting system," Sep. 2010. [Online]. Available: https://www.etsi.org/deliver/etsi_en/302700_302799/302755/01.02.01_40/en_302755v010201o.pdf

[47] ETSI EN 301 545-2 V1.2.1, "Second generation DVB interactive satellite system (DVB-RCS2)," Apr. 2004. [Online]. Available: https://www.etsi.org/deliver/etsi_en/301500_301599/30154502/01.02.01_60/en_30154502v010201p.pdf

[48] ITU-T G.992.3, "Asymmetric digital subscriber line (ADSL) transceivers 2 (ADSL2)," Jul. 2002.

[49] ITU-T G.9960, "Unified high-speed wire-line based home networking transceivers system architecture and physical layer specification," Nov. 2018.

[50] E. SASAKI and T. MARU, "Ultra-high-capacity wireless transmission technology achieving 10 Gbps transmission," *NEC Techn. J.*, vol. 8, no. 2, pp. 70–74, Apr. 2014.

[51] E. Charfi, L. Chaari, and L. Kamoun, "PHY/MAC enhancements and QoS mechanisms for very high throughput WLANs: A survey," *IEEE Commun. Surveys Tuts.*, vol. 15, no. 4, pp. 1714–1735, 2013.

[52] M. Sauter, *From GSM to LTE: An Introduction to Mobile Networks and Mobile Broadband*. John Wiley & Sons, 2010.

[53] S. Banerji and R. S. Chowdhury, "On IEEE 802.11: Wireless LAN technology," *Int. J. Mobile Netw. Commun. Telemat.*, vol. 3, no. 4, pp. 1–19, Aug. 2013.

[54] L. Verma, M. Fakharzadeh, and S. Choi, "Wi-Fi on steroids: 802.11 ac and 802.11 ad," *IEEE Wireless Commun.*, vol. 20, no. 6, pp. 30–35, 2013.

[55] Y. Ghasempour, C. R. da Silva, C. Cordeiro, and E. W. Knightly, "IEEE 802.11 ay: Next-generation 60 GHz communication for 100 Gb/s Wi-Fi," *IEEE Commun. Mag.*, vol. 55, no. 12, pp. 186–192, Oct. 2017.

[56] IEEE 802 LAN/MAN Standards Committee and others, "IEEE standard for information technology-telecommunication and information exchange between systems-local and metropolitan area networks-specific requirements part11: Wireless LAN medium access control (MAC) and physical layer (PHY) specifications amendment1: Radio resource measurement of wireless LANs," *IEEE Std.*, 2009. [Online]. Available: http://standards.ieee.org/getieee802/download/802.11n-2009.pdf

[57] W. Sun, M. Choi, and S. Choi, "IEEE 802.11 ah: A long range 802.11 WLAN at sub 1 GHz," *J. ICT Standardization*, vol. 1, no. 1, pp. 83–108, Jul. 2013.

[58] L. Oliveira, J. J. Rodrigues, S. A. Kozlov, R. A. Rabêlo, and V. H. C. d. Albuquerque, "MAC layer protocols for internet of things: A survey," *Future Internet*, vol. 11, no. 1, p. 16, 2019.

[59] IEEE 802.11 Working Group and others, "IEEE standard for information technology–telecommunications and information exchange between systems–local and metropolitan area networks–specific requirements–part 11: Wireless LAN medium access control (MAC) and physical layer (PHY) specifications amendment 6: Wireless access in vehicular environments," *IEEE Std.*, vol. 802, no. 11, Jul. 2010.

[60] D. Lekomtcev and R. Maršálek, "Comparison of 802.11 af and 802.22 standards–physical layer and cognitive functionality," *Elektro Revue*, vol. 3, no. 2, pp. 12–18, 2012.

[61] IEEE Computer Society LAN/MAN Standards Committee and others, "IEEE standard for information technology-telecommunications and information exchange between systems-local and metropolitan area networks-specific requirements part 11: Wireless LAN medium access control (MAC) and physical layer (PHY) specifications," *IEEE Std.*, 2007.

[62] D. Tse and P. Viswanath, *Fundamentals of Wireless Communication*. Cambridge University Press, 2005.

[63] 3GPP TS 36.211 V 8.9.0 Release 8, "Evolved Universal Terrestrial Radio Access (E-UTRA); Physical channels and modulation," Jan. 2010. [Online]. Available: https://www.etsi.org/deliver/etsi_ts/136200_136299/136211/08.09.00_60/ts_136211v080900p.pdf

[64] 3GPP TS 36.300 V 10.2.0 Release 10, "Evolved Universal Terrestrial Radio Access (E-UTRA) and Evolved Universal Terrestrial Radio Access Network (E-UTRAN); Overall description; Stage 2," Jan. 2011. [Online]. Available: https://www.etsi.org/deliver/etsi_ts/136300_136399/136300/10.02.00_60/ts_136300v100200p.pdf

[65] 3GPP TS 36.306 V 14.2.0 Release 14, "Evolved Universal Terrestrial Radio Access (E-UTRA); User Equipment (UE) radio access capabilities," Apr. 2014. [Online]. Available: https://www.etsi.org/deliver/etsi_ts/136300_136399/136306/14.02.00_60/ts_136306v140200p.pdf

[66] 3GPP TS 36.331 V 15.3.0 Release 15, "Evolved universal terrestrial radio access (E-UTRA); radio resource control (RRC); protocol specification," Oct. 2018. [Online]. Available: https://www.etsi.org/deliver/etsi_ts/136300_136399/136331/15.03.00_60/ts_136331v150300p.pdf

[67] L. Hanzo, Y. Akhtman, J. Akhtman, L. Wang, and M. Jiang, *MIMO-OFDM for LTE, Wi-Fi and WiMAX: Coherent versus non-coherent and cooperative turbo transceivers*. John Wiley & Sons, 2011.

[68] D. Pareit, B. Lannoo, I. Moerman, and P. Demeester, "The history of WiMAX: A complete survey of the evolution in certification and standardization for IEEE 802.16 and WiMAX," *IEEE Commun. Surveys Tuts.*, vol. 14, no. 4, pp. 1183–1211, 2011.

[69] IEEE 802.16 Broadband Wireless Access Working Group and others, "IEEE 802.16 m system description document," *IEEE 802.16 Std.*, Feb. 2009.

[70] I. S. 802.16^{TM}-2017, "IEEE standard for air interface for broadband wireless access systems," *IEEE Std.*, Feb. 2018.

[71] L. Hanzo, P. J. Cherriman, and J. Streit, *Wireless Video Communications: Second to Third Generation and Beyond*. John Wiley & Sons, 2001.

[72] B.-E. Olsson, A. Djupsjöbacka, J. Mårtensson, and A. Alping, "112 Gbit/s RF-assisted dual carrier DP-16-QAM transmitter using optical phase modulator," *Opt. Exp.*, vol. 19, no. 26, pp. B784–B789, 2011.

[73] ITU-J.83 Recommendations, "J.83: Digital multi-programme systems for television, sound and data services for cable distribution," Dec. 2007. [Online]. Available: https://www.itu.int/rec/T-REC-J.83-200712-I/en

[74] ITU-T, Recommendation H.261, "Video codec for audiovisual services at px64 Kbit/s," Mar. 1993.

[75] J. Streit and L. Hanzo, "Quadtree-based parametric wireless videophone systems," *IEEE Trans. Circuits Syst. Video Technol.*, vol. 6, no. 2, pp. 225–237, 1996.

[76] N. Kumar, P. K. Singya, and V. Bhatia, "ASER analysis of hexagonal and rectangular QAM schemes in multiple-relay networks," *IEEE Trans. Veh. Technol.*, vol. 67, no. 2, pp. 1815–1819, Feb. 2018.

[77] P. K. Singya, N. Kumar, and V. Bhatia, "Impact of imperfect CSI on ASER of hexagonal and rectangular QAM for AF relaying network," *IEEE Commun. Lett.*, vol. 22, no. 2, pp. 428–431, Feb. 2018.

[78] P. K. Singya, N. Kumar, V. Bhatia, and M.-S. Alouini, "On performance of hexagonal, cross, and rectangular QAM for multi-relay systems," *IEEE Access*, vol. 7, pp. 60 602–60 616, May 2019.

[79] *Asymmetric digital subscriber line (ADSL) transceivers*. ITUT Std. G.992.1, Jun. 1999.

[80] *Very high speed digital subscriber line transceivers*. ITUT Std. G.993.1, Jun. 2004.

[81] "Digital Video Broadcasting (DVB); framing structure, channel coding and modulation for cable systems," *ETSI Std. EN*, vol. 300, no. 429, Apr. 1998.

[82] S. Colonnese, G. Panci, S. Rinauro, and G. Scarano, "High SNR performance analysis of a blind frequency offset estimator for cross QAM communication," in *Proc. IEEE ICASSP*. IEEE, Mar. 2008, pp. 2825–2828.

[83] K. V. Cartwright, "Blind phase recovery in cross QAM communication systems with eighth-order statistics," *IEEE Signal Process. Lett.*, vol. 8, no. 12, pp. 304–306, Dec. 2001.

[84] S. Abrar and I. M. Qureshi, "Blind equalization of cross-QAM signals," *IEEE Signal Process. Lett.*, vol. 13, no. 12, pp. 745–748, Nov. 2006.

[85] S. H. Han, J. M. Cioffi, and J. H. Lee, "On the use of hexagonal constellation for peak-to-average power ratio reduction of an ODFM signal," *IEEE Trans. Wireless Commun.*, vol. 7, no. 3, pp. 781–786, Mar. 2008.

[86] D. Kapetanovic, H. V. Cheng, W. H. Mow, and F. Rusek, "Optimal two-dimensional lattices for precoding of linear channels," *IEEE Trans. Wireless Commun.*, vol. 12, no. 5, pp. 2104–2113, May 2013.

[87] K. P. Srinath and B. S. Rajan, "Fast-decodable MIDO codes with large coding gain," *IEEE Trans. Inf. Theory*, vol. 60, no. 2, pp. 992–1007, Nov. 2013.

[88] E. Leung and J.-K. Zhang, "Design of uniquely factorable hexagonal constellations for noncoherent SIMO systems," in *Proc. ICNC*. IEEE, Feb. 2016, pp. 1–5.

[89] M. Hekrdla and J. Sykora, "Hexagonal constellations for adaptive physical-layer network coding 2-way relaying," *IEEE Commun. Lett.*, vol. 18, no. 2, pp. 217–220, Jan. 2014.

[90] S. Hosur, M. F. Mansour, and J. C. Roh, "Hexagonal constellations for small cell communication," in *Proc. IEEE GLOBECOM*. IEEE, Dec. 2013, pp. 3270–3275.

[91] C. R. Doerr, L. Zhang, P. Winzer, and A. H. Gnauck, "28-Gbaud InP square or hexagonal 16-QAM modulator," in *Proc. OFC*. OSA, Mar. 2011, p. OMU2.

[92] M. Tanahashi and H. Ochiai, "A multilevel coded modulation approach for hexagonal signal constellation," *IEEE Trans. Wireless Commun.*, vol. 8, no. 10, pp. 4993–4997, Oct. 2009.

[93] S. Hashimoto, K. Ishii, and S. Ogose, "Non-binary turbo coded spatial modulation," in *Proc. IEEE VTC*. IEEE, Sep. 2013, pp. 1–5.

[94] H. Morita, "Nearest-neighbor error correcting codes on a hexagonal signal constellation," in *2015 IEEE ISIT*. IEEE, Jun. 2015, pp. 2480–2484.

[95] W. T. Webb, "QAM: the modulation scheme for future mobile radio communications?" *IET Electron. Commun. Engg. J.*, vol. 4, no. 4, pp. 167–176, Aug. 1992.

[96] W. Webb and R. Steele, "16-level circular QAM transmissions over a Rayleigh fading channel," in *IEE Colloquium on Multi-Level Modulation Techniques and Point-to-Point and Mobile Radio*. IET, Mar. 1990, pp. 6–1.

[97] X. Dong, N. C. Beaulieu, and P. H. Wittke, "Signaling constellations for fading channels," *IEEE Trans. Commun.*, vol. 47, no. 5, pp. 703–714, May 1999.

[98] ——, "Error probabilities of two-dimensional M-ary signaling in fading," *IEEE Trans. Commun.*, vol. 47, no. 3, pp. 352–355, Mar. 1999.

[99] F. Adachi and M. Sawahashi, "Performance analysis of various 16 level modulation schemes under Rayleigh fading," *IET Electron. Lett.*, vol. 28, no. 17, pp. 1579–1581, Aug. 1992.

[100] P. K. Vitthaladevuni, M.-S. Alouini, and J. C. Kieffer, "Exact BER computation for cross QAM constellations," *IEEE Trans. Wireless Commun.*, vol. 4, no. 6, pp. 3039–3050, Dec. 2005.

[101] M. Abdelaziz and T. A. Gulliver, "Triangular Constellations for Adaptive Modulation," *IEEE Trans. Commun.*, vol. 66, no. 2, pp. 756–766, Feb. 2018.

[102] S. Park, "Triangular quadrature amplitude modulation," *IEEE Commun. Lett.*, vol. 11, no. 4, pp. 292–294, Apr. 2007.

[103] S. Park, M. Byeon, and J. Jeon, "Odd-bit triangular quadrature amplitude modulations," in *Proc. PIMRC*, Sep. 2009, pp. 2419–2423.

[104] S. Park and M.-K. Byeon, "Irregularly distributed triangular quadrature amplitude modulation," in *Proc. PIMRC*, Sep. 2008, pp. 1–5.

[105] S. J. Park, "Performance analysis of triangular quadrature amplitude modulation in AWGN channel," *IEEE Commun. Lett.*, vol. 16, no. 6, pp. 765–768, Jun. 2012.

[106] L. Rugini, "Tight upper bounds on the probability of error of quaternary simplex signals," *IEEE Commun. Lett.*, vol. 19, no. 6, pp. 1001–1004, Jun. 2015.

[107] ——, "Symbol error probability of hexagonal QAM," *IEEE Commun. Lett.*, vol. 20, no. 8, pp. 1523–1526, Aug. 2016.

[108] F. Gray, "Pulse code communication. US Patent 2632058," Mar. 1953.

[109] S.-J. Park, "Bit mapping of triangular quadrature amplitude modulation," in *Proc. PIMRC*. IEEE, Sep. 2007, pp. 1–3.

[110] P. K. Singya, N. Kumar, V. Bhatia, and F. A. Khan, "Performance analysis of OFDM based 3-hop AF relaying network over mixed Rician/Rayleigh fading channels," *AEU-Int. J. Electron. Commun.*, vol. 93, pp. 337–347, Sep. 2018.

[111] S. Parvez, P. K. Singya, and V. Bhatia, "On impact of imperfect CSI over hexagonal QAM for TAS/MRC-MIMO cooperative relay network," *IEEE Commun. Lett.*, Jul. 2019.

[112] Z. Qu and I. B. Djordjevic, "On the probabilistic shaping and geometric shaping in optical communication systems," *IEEE Access*, vol. 7, pp. 21 454–21 464, Feb. 2019.

[113] M. P. Yankov, D. Zibar, K. J. Larsen, L. P. Christensen, and S. Forchhammer, "Constellation shaping for fiber-optic channels with QAM and high spectral efficiency," *IEEE Photon. Technol. Lett.*, vol. 26, no. 23, pp. 2407–2410, Sep. 2014.

[114] T. Fehenberger, D. Lavery, R. Maher, A. Alvarado, P. Bayvel, and N. Hanik, "Sensitivity gains by mismatched probabilistic shaping for optical communication systems," *IEEE Photon. Technol. Lett.*, vol. 28, no. 7, pp. 786–789, Jan. 2016.

[115] G. Böcherer, F. Steiner, and P. Schulte, "Bandwidth efficient and rate-matched low-density parity-check coded modulation," *IEEE Trans. Commun.*, vol. 63, no. 12, pp. 4651–4665, Oct. 2015.

[116] T. Fehenberger, A. Alvarado, G. Böcherer, and N. Hanik, "On probabilistic shaping of quadrature amplitude modulation for the nonlinear fiber channel," *IEEE J. Lightw. Technol.*, vol. 34, no. 21, pp. 5063–5073, Jul. 2016.

[117] F. Steiner and G. Böcherer, "Comparison of geometric and probabilistic shaping with application to ATSC 3.0," in *Proc. SCC*. VDE, Feb. 2017, pp. 1–6.

[118] S. Zhang and F. Yaman, "Constellation design with geometric and probabilistic shaping," *Optics Commun.*, vol. 409, pp. 7–12, Feb. 2018.

[119] Z. Qu and I. B. Djordjevic, "Hybrid probabilistic-geometric shaping in optical communication systems," in *IEEE Photon. Conf. (IPC)*. IEEE, Sep. 2018, pp. 1–2.

[120] Z. Qu, I. B. Djordjevic, and J. Anderson, "Two-dimensional constellation shaping in fiber-optic communications," *Applied Sciences*, vol. 9, no. 9, p. 1889, Jan. 2019.

[121] J. Lee, D. Yoon, and K. Cho, "Error performance analysis of M-ary θ-QAM," *IEEE Trans. Veh. Technol.*, vol. 61, no. 3, pp. 1423–1427, Feb. 2012.

[122] T. G. Markiewicz, "Construction and labeling of triangular QAM," *IEEE Commun. Lett.*, vol. 21, no. 8, pp. 1751–1754, May 2017.

[123] D. Sadhwani, "Simple and tightly approximated integrals over κ-μ shadowed fading channel with applications," *IEEE Trans. Veh. Technol.*, vol. 67, no. 10, pp. 10 092–10 096, Jul. 2018.

[124] D. Sadhwani, R. N. Yadav, S. Aggarwal, and D. K. Raghuvanshi, "Simple and accurate SEP approximation of hexagonal-QAM in AWGN channel and its application in parametric α- μ, η- μ, κ- μ fading, and log-normal shadowing," *IET Commun.*, vol. 12, no. 12, pp. 1454–1459, Mar. 2018.

[125] P. Shaik, P. K. Singya, and V. Bhatia, "Performance analysis of QAM schemes for non-regenerative cooperative MIMO network with transmit antenna selection," *AEU-Int. J. Electron. Commun.*, vol. 107, pp. 298–306, Jul. 2019.

[126] K. K. Garg, P. Singya, and V. Bhatia, "Performance analysis of NLOS ultraviolet communications with correlated branches over turbulent channels," *IEEE/OSA J. Opt. Commun. Netw.*, vol. 11, no. 11, pp. 525–535, Nov. 2019.

[127] S. Parvez, P. K. Singya, and V. Bhatia, "On ASER analysis of energy efficient modulation schemes for a device-to-device MIMO relay network," *IEEE Access*, vol. 8, pp. 2499–2512, Dec. 2019.

[128] P. Shaik, K. K. Garg, and V. Bhatia, "On impact of imperfect channel state information on dual-hop nonline-of-sight ultraviolet communication over turbulent channel," *Opt. Eng.*, vol. 59, no. 1, pp. 1 – 14, Jan. 2020.

[129] K. N. Pappi, A. S. Lioumpas, and G. K. Karagiannidis, "θ-QAM: A parametric quadrature amplitude modulation family and its performance in AWGN and fading channels," *IEEE Trans. Commun.*, vol. 58, no. 4, pp. 1014–1019, Mar. 2010.

[130] P. Dupuis, M. Joindot, A. Leclert, and D. Soufflet, "16 QAM modulation for high capacity digital radio system," *IEEE Trans. Commun.*, vol. 27, no. 12, pp. 1771–1782, Dec. 1979.

[131] S. Komaki, I. Horikawa, K. Morita, and Y. Okamoto, "Characteristics of a high capacity 16 QAM digital radio system in multipath fading," *IEEE Trans. Commun.*, vol. 27, no. 12, pp. 1854–1861, Dec. 1979.

[132] J. Oetting, "A comparison of modulation techniques for digital radio," *IEEE Trans. Commun.*, vol. 27, no. 12, pp. 1752–1762, Dec. 1979.

[133] V. Prabhu, "Cochannel interference immunity of high capacity QAM," *IET Electron. Lett.*, vol. 17, no. 19, pp. 680–681, Sep. 1981.

[134] A. Giger and W. Barnett, "Effects of multipath propagation on digital radio," *IEEE Trans. Commun.*, vol. 29, no. 9, pp. 1345–1352, Sep. 1981.

[135] M. Joindot, A. Leclert, J. Oudart, C. Rolland, and P. Vandamme, "Baseband adaptive equalization for a 16 QAM system in the presence of multipath propagation," in *Proc. IEEE ICC)*, Jan. 1981, pp. 13.3.1–13.3.6.

[136] T. Hill and K. Feher, "A performance study of NLA 64-state QAM," *IEEE Trans. Commun.*, vol. 31, no. 6, pp. 821–826, Jun. 1983.

[137] K. Feher, "Digital Communications: Microwave Applications," *Englewood Cliffs, NJ, Prentice-Hall, Inc., 1981. 285 p.*, 1981.

[138] T. Noguti, "6GHz 135MBPS digital radio system with 64QAM modulation," in *Proc. IEEE ICC*, 1983, pp. F2–4.

[139] Y. Saito, M. MUROTANI *et al.*, "Feasibility considerations of high-level QAM multi-carrier system," in *Proc. IEEE ICC*, Jan. 1984, pp. 665–671.

[140] J. McNicol, F. Rivest *et al.*, "Design and application of the RD-4A and RD-6A 64 QAM digital radio systems," in *Proc. IEEE ICC*, Jan. 1984, pp. 646–652.

[141] A. Benveniste and M. Goursat, "Blind equalizers," *IEEE Trans. Commun.*, vol. 32, no. 8, pp. 871–883, Aug. 1984.

[142] R. Steele, "Towards a high-capacity digital cellular mobile radio system," in *Proc. IEE*, vol. 132, no. 5. IET, Aug. 1985, pp. 405–415.

[143] M. Borgne, "Comparison of high-level modulation schemes for high-capacity digital radio systems," *IEEE Trans. Commun.*, vol. 33, no. 5, pp. 442–449, May 1985.

[144] K.-T. Wu and K. Feher, "256-QAM modem performance in distorted channels," *IEEE Trans. Commun.*, vol. 33, no. 5, pp. 487–491, May 1985.

[145] P. Mathiopoulos and K. Feher, "Performance evaluation of a 512-QAM system in distorted channels," in *Proc. IEE*, vol. 133, no. 2. IET, Apr. 1986, pp. 199–204.

[146] M. Shafi and D. Moore, "Further results on adaptive equalizer improvements for 16 QAM and 64 QAM digital radio," *IEEE Trans. Commun.*, vol. 34, no. 1, pp. 59–66, Jan. 1986.

[147] C.-E. Sundberg, W. Wong, and R. Steele, "Logarithmic PCM weighted QAM transmission over Gaussian and Rayleigh fading channels," in *Proc. IEE*, vol. 134, no. 6. IET, Oct. 1987, pp. 557–570.

[148] R. Steele, C.-E. Sundberg, and W. Wong, "Transmission of log-PCM via QAM over Gaussian and Rayleigh fading channels," in *Proc. IEE*, vol. 134, no. 6. IET, Oct. 1987, pp. 539–556.

[149] Y. Nakamura, Y. Saito, and S. Aikawa, "256 QAM modem for multicarrier 400 Mbit/s digital radio," *IEEE J. Sel. Areas Commun.*, vol. 5, no. 3, pp. 329–335, Apr. 1987.

[150] A. Rustako, L. Greenstein, R. Roman, and A. A. Saleh, "Using times-four carrier recovery in M-QAM digital radio receivers," *IEEE J. Sel. Areas Commun.*, vol. 5, no. 3, pp. 524–533, Apr. 1987.

[151] S. Pupolin and L. Greenstein, "Performance analysis of digital radio links with nonlinear transmit amplifiers," *IEEE J. Sel. Areas Commun.*, vol. 5, no. 3, pp. 534–546, Apr. 1987.

[152] O. Andrisano, G. Bianconi, and L. Calandrino, "Adaptive equalization of high capacity M-QAM radio systems on multipath fading channels," *IEEE J. Sel. Areas Commun.*, vol. 5, no. 3, pp. 457–465, Apr. 1987.

[153] K. Vogel, "Orthogonal cochannel operation for high spectrum efficiency based on the example of 16 QAM-140 Mbit/s systems using rolloff 0.19," *IEEE J. Sel. Areas Commun.*, vol. 5, no. 3, pp. 321–328, Apr. 1987.

[154] J. Chamberlin, C. Hester, J. Meyers, T. Mock, F. Moody, R. Simons, E. Bahm, and J. Ritchie, "Design and field test of a 256-QAM DIV modem," *IEEE J. Sel. Areas Commun.*, vol. 5, no. 3, pp. 349–356, Apr. 1987.

[155] B. Collins, T. Fischer, S. Gronemeyer, and R. McGuire, "Application of coded modulation to 1.544-Mbit/s data-in-voice modems for FDM FM and SSB analog radio systems," *IEEE J. Sel. Areas Commun.*, vol. 5, no. 3, pp. 369–377, Apr. 1987.

[156] P. Duvoisin, S. Hsieh, and E. Williamson, "The operation of dual polarized QAM systems in the presence of depolarization crosstalk and differential fading," *IEEE J. Sel. Areas Commun.*, vol. 5, no. 3, pp. 437–447, Apr. 1987.

[157] G. Sebald, B. Lankl, and J. Nossek, "Advanced time-and frequency-domain adaptive equalization in multilevel QAM digital radio systems," *IEEE J. Sel. Areas Commun.*, vol. 5, no. 3, pp. 448–456, Apr. 1987.

[158] M. Borgne, "A new class of adaptive cross-polarization interference cancellers for digital radio systems," *IEEE J. Sel. Areas Commun.*, vol. 5, no. 3, pp. 484–492, Apr. 1987.

[159] B. Baccetti, S. Bellini, G. Filiberti, and G. Tartara, "Full digital adaptive equalization in 64-QAM radio systems," *IEEE J. Sel. Areas Commun.*, vol. 5, no. 3, pp. 466–475, Apr. 1987.

[160] R. Agusti, F. Casadevall, and J. Olmos, "Performance of fractioned and nonfractioned equalizers with high-level QAM," *IEEE J. Sel. Areas Commun.*, vol. 5, no. 3, pp. 476–483, Apr. 1987.

[161] H. Matsue, H. Ohtsuka, and T. Murase, "Digitalized cross-polarization interference canceller for multilevel digital radio," *IEEE J. Sel. Areas Commun.*, vol. 5, no. 3, pp. 493–501, Apr. 1987.

[162] B. Vucetic, D. Skellern, M. Miller, and L. Zhang, "Modelling and simulation of M-QAM digital radio systems ," *Math. Comput. Simulat.*, vol. 30, no. 1, pp. 69 – 73, Feb. 1988.

[163] E. Carpine, N. D'Andrea, U. Mengali, and G. Russo, "Comparative study of modulation techniques for microwave digital radios," in *Proc. IEEE GLOBECOM*. IEEE, 1988, pp. 265–269.

[164] J. C. Chuang, "The effects of time-delay spread on QAM with non-linearity switched filters in a portable radio communications channel," *IEEE Trans. Veh. Technol.*, vol. 38, no. 1, pp. 9–13, Feb. 1989.

[165] J. W. Craig, "A new simple and exact result for calculating the probability of error for two-dimensional signal constellations," in *Proc. IEEE MILCOM*, Nov. 1991, pp. 571–575.

[166] M. K. Simon, S. M. Hinedi, and W. C. Lindsey, *Digital Communication Techniques: Signal Design and Detection*. Englewood Cliffs, NJ: Prentice Hall, 1995.

[167] L. Hanzo, R. Steele, and P. Fortune, "A subband coding, BCH coding, and 16-QAM system for mobile radio speech communications," *IEEE Trans. Veh. Technol.*, vol. 39, no. 4, pp. 327–339, Nov. 1990.

[168] W. T. Webb, "Modulation methods for PCNs," *IEEE Commun. Mag.*, vol. 30, no. 12, pp. 90–95, Dec. 1992.

[169] T. Sunaga and S. Sampei, "Performance of multi-level QAM with post-detection maximal ratio combining space diversity for digital land-mobile radio communications," *IEEE Trans. Veh. Technol.*, vol. 42, no. 3, pp. 294–301, Aug. 1993.

[170] S. Sampei and T. Sunaga, "Rayleigh fading compensation for QAM in land mobile radio communications," *IEEE Trans. Veh. Technol.*, vol. 42, no. 2, pp. 137–147, May. 1993.

[171] J. Du, Y. Kamio, H. Sasaoka, and B. Vucetic, "New 32-QAM trellis codes for fading channels," *IET Electron. Lett.*, vol. 29, no. 20, pp. 1745–1746, Sep. 1993.

[172] L. M. Jalloul and J. M. Holtzman, "Performance analysis of DS/CDMA with noncoherent M-ary orthogonal modulation in multipath fading channels," *IEEE J. Sel. Areas Commun.*, vol. 12, no. 5, pp. 862–870, Jun. 1994.

[173] A. Aghamohammadi and H. Meyr, "On the error probability of linearly modulated signals on Rayleigh frequency-flat fading channels," *IEEE Trans. Commun.*, vol. 38, no. 11, pp. 1966–1970, Nov. 1990.

[174] M. G. Shayesteh and A. Aghamohammadi, "On the error probability of linearly modulated signals on frequency-flat Ricean, Rayleigh, and AWGN channels," *IEEE Trans. Commun.*, vol. 43, no. 2/3/4, pp. 1454–1466, Feb. 1995.

[175] J. Torrance and L. Hanzo, "Optimisation of switching levels for adaptive modulation in slow Rayleigh fading," *IET Electron. Lett.*, vol. 32, no. 13, pp. 1167–1169, Jun. 1996.

[176] A. J. Goldsmith and S.-G. Chua, "Adaptive coded modulation for fading channels," *IEEE Trans. Commun.*, vol. 46, no. 5, pp. 595–602, May 1998.

[177] J. Lu, T. T. Tjhung, and C. C. Chai, "Error probability performance of L-branch diversity reception of MQAM in Rayleigh fading," *IEEE Trans. Commun.*, vol. 46, no. 2, pp. 179–181, Feb. 1998.

[178] M.-S. Alouini and A. J. Goldsmith, "A unified approach for calculating error rates of linearly modulated signals over generalized fading channels," *IEEE Trans. Commun.*, vol. 47, no. 9, pp. 1324–1334, Sep. 1999.

[179] V. K. Lau and S. V. Maric, "Variable rate adaptive modulation for DS-CDMA," *IEEE Trans. Commun.*, vol. 47, no. 4, pp. 577–589, Apr. 1999.

[180] C. H. Wong and L. Hanzo, "Upper-bound performance of a wideband burst-by-burst adaptive modem," in *Proc. IEEE VTC*, vol. 3. IEEE, May 1999, pp. 1851–1855.

[181] M.-S. Alouini, X. Tang, and A. J. Goldsmith, "An adaptive modulation scheme for simultaneous voice and data transmission over fading channels," *IEEE J. Sel. Areas Commun.*, vol. 17, no. 5, pp. 837–850, May 1999.

[182] X. Qiu and K. Chawla, "On the performance of adaptive modulation in cellular systems," *IEEE Trans. Commun.*, vol. 47, no. 6, pp. 884–895, Jun. 1999.

[183] J. M. Torrance, L. Hanzo, and T. Keller, "Interference aspects of adaptive modems over slow Rayleigh fading channels," *IEEE Trans. Veh. Technol.*, vol. 48, no. 5, pp. 1527–1545, Sep. 1999.

[184] X. Tang, M. S. Alouini, and A. J. Goldsmith, "Effect of channel estimation error on M-QAM BER performance in Rayleigh fading," *IEEE Trans. Commun.*, vol. 47, no. 12, pp. 1856–1864, Dec. 1999.

[185] L.-L. Yang and L. Hanzo, "A recursive algorithm for the error probability evaluation of M-QAM," *IEEE Commun. Lett.*, vol. 4, no. 10, pp. 304–306, Oct. 2000.

[186] K. J. Hole, H. Holm, and G. E. Oien, "Adaptive multidimensional coded modulation over flat fading channels," *IEEE J. Sel. Areas Commun.*, vol. 18, no. 7, pp. 1153–1158, Jul. 2000.

[187] P. Ormeci, X. Liu, D. L. Goeckel, and R. D. Wesel, "Adaptive bit-interleaved coded modulation," *IEEE Trans. Commun.*, vol. 49, no. 9, pp. 1572–1581, Sep. 2001.

[188] J. S. Blogh, P. J. Cherriman, and L. Hanzo, "Dynamic channel allocation techniques using adaptive modulation and adaptive antennas," *IEEE J. Sel. Areas Commun.*, vol. 19, no. 2, pp. 312–321, Feb. 2001.

[189] S. T. Chung and A. J. Goldsmith, "Degrees of freedom in adaptive modulation: a unified view," *IEEE Trans. Commun.*, vol. 49, no. 9, pp. 1561–1571, Sep. 2001.

[190] K. Cho and D. Yoon, "On the general BER expression of one-and two-dimensional amplitude modulations," *IEEE Trans. Commun.*, vol. 50, no. 7, pp. 1074–1080, Nov. 2002.

[191] M. M. Wang, W. Xiao, and T. Brown, "Soft decision metric generation for QAM with channel estimation error," *IEEE Trans. Commun.*, vol. 50, no. 7, pp. 1058–1061, Nov. 2002.

[192] S. A. Jafar and A. Goldsmith, "Adaptive multirate CDMA for uplink throughput maximization," *IEEE Trans. Wireless Commun.*, vol. 2, no. 2, pp. 218–228, Mar. 2003.

[193] B. Choi and L. Hanzo, "Optimum mode-switching-assisted constant-power single-and multicarrier adaptive modulation," *IEEE Trans. Veh. Technol.*, vol. 52, no. 3, pp. 536–560, May 2003.

[194] S. Vishwanath and A. Goldsmith, "Adaptive turbo-coded modulation for flat-fading channels," *IEEE Trans. Commun.*, vol. 51, no. 6, pp. 964–972, Jun. 2003.

[195] K. L. Baum, T. A. Kostas, P. J. Sartori, and B. K. Classon, "Performance characteristics of cellular systems with different link adaptation strategies," *IEEE Trans. Veh. Technol.*, vol. 52, no. 6, pp. 1497–1507, Nov. 2003.

[196] S. Falahati, A. Svensson, T. Ekman, and M. Sternad, "Adaptive modulation systems for predicted wireless channels," *IEEE Trans. Commun.*, vol. 52, no. 2, pp. 307–316, Mar. 2004.

[197] Shoumin Liu and Zhi Tian, "Near-optimum soft decision equalization for frequency selective MIMO channels," *IEEE Trans. Signal Process.*, vol. 52, no. 3, pp. 721–733, Mar. 2004.

[198] G. Oien, H. Holm, and K. J. Hole, "Impact of channel prediction on adaptive coded modulation performance in Rayleigh fading," *IEEE Trans. Veh. Technol.*, vol. 53, no. 3, pp. 758–769, May 2004.

[199] L. Cao and N. C. Beaulieu, "Exact error-rate analysis of diversity 16-QAM with channel estimation error," *IEEE Trans. Commun.*, vol. 52, no. 6, pp. 1019–1029, Jun. 2004.

[200] X. Cai and G. B. Giannakis, "Adaptive PSAM accounting for channel estimation and prediction errors," *IEEE Trans. Wireless Commun.*, vol. 4, no. 1, pp. 246–256, Jan. 2005.

[201] T. Yoo, R. J. Lavery, A. Goldsmith, and D. J. Goodman, "Throughput optimization using adaptive techniques," *IEEE Commun. Lett.*, p. 18, Jan. 2006.

[202] A. Lozano, A. M. Tulino, and S. Verdú, "Optimum power allocation for parallel Gaussian channels with arbitrary input distributions," *IEEE Trans. Inf. Theory*, vol. 52, no. 7, pp. 3033–3051, Jul. 2006.

[203] K.-B. Song, A. Ekbal, S. T. Chung, and J. M. Cioffi, "Adaptive modulation and coding (AMC) for bit-interleaved coded OFDM (BIC-OFDM)," *IEEE Trans. Wireless Commun.*, vol. 5, no. 7, pp. 1685–1694, Aug. 2006.

[204] A. Conti, M. Z. Win, and M. Chiani, "Slow adaptive M-QAM with diversity in fast fading and shadowing," *IEEE Trans. Commun.*, vol. 55, no. 5, pp. 895–905, May 2007.

[205] F. Meshkati, A. J. Goldsmith, H. V. Poor, and S. C. Schwartz, "A game-theoretic approach to energy-efficient modulation in CDMA networks with delay QoS constraints," *IEEE J. Sel. Areas Commun.*, vol. 25, no. 6, pp. 1069–1078, Jul. 2007.

[206] P. K. Vitthaladevuni and M.-S. Alouini, "BER computation of 4/M-QAM hierarchical constellations," *IEEE Trans. Broadcast.*, vol. 47, no. 3, pp. 228–239, Sep. 2001.

[207] D. Dixit and P. R. Sahu, "Symbol error rate of rectangular QAM with best-relay selection in cooperative systems over Rayleigh fading channels," *IEEE Commun. Lett.*, vol. 16, no. 4, pp. 466–469, Apr. 2012.

[208] ——, "Performance of L-branch MRC receiver in η-μ and κ-μ fading channels for QAM signals," *IEEE Wireless Commun. Lett.*, vol. 1, no. 4, pp. 316–319, Aug. 2012.

[209] J. P. Peña-Martín, J. M. Romero-Jerez, and C. Tellez-Labao, "Performance of selection combining diversity in $\eta - \mu$ fading channels with integer values of μ," *IEEE Trans. Veh. Technol.*, vol. 64, no. 2, pp. 834–839, Feb. 2015.

[210] D. Dixit and P. R. Sahu, "Performance of dual-hop DF relaying systems with QAM schemes over mixed η-μ and κ-μ fading channels," *Wiley Trans. Emerg. Telecommun. Technol.*, vol. 28, no. 11, p. e3179, Nov. 2017.

[211] K. Miyauchi, S. Seki, and H. Ishio, "New technique for generating and detecting multilevel signal formats," *IEEE Trans. Commun.*, vol. 24, no. 2, pp. 263–267, Feb. 1976.

[212] I. Horikawa, T. Murase, and Y. Saito, "Design and performances of a 200 Mbit/s 16 QAM digital radio system," *IEEE Trans. Commun.*, vol. 27, no. 12, pp. 1953–1958, Dec. 1979.

[213] V. Prabhu, "The detection efficiency of 16-ary QAM," *Bell Syst. Tech. J.*, vol. 59, no. 4, pp. 639–656, Apr. 1980.

[214] H. Yamamoto, "Advanced 16-QAM techniques for digital microwave radio," *IEEE Commun. Mag.*, vol. 19, no. 3, pp. 36–45, May 1981.

[215] D. Morais and K. Feher, "NLA-QAM: A Method for Generating High-Power QAM Signals Through Nonlinear Amplification," *IEEE Trans. Commun.*, vol. 30, no. 3, pp. 517–522, Mar. 1982.

[216] K. Feher, "Digital Communications: Satellite/Earth Station Engineering," *Englewood Cliffs, NJ, Prentice-Hall, Inc., 1983, 492 p.*, 1983.

[217] G. Foschini, "Equalizing without altering or detecting data," *Bell Syst. Tech. J.*, vol. 64, no. 8, pp. 1885–1911, Oct. 1985.

[218] K. Feher, "1024-QAM and 256-QAM coded modems for microwave and cable system applications," *IEEE J. Sel. Areas Commun.*, vol. 5, no. 3, pp. 357–368, Apr. 1987.

[219] H. Sinnreich and D. Stom, "System parameters and performance of high speed modems on analog radio," *IEEE J. Sel. Areas Commun.*, vol. 5, no. 3, pp. 342–348, Apr. 1987.

[220] J. Choi and V. Chan, "Predicting and adapting satellite channels with weather-induced impairments," *IEEE Trans. Aerosp. Electron. Syst.*, vol. 38, no. 3, pp. 779–790, Dec. 2002.

[221] M. A. Díaz, N. Courville, C. Mosquera, G. Liva, and G. E. Corazza, "Non-linear interference mitigation for broadband multimedia satellite systems," in *Proc. IEEE IWSSC*. IEEE, Sep. 2007, pp. 61–65.

[222] T. Hwang, C. Yang, G. Wu, S. Li, and G. Y. Li, "OFDM and its wireless applications: A survey," *IEEE Trans. Veh. Technol.*, vol. 58, no. 4, pp. 1673–1694, Aug. 2008.

[223] A. F. Molisch, *Wireless Communications*. John Wiley & Sons, 2012, vol. 34.

[224] P. K. Singya, N. Kumar, and V. Bhatia, "Mitigating NLD for wireless networks: Effect of nonlinear power amplifiers on future wireless communication networks," *IEEE Microwave Mag.*, vol. 18, no. 5, pp. 73–90, Jul. 2017.

[225] B. Hirosaki, "An Orthogonally Multiplexed QAM System Using the Discrete Fourier Transform," *IEEE Trans. Commun.*, vol. 29, no. 7, pp. 982–989, Jun. 1981.

[226] C. RoBing and V. Tarokh, "A construction of OFDM 16-QAM sequences having low peak powers," *IEEE Trans. Inf. Theory*, vol. 47, no. 5, pp. 2091–2094, Jul. 2001.

[227] A. G. Marqués, F. F. Digham, and G. B. Giannakis, "Optimizing power efficiency of OFDM using quantized channel state information," *IEEE J. Sel. Areas Commun.*, vol. 24, no. 8, pp. 1581–1592, Jul. 2006.

[228] Z. Q. Taha and X. Liu, "Low PMEPR code based on star-16-QAM constellation for OFDM," *IEEE Commun. Lett.*, vol. 11, no. 9, pp. 747–749, Sep. 2007.

[229] G. Miao, N. Himayat, and G. Y. Li, "Energy-efficient link adaptation in frequency-selective channels," *IEEE Trans. Commun.*, vol. 58, no. 2, pp. 545–554, Feb. 2010.

[230] A. Annamalai, C. Tellambura, and V. K. Bhargava, "Exact evaluation of maximal-ratio and equal-gain diversity receivers for M-ary QAM on Nakagami fading channels," *IEEE Trans. Commun.*, vol. 47, no. 9, pp. 1335–1344, Sep. 1999.

[231] S. Catreux, P. F. Driessen, and L. J. Greenstein, "Attainable throughput of an interference-limited multiple-input multiple-output (MIMO) cellular system," *IEEE Trans. Commun.*, vol. 49, no. 8, pp. 1307–1311, Aug. 2001.

[232] ——, "Data throughputs using multiple-input multiple-output (MIMO) techniques in a noise-limited cellular environment," *IEEE Trans. Wireless Commun.*, vol. 1, no. 2, pp. 226–235, Aug. 2002.

[233] P. Xia, S. Zhou, and G. B. Giannakis, "Adaptive MIMO-OFDM based on partial channel state information," *IEEE Trans. signal process.*, vol. 52, no. 1, pp. 202–213, Jan. 2004.

[234] S. Zhou and G. B. Giannakis, "Adaptive modulation for multiantenna transmissions with channel mean feedback," *IEEE Trans. Wireless Commun.*, vol. 3, no. 5, pp. 1626–1636, Oct. 2004.

[235] ——, "How accurate channel prediction needs to be for transmit-beamforming with adaptive modulation over Rayleigh MIMO channels?" *IEEE Trans. Wireless Commun.*, vol. 3, no. 4, pp. 1285–1294, Jun. 2004.

[236] C. Windpassinger, R. F. Fischer, T. Vencel, and J. B. Huber, "Precoding in multiantenna and multiuser communications," *IEEE Trans. Wireless Commun.*, vol. 3, no. 4, pp. 1305–1316, Jul. 2004.

[237] Z. Zhou, B. Vucetic, M. Dohler, and Y. Li, "MIMO systems with adaptive modulation," *IEEE Trans. Veh. Technol.*, vol. 54, no. 5, pp. 1828–1842, Nov. 2005.

[238] Y. J. Zhang and K. B. Letaief, "An efficient resource-allocation scheme for spatial multiuser access in MIMO/OFDM systems," *IEEE Trans. Commun.*, vol. 53, no. 1, pp. 107–116, Feb. 2005.

[239] P. Xia, S. Zhou, and G. B. Giannakis, "Multiantenna adaptive modulation with beamforming based on bandwidth-constrained feedback," *IEEE Trans. Commun.*, vol. 53, no. 3, pp. 526–536, Apr. 2005.

[240] D. P. Palomar and S. Barbarossa, "Designing MIMO communication systems: Constellation choice and linear transceiver design," *IEEE Trans. Signal Process.*, vol. 53, no. 10, pp. 3804–3818, Sep. 2005.

[241] B. Xia and J. Wang, "Analytical study of QAM with interference cancellation for high-speed multicode CDMA," *IEEE Trans. Veh. Technol.*, vol. 54, no. 3, pp. 1070–1080, May 2005.

[242] Y. Ko and C. Tepedelenlioglu, "Orthogonal space-time block coded rate-adaptive modulation with outdated feedback," *IEEE Trans. Wireless Commun.*, vol. 5, no. 2, pp. 290–295, Mar. 2006.

[243] J. L. Vicario, M. A. Lagunas, and C. Antón-Haro, "A cross-layer approach to transmit antenna selection," *IEEE Trans. Wireless Commun.*, vol. 5, no. 8, pp. 1993–1997, Sep. 2006.

[244] S. Yang and J.-C. Belfiore, "Optimal space–time codes for the MIMO amplify-and-forward cooperative channel," *IEEE Trans. Inf. Theory*, vol. 53, no. 2, pp. 647–663, Jan. 2007.

[245] M. Haleem, C. Mathur, R. Chandramouli, and K. Subbalakshmi, "Opportunistic encryption: A trade-off between security and throughput in wireless networks," *IEEE Trans. Depend. Secure Comput.*, vol. 4, no. 4, pp. 313–324, Nov. 2007.

[246] Y. Ding, J.-K. Zhang, and K. M. Wong, "The amplify-and-forward half-duplex cooperative system: Pairwise error probability and precoder design," *IEEE Trans. Signal Process.*, vol. 55, no. 2, pp. 605–617, Jan. 2007.

[247] X. Yu, S.-H. Leung, W. H. Mow, and W.-K. Wong, "Performance of variable-power adaptive modulation with space–time coding and imperfect CSI in MIMO systems," *IEEE Trans. Veh. Technol.*, vol. 58, no. 4, pp. 2115–2120, Jul. 2008.

[248] W. W. Ho and Y.-C. Liang, "Optimal resource allocation for multiuser MIMO-OFDM systems with user rate constraints," *IEEE Trans. Veh. Technol.*, vol. 58, no. 3, pp. 1190–1203, Jun. 2008.

[249] C.-B. Chae, T. Tang, R. W. Heath Jr, and S. Cho, "MIMO relaying with linear processing for multiuser transmission in fixed relay networks," *IEEE Trans. Signal Process.*, vol. 56, no. 2, pp. 727–738, Feb. 2008.

[250] J. Jeganathan, A. Ghrayeb, L. Szczecinski, and A. Ceron, "Space shift keying modulation for MIMO channels," *IEEE Trans. Wireless Commun.*, vol. 8, no. 7, pp. 3692–3703, Jul. 2009.

[251] K.-J. Lee, H. Sung, E. Park, and I. Lee, "Joint optimization for one and two-way MIMO AF multiple-relay systems," *IEEE Trans. Wireless Commun.*, vol. 9, no. 12, pp. 3671–3681, Oct. 2010.

[252] C.-A. Shen, A. M. Eltawil, K. N. Salama, and S. Mondal, "A best-first soft/hard decision tree searching MIMO decoder for a 4×4 64-QAM system," *IEEE Trans. Very Large Scale Integr. (VLSI) Syst.*, vol. 20, no. 8, pp. 1537–1541, Jul. 2011.

[253] T. Datta, N. Srinidhi, A. Chockalingam, and B. S. Rajan, "A hybrid RTS-BP algorithm for improved detection of large-MIMO M-QAM signals," in *Proc. NCC*. IEEE, Jan. 2011, pp. 1–5.

[254] S. Sugiura, C. Xu, S. X. Ng, and L. Hanzo, "Reduced-complexity coherent versus non-coherent QAM-aided space-time shift keying," *IEEE Trans. Commun.*, vol. 59, no. 11, pp. 3090–3101, Oct. 2011.

[255] A. K. Sadek, W. Su, and K. R. Liu, "Multinode cooperative communications in wireless networks," *IEEE Trans. Signal Process.*, vol. 55, no. 1, pp. 341–355, Dec. 2006.

[256] R. Chen, R. W. Heath, and J. G. Andrews, "Transmit selection diversity for unitary precoded multiuser spatial multiplexing systems with linear receivers," *IEEE Trans. Signal Process.*, vol. 55, no. 3, pp. 1159–1171, Mar. 2007.

[257] N. Kim, Y. Lee, and H. Park, "Performance analysis of MIMO system with linear MMSE receiver," *IEEE Trans. Wireless Commun.*, vol. 7, no. 11, pp. 4474–4478, Dec. 2008.

[258] Y. Ma, D. Zhang, A. Leith, and Z. Wang, "Error performance of transmit beamforming with delayed and limited feedback," *IEEE Trans. Wireless Commun.*, vol. 8, no. 3, pp. 1164–1170, Mar. 2009.

[259] Y. Lee, M.-H. Tsai, and S.-I. Sou, "Performance of decode-and-forward cooperative communications with multiple dual-hop relays over Nakagami-m fading channels," *IEEE Trans. Wireless Commun.*, vol. 8, no. 6, pp. 2853–2859, Jun. 2009.

[260] N. Kim and H. Park, "Bit error performance of convolutional coded MIMO system with linear MMSE receiver," *IEEE Trans. Wireless Commun.*, vol. 8, no. 7, pp. 3420–3424, Jul. 2009.

[261] J. M. Romero-Jerez and A. J. Goldsmith, "Performance of multichannel reception with transmit antenna selection in arbitrarily distributed Nagakami fading channels," *IEEE Trans. Wireless Commun.*, vol. 8, no. 4, Apr. 2009.

[262] Z. Chen, Z. Chi, Y. Li, and B. Vucetic, "Error performance of maximal-ratio combining with transmit antenna selection in flat Nakagami-m fading channels," *IEEE Trans. Wireless Commun.*, vol. 8, no. 1, pp. 424–431, Feb. 2009.

[263] S. Chen, W. Wang, X. Zhang, and D. Zhao, "Performance of amplify-and-forward MIMO relay channels with transmit antenna selection and maximal-ratio combining," in *Proc. IEEE WCNC*. IEEE, Apr. 2009, pp. 1–6.

[264] J.-S. Kim, S.-H. Moon, and I. Lee, "A new reduced complexity ML detection scheme for MIMO systems," *IEEE Trans. Commun.*, vol. 58, no. 4, pp. 1302–1310, Mar. 2010.

[265] H. A. Suraweera, G. K. Karagiannidis, Y. Li, H. K. Garg, A. Nallanathan, and B. Vucetic, "Amplify-and-forward relay transmission with end-to-end antenna selection," in *Proc. IEEE WCNC*. IEEE, Apr. 2010, pp. 1–6.

[266] H. Kim, N. Kim, W. Choi, and H. Park, "Performance of multiuser transmit diversity in spatially correlated channels," *IEEE Commun. Lett.*, vol. 14, no. 9, pp. 824–826, Aug. 2010.

[267] J. Wang, O. Wen, H. Chen, and S. Li, "Power allocation between pilot and data symbols for MIMO systems with MMSE detection under MMSE channel estimation," *EURASIP J. Wireless Commun. Netw.*, vol. 2011, pp. 1–9, Dec. 2011.

[268] C. Song, K.-J. Lee, and I. Lee, "Performance analysis of MMSE-based amplify and forward spatial multiplexing MIMO relaying systems," *IEEE Trans. Commun.*, vol. 59, no. 12, pp. 3452–3462, Oct. 2011.

[269] P. Liu and I.-M. Kim, "Exact and closed-form error performance analysis for hard MMSE-SIC detection in MIMO systems," *IEEE Trans. Commun.*, no. 9, pp. 2463–2477, Jun. 2011.

[270] H. A. Suraweera, P. J. Smith, A. Nallanathan, and J. S. Thompson, "Amplify-and-forward relaying with optimal and suboptimal transmit antenna selection," *IEEE Trans. Wireless Commun.*, vol. 10, no. 6, pp. 1874–1885, Apr. 2011.

[271] M. Torabi and D. Haccoun, "Performance analysis of joint user scheduling and antenna selection over MIMO fading channels," *IEEE Signal Process. Lett.*, vol. 18, no. 4, pp. 235–238, Apr. 2011.

[272] A. F. Coskun and O. Kucur, "Performance analysis of joint single transmit and receive antenna selection in Nakagami-m fading channels," *IEEE Commun. Lett.*, vol. 15, no. 2, pp. 211–213, Feb. 2011.

[273] ——, "Performance analysis of maximal-ratio transmission/receive antenna selection in Nakagami- m fading channels with channel estimation errors and feedback delay," *IEEE Trans. Veh. Technol.*, vol. 61, no. 3, pp. 1099–1108, Mar. 2012.

[274] A. Bansal, M. R. Bhatnagar, A. Hjorungnes, and Z. Han, "Low-complexity decoding in DF MIMO relaying system," *IEEE Trans. Veh. Technol.*, vol. 62, no. 3, pp. 1123–1137, Nov. 2012.

[275] E. Eraslan, B. Daneshrad, and C.-Y. Lou, "Performance indicator for MIMO MMSE receivers in the presence of channel estimation error," *IEEE Wireless Commun. Lett.*, vol. 2, no. 2, pp. 211–214, Feb. 2013.

[276] M. Arti and M. R. Bhatnagar, "Maximal ratio transmission in AF MIMO relay systems over Nakagami-m fading channels," *IEEE Trans. Veh. Technol.*, vol. 64, no. 5, pp. 1895–1903, Jul. 2014.

[277] D. Zhao, H. Zhao, M. Jia, and W. Xiang, "Smart relaying for selection combining based decode-and-forward cooperative networks," *IEEE Commun. Lett.*, vol. 18, no. 1, pp. 74–77, Jan. 2014.

[278] H. Kim, T. Kim, M. Min, and G. Im, "Low-complexity detection scheme for cooperative MIMO systems with decode-and-forward relays," *IEEE Trans. Commun.*, vol. 63, no. 1, pp. 94–106, Jan. 2015.

[279] C. Song, K.-J. Lee, and I. Lee, "Designs of MIMO amplify-and-forward wireless relaying networks: Practical challenges and solutions based on MSE decomposition," *IEEE Access*, vol. 5, pp. 9223–9234, May 2017.

[280] A. J. Al-Askery, C. C. Tsimenidis, S. Boussakta, and J. A. Chambers, "Performance analysis of coded massive MIMO-OFDM systems using effective matrix inversion," *IEEE Trans. Commun.*, vol. 65, no. 12, pp. 5244–5256, Sep. 2017.

[281] P. L. Yeoh, M. Elkashlan, N. Yang, D. B. da Costa, and T. Q. Duong, "Unified analysis of transmit antenna selection in MIMO multirelay networks," *IEEE Trans. Veh. Technol.*, vol. 62, no. 2, pp. 933–939, Nov. 2012.

[282] P. Yang, Y. Xiao, Y. L. Guan, S. Li, and L. Hanzo, "Transmit antenna selection for multiple-input multiple-output spatial modulation systems," *IEEE Trans. Commun.*, vol. 64, no. 5, pp. 2035–2048, Mar. 2016.

[283] P. Siohan, C. Siclet, and N. Lacaille, "Analysis and design of OFDM/OQAM systems based on filterbank theory," *IEEE Trans. Signal Process.*, vol. 50, no. 5, pp. 1170–1183, Aug. 2002.

[284] R. Y. Mesleh, H. Haas, S. Sinanovic, C. W. Ahn, and S. Yun, "Spatial modulation," *IEEE Trans. Veh. Technol.*, vol. 57, no. 4, pp. 2228–2241, Jul. 2008.

[285] S. Hong, M. Sagong, C. Lim, S. Cho, K. Cheun, and K. Yang, "Frequency and quadrature-amplitude modulation for downlink cellular

OFDMA networks," *IEEE J. Sel. Areas Commun.*, vol. 32, no. 6, pp. 1256–1267, Jun. 2014.

[286] C.-B. Ha, Y.-H. You, and H.-K. Song, "Machine learning model for adaptive modulation of multi-stream in MIMO-OFDM system," *IEEE Access*, vol. 7, pp. 5141–5152, Dec. 2018.

[287] V. Tarokh, H. Jafarkhani, and A. R. Calderbank, "Space-time block codes from orthogonal designs," *IEEE Trans. Inf. Theory*, vol. 45, no. 5, pp. 1456–1467, Jul. 1999.

[288] H.-Y. Liu and R. Y. Yen, "Error probability for orthogonal space-time block code diversity system using rectangular QAM transmission over Rayleigh fading channels," *IEEE Trans. Signal Process.*, vol. 54, no. 4, pp. 1230–1241, Mar. 2006.

[289] Y. Han, S. H. Ting, C. K. Ho, and W. H. Chin, "Performance bounds for two-way amplify-and-forward relaying," *IEEE Trans. Wireless Commun.*, vol. 8, no. 1, pp. 432–439, Feb. 2009.

[290] S. Yang, T. Lv, and L. Hanzo, "Semidefinite programming relaxation based virtually antipodal detection for MIMO systems using Gray-coded high-order QAM," *IEEE Trans. Veh. Technol.*, vol. 62, no. 4, pp. 1667–1677, Dec. 2012.

[291] G. Wang and X.-G. Xia, "An orthogonal space-time coded CPM system with fast decoding for two transmit antennas," *IEEE Trans. Inf. Theory*, vol. 50, no. 3, pp. 486–493, Mar. 2004.

[292] L. Yang and J. Qin, "Performance of Alamouti scheme with transmit antenna selection for M-ray signals," *IEEE Trans. Wireless Commun.*, vol. 5, no. 12, pp. 3365–3369, Dec. 2006.

[293] A. Bansal, M. R. Bhatnagar, and A. Hjorungnes, "Decoding and performance bound of demodulate-and-forward based distributed Alamouti STBC," *IEEE Trans. Wireless Commun.*, vol. 12, no. 2, pp. 702–713, Dec. 2012.

[294] M. Kulkarni, L. Choudhary, B. Kumbhani, and R. S. Kshetrimayum, "Performance analysis comparison of transmit antenna selection with maximal ratio combining and orthogonal space time block codes in equicorrelated Rayleigh fading multiple input multiple output channels," *IET Commun.*, vol. 8, no. 10, pp. 1850–1858, Jun. 2014.

[295] A. Wiesel, Y. C. Eldar, and S. Shamai, "Semidefinite relaxation for detection of 16-QAM signaling in MIMO channels," *IEEE Signal Process. Lett.*, no. 9, pp. 653–656, Aug. 2005.

[296] N. D. Sidiropoulos and Z.-Q. Luo, "A semidefinite relaxation approach to MIMO detection for high-order QAM constellations," *IEEE Signal Process. Lett.*, vol. 13, no. 9, pp. 525–528, Aug. 2006.

[297] Y. Yang, C. Zhao, P. Zhou, and W. Xu, "MIMO detection of 16-QAM signaling based on semidefinite relaxation," *IEEE Signal Process. Lett.*, vol. 14, no. 11, pp. 797–800, Nov. 2007.

[298] Z. Mao, X. Wang, and X. Wang, "Semidefinite programming relaxation approach for multiuser detection of QAM signals," *IEEE Trans. Wireless Commun.*, vol. 6, no. 12, pp. 4275–4279, Dec. 2007.

[299] A. Mobasher, M. Taherzadeh, R. Sotirov, and A. K. Khandani, "A near-maximum-likelihood decoding algorithm for MIMO systems based on semi-definite programming," *IEEE Trans. Inf. Theory*, vol. 53, no. 11, pp. 3869–3886, Oct. 2007.

[300] W.-K. Ma, C.-C. Su, J. Jaldén, T.-H. Chang, and C.-Y. Chi, "The equivalence of semidefinite relaxation MIMO detectors for higher-order QAM," *IEEE J. Sel. Topics Signal Process.*, vol. 3, no. 6, pp. 1038–1052, Dec. 2009.

[301] J. N. Laneman, D. N. Tse, and G. W. Wornell, "Cooperative diversity in wireless networks: Efficient protocols and outage behavior," *IEEE Trans. Inf. Theory*, vol. 50, no. 12, pp. 3062–3080, Nov. 2004.

[302] K. R. Liu, A. K. Sadek, W. Su, and A. Kwasinski, *Cooperative Communications and Networking*. Cambridge University Press, 2009.

[303] A. Annamalai and C. Tellambura, "Error rates for Nakagami-m fading multichannel reception of binary and M-ary signals," *IEEE Trans. Commun.*, vol. 49, no. 1, pp. 58–68, Jan. 2001.

[304] M. Z. Win and J. H. Winters, "Virtual branch analysis of symbol error probability for hybrid selection/maximal-ratio combining in Rayleigh fading," *IEEE Trans. Commun.*, vol. 49, no. 11, pp. 1926–1934, Nov. 2001.

[305] R. U. Nabar, H. Bolcskei, and F. W. Kneubuhler, "Fading relay channels: Performance limits and space-time signal design," *IEEE J. Sel. Areas Commun.*, vol. 22, no. 6, pp. 1099–1109, Aug. 2004.

[306] A. Annamalai, C. Tellambura, and V. K. Bhargava, "A general method for calculating error probabilities over fading channels," *IEEE Trans. Commun.*, vol. 53, no. 5, pp. 841–852, May 2005.

[307] A. Ribeiro, X. Cai, and G. B. Giannakis, "Symbol error probabilities for general cooperative links," *IEEE Trans. Wireless Commun.*, vol. 4, no. 3, pp. 1264–1273, May 2005.

[308] W. Su, A. K. Sadek, and K. R. Liu, "SER performance analysis and optimum power allocation for decode-and-forward cooperation protocol in wireless networks," in *Proc. IEEE WCNC*, vol. 2. IEEE, Mar. 2005, pp. 984–989.

[309] Y. Zhao, R. Adve, and T. J. Lim, "Symbol error rate of selection amplify-and-forward relay systems," *IEEE Commun. Lett.*, vol. 10, no. 11, pp. 757–759, Dec. 2006.

[310] L. Le and E. Hossain, "Multihop cellular networks: Potential gains, research challenges, and a resource allocation framework," *IEEE Commun. Mag.*, vol. 45, no. 9, pp. 66–73, Oct. 2007.

[311] Y. Ma and J. Jin, "Effect of channel estimation errors on M-QAM with MRC and EGC in Nakagami fading channels," *IEEE Trans. Veh. Technol.*, vol. 56, no. 3, pp. 1239–1250, May 2007.

[312] S. Ikki and M. H. Ahmed, "Performance analysis of cooperative diversity wireless networks over Nakagami-m fading channel," *IEEE Commun. Lett.*, vol. 11, no. 4, pp. 334–336, Apr. 2007.

[313] W. Su, A. K. Sadek, and K. R. Liu, "Cooperative communication protocols in wireless networks: performance analysis and optimum power allocation," *Wireless Personal Commun.*, vol. 44, no. 2, pp. 181–217, Jan. 2008.

[314] Y. Ma, N. Yi, and R. Tafazolli, "Bit and power loading for OFDM-based three-node relaying communications," *IEEE Trans. Signal Process.*, vol. 56, no. 7, pp. 3236–3247, Jun. 2008.

[315] Z. Zhou, S. Zhou, S. Cui, and J.-H. Cui, "Energy-efficient cooperative communication in a clustered wireless sensor network," *IEEE Trans. Veh. Technol.*, vol. 57, no. 6, pp. 3618–3628, Feb. 2008.

[316] A. Maaref and S. Aïssa, "Exact error probability analysis of rectangular QAM for single-and multichannel reception in Nakagami-m fading channels," *IEEE Trans. Commun.*, vol. 57, no. 1, pp. 214–221, Jan. 2009.

[317] M. R. Bhatnagar, "Decode-and-forward-based differential modulation for cooperative communication system with unitary and nonunitary constellations," *IEEE Trans. Veh. Technol.*, vol. 61, no. 1, pp. 152–165, Nov. 2011.

[318] O. Amin and M. Uysal, "Optimal bit and power loading for amplify-and-forward cooperative OFDM systems," *IEEE Trans. Wireless Commun.*, vol. 10, no. 3, pp. 772–781, Jan. 2011.

[319] M. R. Bhatnagar and A. Hjorungnes, "ML decoder for decode-and-forward based cooperative communication system," *IEEE Trans. Wireless Commun.*, vol. 10, no. 12, pp. 4080–4090, Oct. 2011.

[320] Z. Ghassemlooy, S. Arnon, M. Uysal, Z. Xu, and J. Cheng, "Emerging optical wireless communications-advances and challenges," *IEEE J. Sel. Areas Commun.*, vol. 33, no. 9, pp. 1738–1749, Jul. 2015.

[321] R. Mitra and V. Bhatia, "Precoded chebyshev-NLMS-based predistorter for nonlinear LED compensation in NOMA-VLC," *IEEE Trans. Commun.*, vol. 65, no. 11, pp. 4845–4856, Nov. 2017.

[322] M. Z. Chowdhury, M. T. Hossan, A. Islam, and Y. M. Jang, "A comparative survey of optical wireless technologies: Architectures and applications," *IEEE Access*, vol. 6, pp. 9819–9840, Jan. 2018.

[323] M. Uysal and H. Nouri, "Optical wireless communicationsAn emerging technology," in *Proc. ICTON*. IEEE, Jul. 2014, pp. 1–7.

[324] Z. Zeng, S. Fu, H. Zhang, Y. Dong, and J. Cheng, "A survey of underwater optical wireless communications," *IEEE Commun. Surveys Tuts.*, vol. 19, no. 1, pp. 204–238, Oct. 2016.

[325] M.-A. Khalighi, S. Long, S. Bourennane, and Z. Ghassemlooy, "PAM- and CAP-based transmission schemes for visible-light communications," *IEEE Access*, vol. 5, pp. 27 002–27 013, Oct. 2017.

[326] R. Mitra and V. Bhatia, "Minimum Error Entropy Criterion Based Channel Estimation for Massive-MIMO in VLC," *IEEE Trans. Veh. Technol.*, vol. 68, no. 1, pp. 1014–1018, Nov. 2018.

[327] J. B. Carruthers and J. M. Kahn, "Multiple-subcarrier modulation for nondirected wireless infrared communication," *IEEE J. Sel. Areas Commun.*, vol. 14, no. 3, pp. 538–546, Apr. 1996.

[328] J. Vučić, C. Kottke, S. Nerreter, K.-D. Langer, and J. W. Walewski, "513 Mbit/s visible light communications link based on DMT-modulation of a white LED," *J. Lightw. Technol.*, vol. 28, no. 24, pp. 3512–3518, Dec. 2010.

[329] G. Ntogari, T. Kamalakis, J. Walewski, and T. Sphicopoulos, "Combining illumination dimming based on pulse-width modulation with visible-light communications based on discrete multitone," *IEEE/OSA J. Opt. Commun. Netw.*, vol. 3, no. 1, pp. 56–65, Jan. 2011.

[330] A. Khalid, G. Cossu, R. Corsini, P. Choudhury, and E. Ciaramella, "1-Gb/s transmission over a phosphorescent white LED by using rate-adaptive discrete multitone modulation," *IEEE Photon. J.*, vol. 4, no. 5, pp. 1465–1473, Jul. 2012.

[331] L. Hanzo, H. Haas, S. Imre, D. O'Brien, M. Rupp, and L. Gyongyosi, "Wireless myths, realities, and futures: from 3G/4G to optical and quantum wireless," *Proc. IEEE*, vol. 100, pp. 1853–1888, Apr. 2012.

[332] S. Dimitrov and H. Haas, "Information rate of OFDM-based optical wireless communication systems with nonlinear distortion," *J. Lightw. Technol.*, vol. 31, no. 6, pp. 918–929, Apr. 2012.

[333] A. H. Azhar, T.-A. Tran, and D. O'Brien, "A gigabit/s indoor wireless transmission using MIMO-OFDM visible-light communications," *IEEE Photon. Technol. Lett.*, vol. 25, no. 2, pp. 171–174, Dec. 2012.

[334] Y. Wang, Y. Wang, N. Chi, J. Yu, and H. Shang, "Demonstration of 575-Mb/s downlink and 225-Mb/s uplink bi-directional SCM-WDM visible light communication using RGB LED and phosphor-based LED," *Opt. Exp.*, vol. 21, no. 1, pp. 1203–1208, Jan. 2013.

[335] F. Wu, C. Lin, C. Wei, C. Chen, Z. Chen, H. Huang, and S. Chi, "Performance comparison of OFDM signal and CAP signal over high capacity RGB-LED-based WDM visible light communication," *IEEE Photon. J.*, vol. 5, no. 4, pp. 7 901 507–7 901 507, Jun. 2013.

[336] J.-Y. Sung, C.-W. Chow, and C.-H. Yeh, "Dimming-discrete-multi-tone (DMT) for simultaneous color control and high speed visible light communication," *Opt. Exp.*, vol. 22, no. 7, pp. 7538–7543, Apr. 2014.

[337] Y. Wang, X. Huang, J. Zhang, Y. Wang, and N. Chi, "Enhanced performance of visible light communication employing 512-QAM N-SC-FDE and DD-LMS," *Opt. Exp.*, vol. 22, no. 13, pp. 15 328–15 334, Jun. 2014.

[338] J.-Y. Sung, C.-W. Chow, and C.-H. Yeh, "Is blue optical filter necessary in high speed phosphor-based white light LED visible light communications?" *Opt. Exp.*, vol. 22, no. 17, pp. 20 646–20 651, Aug. 2014.

[339] P. H. Pathak, X. Feng, P. Hu, and P. Mohapatra, "Visible light communication, networking, and sensing: A survey, potential and challenges," *IEEE Commun. Surveys Tuts.*, vol. 17, no. 4, pp. 2047–2077, Sep. 2015.

[340] X. Huang, Z. Wang, J. Shi, Y. Wang, and N. Chi, "1.6 Gbit/s phosphorescent white LED based VLC transmission using a cascaded pre-equalization circuit and a differential outputs PIN receiver," *Opt. Exp.*, vol. 23, no. 17, pp. 22 034–22 042, Aug. 2015.

[341] D. Karunatilaka, F. Zafar, V. Kalavally, and R. Parthiban, "LED based indoor visible light communications: State of the art," *IEEE Commun. Surveys Tuts.*, vol. 17, no. 3, pp. 1649–1678, Mar. 2015.

[342] Y. Wang, X. Huang, L. Tao, J. Shi, and N. Chi, "4.5-Gb/s RGB-LED based WDM visible light communication system employing CAP modulation and RLS based adaptive equalization," *Opt. Exp.*, vol. 23, no. 10, pp. 13 626–13 633, May 2015.

[343] H. Chun, S. Rajbhandari, G. Faulkner, D. Tsonev, E. Xie, J. J. D. McKendry, E. Gu, M. D. Dawson, D. C. O'Brien, and H. Haas, "LED based wavelength division multiplexed 10 Gb/s visible light communications," *J. Lightw. Technol.*, vol. 34, no. 13, pp. 3047–3052, Jul. 2016.

[344] S. Jain, R. Mitra, and V. Bhatia, "Adaptive precoding-based detection algorithm for massive MIMO visible light communication," *IEEE Commun. Lett.*, vol. 22, no. 9, pp. 1842–1845, Jul. 2018.

[345] T. Zhang, Y. Zou, J. Sun, and S. Qiao, "Design of PAM-DMT-based hybrid optical OFDM for visible light communications," *IEEE Wireless Commun. Lett.*, vol. 8, no. 1, pp. 265–268, Sep. 2018.

[346] M. A. Khalighi and M. Uysal, "Survey on free space optical communication: A communication theory perspective," *IEEE Commun. Surveys Tuts.*, vol. 16, no. 4, pp. 2231–2258, Jun. 2014.

[347] H. Ochi, Y. Watanabe, and T. Shimura, "Basic study of underwater acoustic communication using 32-quadrature amplitude modulation," *Jpn. J. App. Phys.*, vol. 44, no. 6S, p. 4689, Jun. 2005.

[348] B. Cochenour, L. Mullen, and A. Laux, "Phase coherent digital communications for wireless optical links in turbid underwater environments," Tech. Rep., Jan. 2007.

[349] M. Kuschnerov, F. N. Hauske, K. Piyawanno, B. Spinnler, M. S. Alfiad, A. Napoli, and B. Lankl, "DSP for coherent single-carrier receivers," *J. Lightw. Technol.*, vol. 27, no. 16, pp. 3614–3622, Jun. 2009.

[350] H. Song and W. Hodgkiss, "Efficient use of bandwidth for underwater acoustic communication," *J. Acous. Soc. Amer.*, vol. 134, no. 2, pp. 905–908, Aug. 2013.

[351] L. Wan, H. Zhou, X. Xu, Y. Huang, S. Zhou, Z. Shi, and J.-H. Cui, "Adaptive modulation and coding for underwater acoustic OFDM," *IEEE J. Oceanic Eng.*, vol. 40, no. 2, pp. 327–336, Jun. 2014.

[352] I. Mizukoshi, N. Kazuhiko, and M. Hanawa, "Underwater optical wireless transmission of 405nm, 968Mbit/s optical IM/DD-OFDM signals," in *Proc. OECC / ACOFT*. IEEE, Jul. 2014, pp. 216–217.

[353] H. M. Oubei, J. R. Duran, B. Janjua, H.-Y. Wang, C.-T. Tsai, Y.-C. Chi, T. K. Ng, H.-C. Kuo, J.-H. He, M.-S. Alouini *et al.*, "4.8 Gbit/s 16-QAM-OFDM transmission based on compact 450-nm laser for underwater wireless optical communication," *Opt. Exp.*, vol. 23, no. 18, pp. 23 302–23 309, Sep. 2015.

[354] J. Xu, Y. Song, X. Yu, A. Lin, M. Kong, J. Han, and N. Deng, "Underwater wireless transmission of high-speed QAM-OFDM signals using a compact red-light laser," *Opt. Exp.*, vol. 24, no. 8, pp. 8097–8109, Apr. 2016.

[355] X. Sun, Z. Zhang, A. Chaaban, T. K. Ng, C. Shen, R. Chen, J. Yan, H. Sun, X. Li, J. Wang *et al.*, "71-Mbit/s ultraviolet-B LED communication link based on 8-QAM-OFDM modulation," *Opt. Exp.*, vol. 25, no. 19, pp. 23 267–23 274, Sep. 2017.

[356] A. Al-Halafi, H. M. Oubei, B. S. Ooi, and B. Shihada, "Real-time video transmission over different underwater wireless optical channels using a directly modulated 520 nm laser diode," *IEEE/OSA J. Opt. Commun. Netw.*, vol. 9, no. 10, pp. 826–832, Oct. 2017.

[357] N. Saeed, A. Celik, T. Y. Al-Naffouri, and M.-S. Alouini, "Underwater optical wireless communications, networking, and localization: A survey," *Ad Hoc Netw.*, vol. 94, p. 101935, Nov. 2019.

[358] K. P. Peppas and C. K. Datsikas, "Average symbol error probability of general-order rectangular quadrature amplitude modulation of optical wireless communication systems over atmospheric turbulence channels," *IEEE/OSA J. Opt. Commun. Netw.*, vol. 2, no. 2, pp. 102–110, Mar. 2010.

[359] M. Z. Hassan, X. Song, and J. Cheng, "Subcarrier intensity modulated wireless optical communications with rectangular QAM," *IEEE/OSA J. Opt. Commun. Netw.*, vol. 4, no. 6, pp. 522–532, Jun. 2012.

[360] M. Z. Hassan, M. J. Hossain, and J. Cheng, "Performance of non-adaptive and adaptive subcarrier intensity modulations in gamma-gamma turbulence," *IEEE Trans. Commun.*, vol. 61, no. 7, pp. 2946–2957, Apr. 2013.

[361] H. D. Trung, D. V. Ngo, H. T. Pham, D. V. Hoang, and L. N. Nguyen, "Performance of FSO systems employing SC-QAM over atmospheric turbulence channels and pointing errors," in *Proc. RIVF*. IEEE, Nov. 2013, pp. 31–36.

[362] H. D. Trung, B. T. Vu, and A. T. Pham, "Performance of free-space optical MIMO systems using SC-QAM over atmospheric turbulence channels," in *Proc. IEEE ICC*. IEEE, Jun. 2013, pp. 3846–3850.

[363] M. Z. Hassan, M. J. Hossain, and J. Cheng, "Exact BER analysis of subcarrier QAM and PSK intensity modulations in strong turbulence," in *Proc. ICNC*. IEEE, Feb. 2014, pp. 478–483.

[364] W. G. Alheadary, K.-H. Park, and M.-S. Alouini, "Performance analysis of subcarrier intensity modulation using rectangular QAM over Malaga turbulence channels with integer and non-integer β," *Wireless Commun. Mob. Comp.*, vol. 16, no. 16, pp. 2730–2742, Nov. 2016.

[365] M. H. Ardakani and M. Uysal, "Relay-assisted OFDM for ultraviolet communications: performance analysis and optimization," *IEEE Trans. Wireless Commun.*, vol. 16, no. 1, pp. 607–618, Nov. 2016.

[366] D. H. Ai, H. D. Trung *et al.*, "Pointing error effects on performance of amplify-and-forward relaying MIMO/FSO systems using SC-QAM signals over log-normal atmospheric turbulence channels," in *Proc. ACIIDS*. Springer, Mar. 2016, pp. 607–619.

[367] H. D. Trung, "Performance analysis of amplify-and-forward relaying FSO/SC-QAM systems over weak turbulence channels and pointing error impairments," *J. Opt. Commun.*, vol. 39, no. 1, pp. 93–100, Dec. 2017.

[368] K. K. Garg, P. K. Singya, and V. Bhatia, "ASER analysis of general order rectangular QAM for dual-hop NLOS UV communication system," in *Proc. NCC*. IEEE, Feb. 2019, pp. 1–6.

[369] I. B. Djordjevic and B. Vasic, "Multilevel coding in M-ary DPSK/differential QAM high-speed optical transmission with direct detection," *J. Lightw. Technol.*, vol. 24, no. 1, pp. 420–428, Feb. 2006.

[370] I. B. Djordjevic and G. T. Djordjevic, "On the communication over strong atmospheric turbulence channels by adaptive modulation and coding," *Opt. Exp.*, vol. 17, no. 20, pp. 18 250–18 262, Sep. 2009.

[371] I. B. Djordjevic, "Adaptive modulation and coding for free-space optical channels," *J. Opt. Commun. Netw.*, vol. 2, no. 5, pp. 221–229, May 2010.

[372] M. Niu, J. Cheng, and J. F. Holzman, "Error rate analysis of M-ary coherent free-space optical communication systems with K-distributed turbulence," *IEEE Trans. Commun.*, vol. 59, no. 3, pp. 664–668, Jan. 2011.

[373] X. Tang, Z. Ghassemlooy, S. Rajbhandari, W. O. Popoola, and C. G. Lee, "Coherent heterodyne multilevel polarization shift keying with spatial diversity in a free-space optical turbulence channel," *J. Lightw. Technol.*, vol. 30, no. 16, pp. 2689–2695, Jun. 2012.

[374] B. T. Vu, C. T. Truong, A. T. Pham, and N. T. Dang, "Performance of rectangular QAM/FSO systems using APD receiver over atmospheric turbulence channels," in *Proc. TENCON*. IEEE, Nov. 2012, pp. 1–5.

[375] B. T. Vu, N. T. Dang, T. C. Thang, and A. T. Pham, "Bit error rate analysis of rectangular QAM/FSO systems using an APD receiver over atmospheric turbulence channels," *IEEE/OSA J. Opt. Commun. Netw.*, vol. 5, no. 5, pp. 437–446, May 2013.

[376] H. D. Trung *et al.*, "Performance of free-space optical communications using SC-QAM signals over strong atmospheric turbulence and pointing errors," in *Proc. IEEE ICCE*. IEEE, Jul. 2014, pp. 42–47.

[377] D. H. Ai, H. D. Trung *et al.*, "AF relay-assisted MIMO/FSO/QAM systems in gamma-gamma fading channels," in *Proc. NICS*. IEEE, Sep. 2016, pp. 147–152.

[378] J. Yang, A. K. Khandani, and N. Tin, "Statistical decision making in adaptive modulation and coding for 3G wireless systems," *IEEE Trans. Veh. Technol.*, vol. 54, no. 6, pp. 2066–2073, Nov. 2005.

[379] N. Y. Ermolova, "Useful integrals for performance evaluation of communication systems in generalised η-μ and κ-μ fading channels," *IET Commun.*, vol. 3, no. 2, pp. 303–308, Feb. 2009.

[380] V. Asghari, D. B. da Costa, and S. Aissa, "Symbol error probability of rectangular QAM in MRC systems with correlated η -μ fading channels," *IEEE Trans. Veh. Technol.*, vol. 59, no. 3, pp. 1497–1503, Dec. 2009.

[381] H. Yu, G. Wei, F. Ji, and X. Zhang, "On the error probability of cross-QAM with MRC reception over generalized η-μ fading channels," *IEEE Trans. Veh. Technol.*, vol. 60, no. 6, pp. 2631–2643, May 2011.

[382] Q. Shi and Y. Karasawa, "Some applications of Lauricella hypergeometric function F_A in performance analysis of wireless communications," *IEEE Commun. Lett.*, vol. 16, no. 5, pp. 581–584, Mar. 2012.

[383] D. Dixit and P. Sahu, "Performance of QAM signaling over TWDP fading channels," *IEEE Trans. Wireless Commun.*, vol. 12, no. 4, pp. 1794–1799, Mar. 2013.

[384] S. Aggarwal, "A Survey-cum-Tutorial on Approximations to Gaussian Q Function for Symbol Error Probability Analysis over Nakagami-m Fading Channels," *IEEE Commun. Surveys Tuts.*, Mar. 2019.

[385] Q. C. Li, H. Niu, A. T. Papathanassiou, and G. Wu, "5G network capacity: Key elements and technologies," *IEEE Veh. Technol. Mag.*, vol. 9, no. 1, pp. 71–78, Jan. 2014.

[386] M. Agiwal, A. Roy, and N. Saxena, "Next generation 5G wireless networks: A comprehensive survey," *IEEE Commun. Surveys Tuts.*, vol. 18, no. 3, pp. 1617–1655, Feb. 2016.

[387] Y. Cai, Z. Qin, F. Cui, G. Y. Li, and J. A. McCann, "Modulation and multiple access for 5G networks," *IEEE Commun. Surveys Tuts.*, vol. 20, no. 1, pp. 629–646, Oct. 2017.

[388] K. Kim, Y. H. Yun, C. Kim, Z. Ho, Y.-H. Cho, and J.-Y. Seol, "Preprocessing based soft-demapper for per-tone MIMO operation in QAM-FBMC systems," in *Proc. PIMRC*. IEEE, Aug. 2015, pp. 507–511.

[389] H. Han, H. Kim, N. Kim, and H. Park, "An enhanced QAM-FBMC scheme with interference mitigation," *IEEE Commun. Lett.*, vol. 20, no. 11, pp. 2237–2240, Aug. 2016.

[390] J. Kim, Y. Park, S. Weon, J. Jeong, S. Choi, and D. Hong, "A new filter-bank multicarrier system: The linearly processed FBMC system," *IEEE Trans. Wireless Commun.*, vol. 17, no. 7, pp. 4888–4898, May 2018.

[391] P. Singh, R. Budhiraja, and K. Vasudevan, "SER analysis of MMSE combining for MIMO FBMC-OQAM systems with imperfect CSI," *IEEE Commun. Lett.*, vol. 23, no. 2, pp. 226–229, Dec. 2018.

[392] P. Singh, H. B. Mishra, A. K. Jagannatham, and K. Vasudevan, "Semi-blind, training, and data-aided channel estimation schemes for MIMO-FBMC-OQAM systems," *IEEE Trans. Signal Process.*, vol. 67, no. 18, pp. 4668–4682, Jul. 2019.

[393] P. Singh, R. Budhiraja, and K. Vasudevan, "Probability of error in MMSE detection for MIMO-FBMC-OQAM systems," *IEEE Trans. Veh. Technol.*, vol. 68, no. 8, pp. 8196–8200, Jun. 2019.

[394] P. Singh, B. U. Rani, R. Budhiraja, and K. Vasudevan, "Receivers for VBLAST FBMC-OQAM systems," *IEEE Commun. Lett.*, Dec. 2019.

[395] M. Di Renzo and H. Haas, "Bit error probability of space-shift keying MIMO over multiple-access independent fading channels," *IEEE Trans. Veh. Technol.*, vol. 60, no. 8, pp. 3694–3711, Sep. 2011.

[396] M. Di Renzo, H. Haas, A. Ghrayeb, S. Sugiura, and L. Hanzo, "Spatial modulation for generalized MIMO: Challenges, opportunities, and implementation," *Proc. IEEE*, vol. 102, no. 1, pp. 56–103, Dec. 2013.

[397] S. Narayanan, M. Shikh-Bahaei, J. Hou, and M. F. Flanagan, "Wireless-powered distributed spatial modulation with energy recycling and finite-energy storage," *IEEE Trans. Wireless Commun.*, vol. 17, no. 10, pp. 6645–6662, Aug. 2018.

[398] M. Wen, B. Zheng, K. J. Kim, M. Di Renzo, T. A. Tsiftsis, K.-C. Chen, and N. Al-Dhahir, "A survey on spatial modulation in emerging wireless systems: Research progresses and applications," *IEEE J. Sel. Areas Commun.*, vol. 37, no. 9, pp. 1949–1972, Jul. 2019.

[399] R. Zhang, L. Yang, and L. Hanzo, "Generalised Pre-Coding Aided Spatial Modulation," *IEEE Trans. Wireless Commun.*, vol. 12, no. 11, pp. 5434–5443, Nov. 2013.

[400] R. Rajashekar, K. V. S. Hari, and L. Hanzo, "Antenna selection in spatial modulation systems," *IEEE Commun. Lett.*, vol. 17, no. 3, pp. 521–524, Mar. 2013.

[401] A. Stavridis, S. Sinanovic, M. Di Renzo, and H. Haas, "Energy evaluation of spatial modulation at a multi-antenna base station," in *Proc. IEEE VTC*, Sep. 2013, pp. 1–5.

[402] S. Cui, A. J. Goldsmith, A. Bahai *et al.*, "Energy-constrained modulation optimization," *IEEE Trans. Wireless Commun.*, vol. 4, no. 5, pp. 2349–2360, Sep. 2005.

[403] S. Cui, R. Madan, A. Goldsmith, and S. Lall, "Joint routing, MAC, and link layer optimization in sensor networks with energy constraints," in *Proc. IEEE ICC*, vol. 2. IEEE, May 2005, pp. 725–729.

[404] S. Cui, R. Madan, A. J. Goldsmith, and S. Lall, "Cross-layer energy and delay optimization in small-scale sensor networks," *IEEE Trans. Wireless Commun.*, vol. 6, no. 10, pp. 3688–3699, Oct. 2007.

[405] J. Li and G. AlRegib, "Distributed estimation in energy-constrained wireless sensor networks," *IEEE Trans. Signal Process.*, vol. 57, no. 10, pp. 3746–3758, May 2009.

[406] G. Miao, N. Himayat, G. Y. Li, and S. Talwar, "Low-complexity energy-efficient scheduling for uplink OFDMA," *IEEE Trans. Commun.*, vol. 60, no. 1, pp. 112–120, Dec. 2011.

[407] G. Miao, "Energy-efficient uplink multi-user MIMO," *IEEE Trans. Wireless Commun.*, vol. 12, no. 5, pp. 2302–2313, Apr. 2013.

[408] L. J. Rodriguez, N. H. Tran, and T. Le-Ngoc, "Performance of full-duplex AF relaying in the presence of residual self-interference," *IEEE J. Sel. Areas Commun.*, vol. 32, no. 9, pp. 1752–1764, Jun. 2014.

[409] M. A. Hoque, M. Siekkinen, and J. K. Nurminen, "Energy efficient multimedia streaming to mobile devices - A survey," *IEEE Commun. Surveys Tuts.*, vol. 16, no. 1, pp. 579–597, Nov. 2012.

[410] J. Zhang, Q. Li, K. J. Kim, Y. Wang, X. Ge, and J. Zhang, "On the performance of full-duplex two-way relay channels with spatial modulation," *IEEE Trans. Commun.*, vol. 64, no. 12, pp. 4966–4982, Aug. 2016.

[411] B. Kumbhani and R. S. Kshetrimayum, "MGF based approximate SER calculation of SM MIMO systems over generalized η-μ and κ-μ fading channels," *Wireless Personal Commun.*, vol. 83, no. 3, pp. 1903–1913, Aug. 2015.

[412] R. Rajashekar, M. Di Renzo, K. Hari, and L. Hanzo, "A generalized transmit and receive diversity condition for feedback-assisted MIMO systems: Theory and applications in full-duplex spatial modulation," *IEEE Trans. Signal Process.*, vol. 65, no. 24, pp. 6505–6519, Dec. 2017.

[413] S. Narayanan, H. Ahmadi, and M. F. Flanagan, "On the performance of spatial modulation MIMO for full-duplex relay networks," *IEEE Trans. Wireless Commun.*, vol. 16, no. 6, pp. 3727–3746, Mar. 2017.

[414] Y. Jin, X.-G. Xia, Y. Chen, and R. Li, "Full-duplex delay diversity relay transmission using bit-interleaved coded OFDM," *IEEE Trans. Commun.*, vol. 65, no. 8, pp. 3250–3258, May 2017.

[415] Y. Naresh and A. Chockalingam, "Performance analysis of full-duplex decode-and-forward relaying with media-based modulation," *IEEE Trans. Veh. Technol.*, vol. 68, no. 2, pp. 1510–1524, Feb. 2018.